ISSN 0973-8916

Current Trends in Biotechnology and Pharmacy

Volume 12 Issue 4 October 2018

www.abap.co.in

Current Trends in Biotechnology and Pharmacy
ISSN 0973-8916 (Print), 2230-7303 (Online)

Editors

Prof.K.R.S. Sambasiva Rao, India
krssrao@abap.co.in

Prof. Karnam S. Murthy, USA
skarnam@vcu.edu

www.abap.co.in

ISSN 0973-8916

Current Trends in Biotechnology and Pharmacy

(An International Scientific Journal)

Volume 12 Issue 4 October 2018

www.abap.co.in

Indexed in Chemical Abstracts, EMBASE, ProQuest, Academic SearchTM, DOAJ, CAB Abstracts, Index Copernicus, Ulrich's Periodicals Directory, Open J-Gate Pharmoinfonet.in Indianjournals.com and Indian Science Abstracts.

Current Trends in Biotechnology and Pharmacy
Vol. 12 (4) October 2018, ISSN 0973-8916 (Print), 2230-7303 (Online)

Association of Biotechnology and Pharmacy

(Regn. No. 28 OF 2007)

The *Association of Biotechnology and Pharmacy (ABAP)* was established for promoting the science of Biotechnology and Pharmacy. The objective of the Association is to advance and disseminate the knowledge and information in the areas of Biotechnology and Pharmacy by organising annual scientific meetings, seminars and symposia.

Members

The persons involved in research, teaching and work can become members of Association by paying membership fees to Association.

The members of the Association are allowed to write the title ***MABAP*** (Member of the Association of Biotechnology and Pharmacy) with their names.

Fellows

Every year, the Association will award Fellowships to the limited number of members of the Association with a distinguished academic and scientific career to be as Fellows of the Association during annual convention. The fellows can write the title ***FABAP*** (Fellow of the Association of Biotechnology and Pharmacy) with their names.

Membership details

(Membership and Journal)		India	SAARC	Others
Individuals	– 1 year	Rs. 600	Rs. 1000	$100
	LifeMember	Rs. 4000	Rs. 6000	$500
Institutions	– 1 year	Rs. 1500	Rs. 2000	$200
(Journal only)	Life member	Rs.10000	Rs.12000	$1200

Individuals can pay in two instalments, however the membership certificate will be issued on payment of full amount. All the members and Fellows will receive a copy of the journal free.

Association of Biotechnology and Pharmacy
(Regn. No. 28 OF 2007)
#5-69-64; 6/19, Brodipet
Guntur – 522 002, Andhra Pradesh, India

Current Trends in Biotechnology and Pharmacy
Vol. 12 (4) October 2018, ISSN 0973-8916 (Print), 2230-7303 (Online)

Current Trends in Biotechnology and Pharmacy

ISSN 0973-8916

Volume 12 (4) **October 2018**

CONTENTS

Current Trends in Biotechnology and Pharmacy
Vol. 12 (4) October 2018, ISSN 0973-8916 (Print), 2230-7303 (Online)

Information to Authors

The *Current Trends in Biotechnology and Pharmacy* is an official international journal of *Association of Biotechnology and Pharmacy*. It is a peer reviewed quarterly journal dedicated to publish high quality original research articles in biotechnology and pharmacy. The journal will accept contributions from all areas of biotechnology and pharmacy including plant, animal, industrial, microbial, medical, pharmaceutical and analytical biotechnologies, immunology, proteomics, genomics, metabolomics, bioinformatics and different areas in pharmacy such as, pharmaceutics, pharmacology, pharmaceutical chemistry, pharma analysis and pharmacognosy. In addition to the original research papers, review articles in the above mentioned fields will also be considered.

Call for papers

The Association is inviting original research or review papers and short comunications in any of the above mentioned research areas for publication in Current Trends in Biotechnology and Pharmacy. The manuscripts should be concise, typed in double space in a general format containing a title page with a short running title and the names and addresses of the authors for correspondence followed by Abstract (350 words), 3 – 5 key words, Introduction, Materials and Methods, Results and Discussion, Conclusion, References, followed by the tables, figures and graphs on separate sheets. For quoting references in the text one has to follow the numbering of references in parentheses and full references with appropriate numbers at the end of the text in the same order. References have to be cited in the format below.

Mahavadi, S., Rao, R.S.S.K. and Murthy, K.S. (2007). Cross-regulation of VAPC2 receptor internalization by m2 receptors via c-Src-mediated phosphorylation of GRK2. Regulatory Peptides, 139: 109-114.

Lehninger, A.L., Nelson, D.L. and Cox, M.M. (2004). Lehninger Principles of Biochemistry, (4th edition), W.H. Freeman & Co., New York, USA, pp. 73-111.

Authors have to submit the figures, graphs and tables of the related research paper/article in Adobe Photoshop of the latest version for good illumination and allignment.

Authors can submit their papers and articles either to the editor or any of the editorial board members for onward transmission to the editorial office. Members of the editorial board are authorized to accept papers and can recommend for publication after the peer reviewing process. The email address of editorial board members are available in website www.abap.in. For submission of the articles directly, the authors are advised to submit by email to krssrao@abap.co.in or krssrao@yahoo.com.

Authors are solely responsible for the data, presentation and conclusions made in their articles/research papers. It is the responsibility of the advertisers for the statements made in the advertisements.

Current Trends in Biotechnology and Pharmacy
Vol. 12 (4) 311-317, October 2018, ISSN 0973-8916 (Print), 2230-7303 (Online)

Compatibility and stability of ceftriaxone sodium with peritoneal dialysis solution

Osama Javed, Khalid Hussain; Muhammad Shahzad Aslam*
University College of Pharmacy, University of the Punjab, Lahore, Pakistan
* Department of Pharmaceutical Chemistry, Faculty of Pharmacy, Ziauddin University, Karachi, Pakistan
aslammuhammadshahzad@gmail.com

Abstract

Drug compatibility and stability with the diluents is important expected therapeutic outcome. The administration of incompatible and unstable antibiotics admixtures is associated with several life threatening clinical situations. For the treatment of peritonitis or peritoneal infection, antibiotics are delivered at the site through peritoneal dialysis solution. Therefore, the investigation of compatibility and stability of antibiotic with peritoneal dialysis is imperative. To address this matter, the present study is aimed to determine the compatibility and stability of ceftriaxone sodium in isotonic and hypertonic peritoneal dialysis solutions. For such purposes, a spectroscopic method was developed and validated for the determination of ceftriaxone sodium in the presence of peritoneal dialysis solutions. Then the compatibility and stability of the antibiotic in both the peritoneal dialysis solutions at 4°C, 25°C and 40°C for 48 h using three concentrations of the drug such as 250 mg/L, 500 mg/L and 1000 mg/L. The aliquots were drawn from the admixtures at regular intervals and analyzed to determine the drug contents using UV spectrophotometry. The results of the study showed that the drug was stable for 10 days at 4°C, 28 h at 25°C and 8 h at 40°C in both the peritoneal dialysis solutions. The drug was found to be following the 1st order degradation at all the three temperatures. It is concluded from results of the present study that ceftriaxone sodium is compatible and stable with isotonic and hypertonic peritoneal dialysis solutions.

Introduction

CFX-Na is a crystalline, white hygroscopic powder and has a good water solubility. It is slightly soluble in ethanol and in methanol it shows sparingly solubility. The pH of 1% aqueous solution is approximately 6.7. It is optimum to store it under 25°C and should be shielded from light. It is recommended that the reconstituted solutions must be used immediately after preparation but they are stable for up to 24 h when stored in the refrigerator. The present study aimed to investigate compatibility and stability of ceftriaxone sodium and PD solutions at three different temperatures. To develop and validate UV spectroscopic method for the determination of ceftriaxone sodium in PD solutions. Compatibility and stability of the antibiotic and PD solutions.

Materials and methods

Preparation of admixtures

Three sample solutions were made by dissolving the quantity of CFX-Na equivalent to 25 mg, 50 mg and 100 mg in 100 ml isotonic PD solution. Similarly three sample solutions were also made by dissolving the quantity of CFX-Na equivalent to 25 mg, 50 mg and 100 mg in 100 ml hypertonic PD solution.

Processing of admixtures : The solutions of each concentration in isotonic PD solution were stored at three different temperatures such as 4°C, 25°C and 40°C for 48 h. Similarly, the solutions of each concentration in hypertonic PD solutions were

stored at three different temperatures such as 4°C, 25°C and 40°C for 48 h. The physicochemical changes like color changes, precipitation, turbidity and clarity of the solutions were observed for 48 h at regular intervals.

Analysis of aliquots : One hundred micro liters aliquots were withdrawn at 0 (premixing), 15, 30, 45, 60, 120, 360, 720, 1440 and 2880 minutes and diluted up to 10 ml with isotonic PD solution. Same procedure was repeated for dilution with hypertonic PD solution, for the solutions which were formed in hypertonic PD solution. Then the aliquots of CFX-Na were analyzed by using spectrophotometer at $ë_{max}$ of 276nm. All readings were taken in triplicate by using isotonic PD solution as a blank for the solutions which were made in isotonic PD solution. Similarly, hypertonic PD solution was used as a blank for the solutions which were made in hypertonic PD solution.

Evaluation of chemical kinetic parameters

Order of the reaction : Chemical kinetics of the reaction were determined by graphic method as zero, first and second order [1]. Graphs were plotted for zero order, first order and second order kinetics for each of the solution stored at 4°C, 25°C and 40°C. The correlation coefficient of each of the graph at each temperature was evaluated and order of the chemical reaction with the best linearity was taken. The reaction rate constant (K) for zero order kinetic was calculated at each temperature from slope of the curve of % concentration remaining after 48h versus time, for first order by logarithm of % concentration remaining versus time and for second order by inverse of the concentration remaining (1/C) versus time [2].

Activation energy (Ea) : Activation energy (Ea), the energy required to move a molecule from initial state to the transitional state or the minimum energy needed for the reaction to occur. Rate constant K was used to ascertain Ea by taking natural logarithm (ln K) or logarithm (log K) on y-axis and reciprocal of absolute temperature (1/T) in Kelvin on x-axis (Pugh *et al.,* 2002). It can be calculated from the slope of the straight line of the plot (-Ea/2.303 R or Ea/R) [2].

Frequency Factor (A) : It is also called the pre-exponential factor or the steric factor. It determines factors like frequency of collision and their orientation. It can be calculated from the intercept (log A or ln A) taken from the plot of ln K versus 1/T [2]. Then Arrhenius equation was used to determine the reaction rate constant for each of the solution of CFX-Na in isotonic and hypertonic PD solutions stored at 4°C (277.15 K), 25°C (298.15) and 40°C (313.15 K).

Results and discussion

Physical changes of the CFX-Na in PD solutions : Different parameters were assessed during physical study like color changes, precipitation, clarity of solution and turbidity. No physical changes were observed in the solutions of CFX-Na in isotonic PD solution as well as in hypertonic PD solution, which were stored at 4°C, 25°C and 40°C for the time period of 48 h. Parameters for physical study like color changes, precipitation, clarity of solution and turbidity were assessed at all the three temperatures. No color change was observed in the solutions of CFX-Na in isotonic as well as in hypertonic PD solution, even after the storage time of 48 h at all the three temperatures i.e., 4°C, 25°C and 40°C. No precipitation was seen in the solutions of CFX-Na in isotonic PD solution neither in the solutions of CFX-Na in hypertonic PD solutions after keeping the solutions in storage upto 48 h at all the three temperatures. Solutions of CFX-Na in both PD solutions were crystal clear and no turbidity was found at all three temperatures during complete physical study of 48 h.

Degradation kinetics of admixtures at different temperatures : Compatibility and stability of CFX-Na with isotonic PD solution and CFX-Na with hypertonic PD solution was also studied by investigating their order of reactions at all three temperatures and the curve with the best linearity was taken as order of reaction. The graphs of percentage degradation versus time in minutes of all the three concentrations in isotonic PD solution

Vol. 12 (4) 311-317, October 2018, ISSN 0973-8916 (Print), 2230-7303 (Online)

Table 1- Parameters for physical changes observed during stability study

Color changes			
Drug Sample	4°C	25°C	40°C
CFX-Na in isotonic PD solution	No change	No change	No change
CFX-Na in hypertonic PD solution	No change	No change	No change
	Precipitation observed		
CFX-Na in isotonic PD solution	Absent	Absent	Absent
CFX-Na in hypertonic PD solution	Absent	Absent	Absent
	Clarity test		
CFX-Na in isotonic PD solution	Clear	Clear	Clear
CFX-Na in hypertonic PD solution	Clear	Clear	Clear
	Turbidity observed		
CFX-Na in isotonic PD solution	No turbidity	No turbidity	No turbidity
CFX-Na in hypertonic PD solution	No turbidity	No turbidity	No turbidity

are shown in the Figure 3.1, 3.2 and 3.3 respectively.

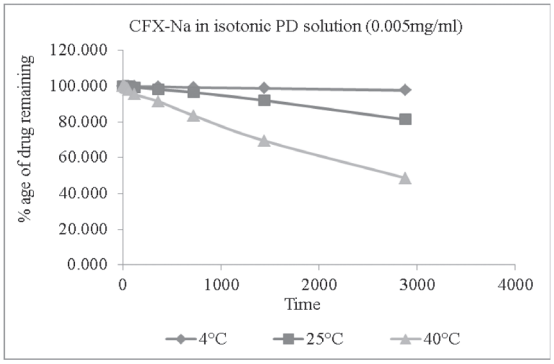

Fig. 1: % age of remaining CFX-Na in isotonic PD solution at concentration of 0.0025 mg/ml

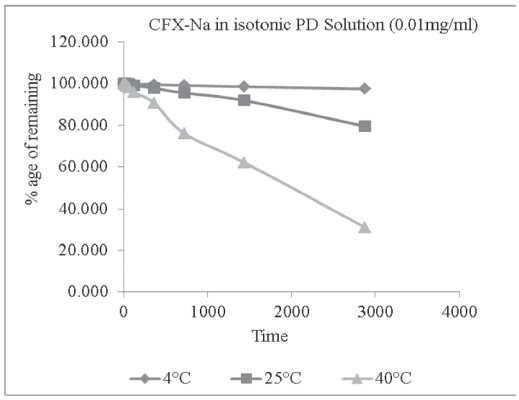

Figure 2: % age of remaining CFX-Na in isotonic PD solution at concentration of 0.005 mg/ml

The above curves indicate that the drug is more stable at lower temperature than higher temperature. Drug is most stable at 4°C and it is least stable at 40°C. The degradation curves of CFX-Na in the hypertonic PD solution at the same three temperatures and concentrations are shown in the Figures 3.4, 3.5 and 3.6 respectively.

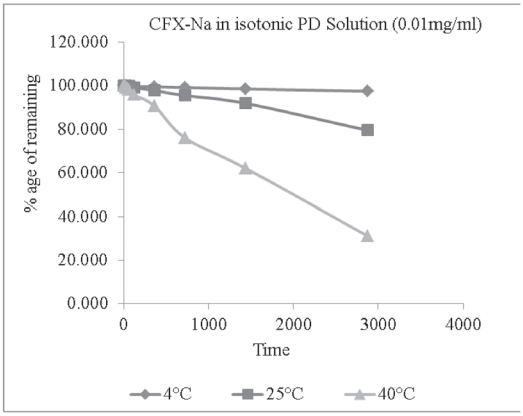

Fig. 3: % age of remaining CFX-Na in isotonic PD solution at concentration of 0.01mg/ml

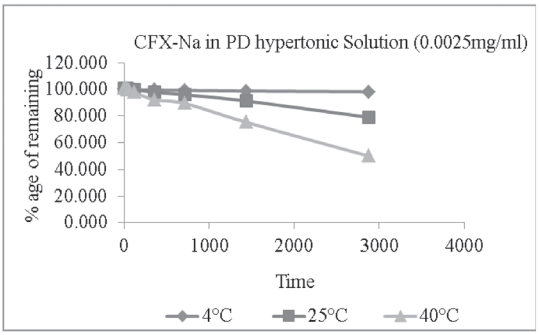

Fig. 4: % age of remaining CFX-Na in hypertonic PD solution at concentration of 0.0025 mg/ml

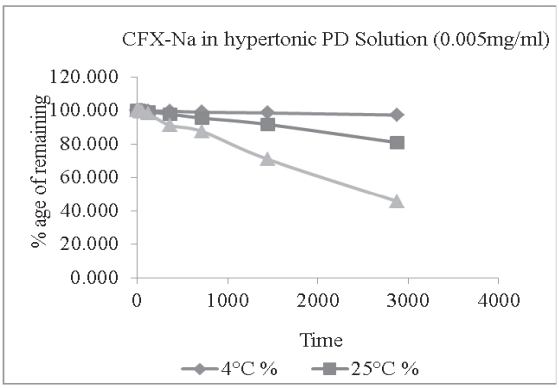

Fig. 5: % age of remaining CFX-Na in hypertonic PD solution at concentration of 0.005 mg/ml

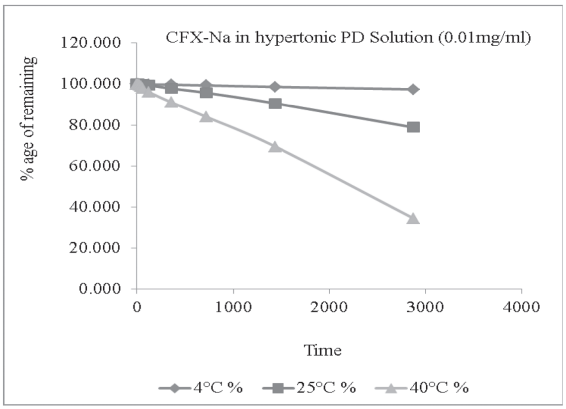

Fig. 6: % age of remaining CFX-Na in hypertonic PD solution at concentration of 0.01 mg/ml

The study conducted in hypertonic PD solution also showed similar results as shown for the isotonic PD solution. The rate of degradation was maximum at temperature 40°C and was found to be minimum at temperature 4°C. The graphs of reaction order in isotonic PD solution at three temperatures are shown in Figure 3.7. 3.8 and 3.9 respectively.

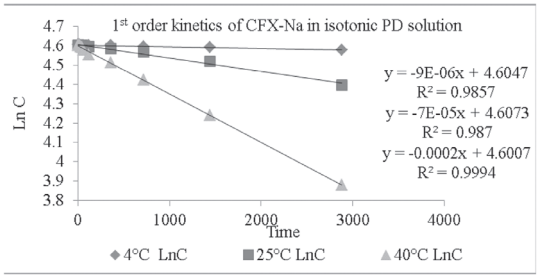

Fig. 7: 1st order degradation kinetics of CFX-Na in isotonic PD solution at 0.0025 mg/ml concentration.

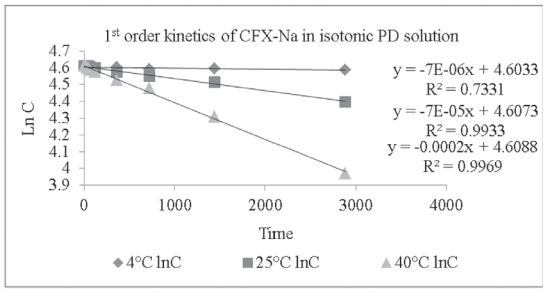

Fig. 8: 1st order degradation kinetics of CFX-Na isotonic PD solution at 0.005 mg/ml concentration.

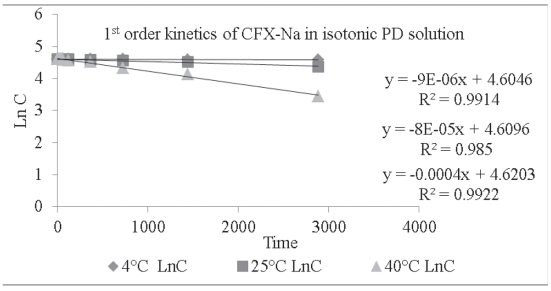

Fig. 9: 1st order degradation kinetics of CFX-Na isotonic PD solution at 0.01 mg/ml concentration.

It can be seen from the graph of order of reaction that the value of correlation coefficient is almost approaching to '1' in all the curves. So it can be concluded that drug degradation follows 1st order kinetics at all the three concentrations i.e., 0.0025 mg/ml, 0.005 mg/ml and 0.01 mg/ml in isotonic PD solution. The slope of the degradation curve was minimum at 4°C and maximum at 40°C so the degradation was minimum at 4°C and maximum at 40°C. The graphs of 1st order reaction in hypertonic PD solution are shown in figures 3.10, 3.11 and 3.12.

The above graphs show that the degradation follows 1st order kinetics at all three temperatures in hypertonic PD solution. The concentration has no effect on the order of reaction and the degradation followed 1st order kinetics at all three concentrations.

Arrhenius plots : Effect of temperature on rate of reaction was studied by taking Arrhenius plots of degradation rates. It was proved from the results of order of reaction because the reaction order was independent of the concentration of drug, so the Arrhenius plot was taken only for a single concentration of drug i.e., 0.0025 mg/ml. The reaction velocity or degradation rate constant (K) of the CFX-Na in peritoneal PD solutions at a concentration of 0.0025 mg/ml was taken from the slope of their curves of logarithm of concentration remaining (LnC) versus time. Rate constant of CFX-Na degradation was determined by extrapolating the graphs of (LnK) versus inverse of temperature (1/T Kelvin^{-1}). Results of plots in isotonic and hypertonic PD solution are shown in figure 3.13 and 3.14 respectively.

Activation energy (Ea) for each combination was calculated by multiplying slope of the straight line of the respective Arrhenius plot with gas constant (R= 8.314 KJ mol^{-1}) whereas pre-exponential factor or frequency factor (A) was calculated from the intercept of the curves. Degradation rate constant (K), activation energy (Ea) and frequency factor (A) of above stated combinations are presented in Table 3.2.

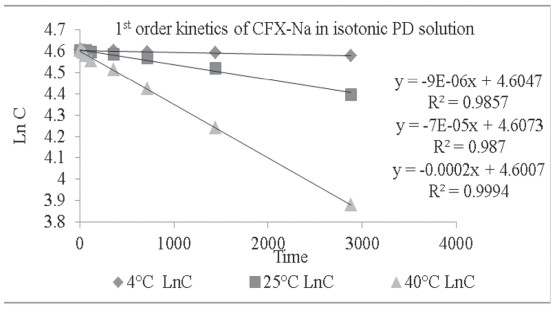

Fig. 10: 1st order degradation kinetics of CFX-Na in hypertonic PD solution at 0.0025 mg/ml concentration.

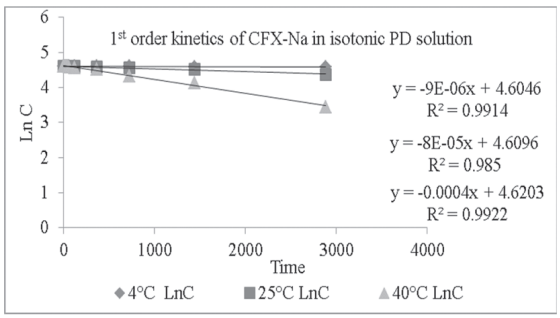

Fig. 11: 1st order degradation kinetics of CFX-Na in hypertonic PD solution at 0.005 mg/ml concentration.

Vol. 12 (4) 311-317, October 2018, ISSN 0973-8916 (Print), 2230-7303 (Online)

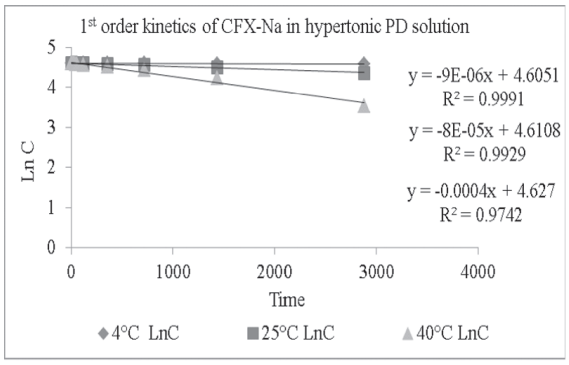

Fig. 12: 1st order degradation kinetics of CFX-Na in hypertonic PD solution at 0.01 mg/ml concentration.

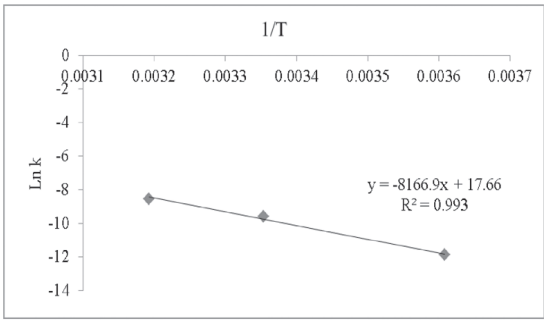

Fig. 13: Arrhenius plot of CFX-Na (0.0025 mg/ml) in isotonic PD solution

The above mentioned results show that the value of degradation rate constant (K) is maximum at 40˚C and minimum at 4°C, so the rate of degradation is maximum at 40°C. The value of 'K'

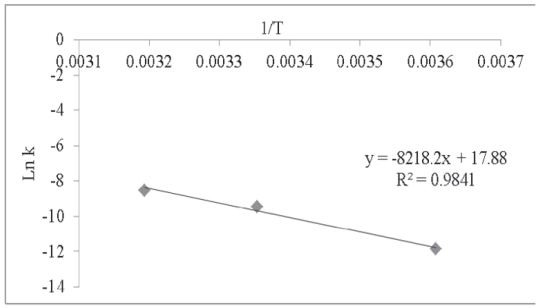

Fig. 14: Arrhenius plot of CFX-Na (0.0025 mg/ml) in hypertonic PD solution.

is slightly greater in the hypertonic PD solution. It means the degradation rate is slightly faster in hypertonic PD solution than in the isotonic PD solution. The frequency factor 'A' is also greater in hypertonic PD solution. The shelf life of the CFX-Na in isotonic and hypertonic PD solutions was calculated and showed in Table 3.3.

The results shown in Table 3.3 indicate that as the temperature increases, the shelf life of CTX-Na decreases. The results also indicate that the drug showed a slightly lesser shelf life in hypertonic PD solution than in the isotonic PD solution. The shelf life of drug was almost 10 days in isotonic PD solution and 9.5 days in hypertonic PD solution at 4°C. At 25°C, the drug remained stable for almost 30 h in isotonic and for 28 h in hypertonic PD solution. Least shelf life was shown at 40°C where the drug remained stable for only about 8 h

Table 2: Rate constant (K), activation energy (Ea) and frequency factor (A) of all the combinations stored at 4°C, 25°C and 40°C for 48 h

Name of drug	K4°C	K25°C	K40°C	Ea (KJ mol^{-1})	A (S^{-1})
CFX-Na in isotonic PD solution	0.0000074	0.000059	0.00022	67.89961	46734817.4
CFX-Nain hypertonic PD solution	0.0000077	0.0000625	0.000233	68.32611	58235168.5

Ceftriaxone sodium (CFX-Na); PD (Peritoneal dialysis)

Table 3: Shelf life of CFX-Na in isotonic and hypertonic PD solutions stored at 4°C, 25°C and 40°C for 48 h

Name of drug	Shelf Life (h) 4°C	Shelf Life (h)25°C	Shelf Life (h)40°C
CFX-Na in isotonic PD solution	236.49	29.66	7.95
CFX-Na in hypertonic PD solution	227.3	28.0	7.5

Ceftriaxone sodium (CFX-Na); PD (Peritoneal dialysis)

and 7.5 h in isotonic and hypertonic PD solution respectively. It was found in recent result that ceftriaxone disodum was more stable in water than isotonic solution [3].

Conclusion

Ceftriaxone sodium is a commonly used antibiotic for the prevention of peritonitis in patients of peritoneal dialysis. In most of the times, the drug is mixed with the dialyzing fluid at the time of administration, but if the admixture of drug and dialyzing fluid is required to be stored for some time, this solution must have to remain stable during that storage time. The present stability study of CFX-Na in isotonic and hypertonic PD solution has shown that as the temperature is increased, the drug degradation becomes faster. The degradation products are also soluble in the PD solutions so there is no precipitation or coloration produced in the admixtures after storage for 48 h. Moreover, the drug did not show any suspended particle with the passage of time. The increased degradation of drug is attributable to the increased kinetic energy of the molecules. Due to increased kinetic energy, molecular collision is increased. As the reaction rate is directly proportional to the collision of reactant molecules with one another. So, the degradation rate is also increased at increased temperature. The degradation rate was also greater in the hypertonic PD solution and can also be justified from the frequency factor obtained from the Arrhenius plots. The frequency factor was found to be greater in hypertonic PD solution. Due to the greater rate of degradation, the drug showed shorter shelf life at increased temperature. So, if the admixture is to be administered in a warm environment, it should be used immediately after mixing the CFX-Na in peritoneal dialysis solution. If storage is necessary, it must be stored in refrigerator at 4°C, at which the drug is stable for almost 10 days. The drug degradation follows 1st order kinetics at 0°C, 25°C and 40°C in both types of PD solutions. It means the increase in concentration does not affect the drug degradation rate, but effect of temperature is dominant and the rate of degradation is very slow at 4°C. Overall, it can be suggested by this study that the ceftriaxone sodium is compatible with peritoneal dialysis solutions.

Reference:

[1] Murphy, B., C. Murphy & B. J. Hathaway (1997) A Working Method Approach for Introductory Physical Chemistry Calculations. Royal Society of Chemistry: London, pp. 115-7

[2] Karim, S., Baie, S. H., Hay, Y. K., Latif, A., Shamim, R., Hussain, K., & Bukhari, N. I. (2013). Stability study of paracetamol and omeprazole pellets formulated through sieving-spheronisation. Lat. Am. J. Pharm, 32(3), 431-6. Chicago

[3] Cantón, E., Esteban, M. J., & Rius, F. (1993). Factors affecting the stability of ceftriaxone sodium in solution on storage. International journal of pharmaceutics, 92(1-3), 47-53.

Current Trends in Biotechnology and Pharmacy
Vol. 12 (4) 318-333, October 2018, ISSN 0973-8916 (Print), 2230-7303 (Online)

Development of Murine Monoclonal Antibodies, Characterization and Quantification of Diphtheria Toxoid in Vaccine Batches

Praveen Alagangula[1, 2], Sridevi V Nimmagadda[1], Vidyasagar Pitta[1], Dipankar Das[1], Ralla Kumar[1], Shukra M Aavula[1], Mohammed Furman Ali[1], Premalatha Dasari[1], Rajendra Lingala[1]*

[1]Indian Immunologicals Limited, Rakshapuram, Gachibowli, Hyderabad- 500032, Telangana, India.
[2]Department of Biotechnology, Jawaharlal Nehru Technological University, Kukatpally, Hyderabad- 500085
*Corresponding author - rajendra.lingala@indimmune.com

Abstract

Diphtheria is caused by *Cornybacteria diphtheria* and it is one of the contagious diseases with a mortality rate of 5% to 10% worldwide. Though the mass immunization of diphtheria vaccine reduces the mortality, but the immediate effective treatment for this disease involves the administration of anti-diphtheria polyclonal antibodies or diphtheria antitoxin (DAT) produced from Equines. However the availability of anti-diphtheria polyclonal antibody is very limited due to the less number of manufacturers. Hence the development of monoclonal antibodies (mAbs) with neutralizing capability may act as a potent alternate candidate to DAT or as an effective therapeutic agent. In the present study, we have developed and characterized five mouse monoclonal antibodies against diphtheria toxoid. The specificity of the mAbs was established by its non-reactivity towards other toxins by indirect ELISA (Enzyme linked Immunosorbent assay) and competitive ELISA with the commercial mAb. The non-competing mAbs were used to develop immunocapture ELISA for the quantification of toxoid content in in-process samples during manufacture of the vaccine. The r^2 value obtained by the regression analysis was 0.996. This ELISA can be adapted to measure the toxoid content and blending of the vaccine can be performed based on the estimated toxoid. The neutralizing activity of the mAbs against diphtheria toxin was performed by *in vitro* cell based neutralization assay using Vero cells. The cytotoxicity assay demonstrated that mAb neutralized the toxin in a concentration dependent manner. We have further shown that the mAb binds to the receptor binding domain of diphtheria toxin and it blocks the toxin from binding to the heparin-binding epidermal growth factor like growth factor by ELISA.These monoclonal antibodies may have a potential in development of therapeutics and diagnostics.

Key words: Monoclonal antibodies, Diphtheria toxin, ELISA, *In vitro* neutralization

Introduction:

Corynebacterium diphtheria is a gram positive bacterium that causes the infectious disease, diphtheria in the upper respiratory tract of humans (1). The potent toxin produced by *Corynebacterium* plays a major role in inhibition of protein synthesis in eukaryotic cells resulting in cell death (2). The classical form of diphtheria results when the bacterium is infected with a bacteriophage carrying the structural gene for biosynthesis of the toxin responsible for clinical disease. The clinical presentation includes a fibrous, adherent pharyngeal membrane and causes severe systemic toxicity, myocarditis and

peripheral neuritis. Diphtheria toxin is produced as a single polypeptide chain with the disulfide bond linking two fragments which is fragment A and fragment B. Fragment A is known as catalytic domain,a potent enzyme that acts intra cellular to block protein synthesis. Fragment B domain contains a translocation and receptor region. It is responsible for the recognition of receptors on mammalian cells and translocation of fragment A into cells (3,4).

Until recently, diphtheria was known to be a rare disease in industrialized countries with well-established routine childhood vaccination programs (5). After primary vaccination, anti-diphtheria antibodies wane in absence of boosting. As waning of antibodies in adults has been documented in various studies in Australia, New Zealand, Germany and Poland (6). The importance of maintaining adequate population immunity against diphtheria has drawn attention when diphtheria epidemic re-emerged in several eastern European countries in 1990s, with a high proportion of adult cases (7). Diphtheria is preventable by vaccination,however the disease seems to continue due to regional variations in compliance to vaccination, insufficient booster regimens and deterioration of the immune system.According to WHO, 4,500-5,500 cases were reported annually, with the majority occurring in India and Indonesia (8).

The protective role of antisera raised in horses against the toxin to treat human diphtheria as an alternative were reported earlier in the late nineteenth century (3, 9). However, the usage of equine polyclonal antiserum has limitations causing serum sickness, allergic reactions to the recipient and high regulatory requirements for the safe manufacture of blood derived products (10,11). Hence, development of high binding and neutralizing monoclonal antibodies would be safe and better alternative to equine DAT and many resource poor countries would benefit greatly (12).

According to World Health Organization (WHO), circulating diphtheria antitoxin level of 0.01 IU/ml, as determined by the neutralization test, provides basic clinical immunity against the disease, and a higher titer would be required to provide full protection (13). The discovery of potent neutralizing antibodies against the diphtheria toxin holds great promise as potential therapeutics (14).Murine monoclonal antibodies against diphtheria can be used as an alternative to equine serum (15). These monoclonal antibodies (mAbs) can also be used for diagnosis and in maintaining of quality in vaccine manufacture (16) .The evaluation of potency in diphtheria toxoid vaccine for lot release is being performed in guinea pigs through intradermal challenge test or by performing serological assays in mice (17).To demonstrate that the vaccine batches induce a protective immune response, a quite large number of animals are required and this *in vivo* tests accuracy and precision was found to remain contentious.Vaccine manufacturers are determining the potency by *in vitro* ELISA based assays which are correlating well with the *in vivo* tests.Monoclonal antibody assays are being used in diphtheria vaccines to demonstrate the safety (18). As compared to polyclonal antibody products, the advantage of monoclonal antibodies is the fact that they consist of one antibody molecule with singular specificity, the neutralizing activity of which contained in one microgram of purified mAb can be determined by evaluating the mAb relative to the FDA diphtheria anti-toxin standard expressed in IU.

In the present study, we describe the identification of an anti-diphtheria antibodies isolated from antibody secreting cells generated from immunized mice. The selected monoclonal antibodies were characterized for their binding activity and specificity towards diphtheria toxin by ELISA based methods. These antibodies shown neutralization of toxin in a cell based assays and also prevented the toxin from binding to the receptor HB-EGF. Selected the two non-competing antibodies and developed an immunocapture ELISA for the quantification of diphtheria toxoid content in vaccine in-process samples.

Vol. 12 (4) 318-333, October 2018, ISSN 0973-8916 (Print), 2230-7303 (Online)

Materials and methods:

Reagents and chemicals: Diphtheria toxoid standard (1100 Lf/ml) was purchased from NIBSC (UK). Myeloma partner SP2/mIL-6, Human MAb against diphtheria toxoid 16M3F10.1C (HB-8363) and Vero cells were obtained from ATCC (USA). Hypoxanthine-aminopterin-thymidine (HAT), Hypoxanthine-thymidine (HT) and Goat anti-mouse IgG Fc specific HRPO conjugate was obtained from Sigma (St. Louis, Missouri, USA). Isotype kit was purchased from Roche Diagnostics (Mannheim, Germany).

Immunization of mice: All the animal experiments were approved by Institutional Animal Ethics Committee (IAEC) and performed accordingly. The animals were purchased from National Institute of Nutrition (NIN), Hyderabad. Four to six weeks old female BALB/c mice were hyper-immunized with diphtheria toxoid. Briefly, mice were immunized intraperitoneal with diphtheria toxoid (50 µg/dose/animal) emulsified with equal volume of Freund's complete adjuvant. After an interval of two weeks, booster doses were administered intraperitoneal with diphtheria toxoid (25 µg/dose/animal) mixed with equal volume of Freund's incomplete adjuvant. Subsequently, after one week interval, blood was collected from the retro-orbital sinus of the mice and incubated at room temperature for 4 hours. Serum was separated from blood by centrifugation at 10,000 rpm for 5 minutes and tested for end-point titer by indirect ELISA. After last booster, mice were kept under observation for one month. Four days prior to fusion, diphtheria toxoid was administered to mice by intravenous route (10 µg/animal) for three consecutive days and were kept under observation for a day before performing spleenectomy.

Generation of monoclonal antibodies: The development of hybridomas was performed by fusing myeloma partner, Sp2/m IL-6 and hyper immunized mouse spleenocytes as per standard procedure (19). Briefly, 10 x 10^6 cells of mouse myeloma partner (Sp2/m IL-6) were suspended in DMEM medium. High titer mouse spleenocytes, 100 x 10^6 cells were isolated and fused with Sp2/m IL-6 cells at a ratio of 10:1 in the presence of polyethylene glycol (PEG 1500). After fusion, hypoxanthine-aminopterin-thymidine (HAT) medium was used as selective media for the growth of hybrid cells. Hybridomas were seeded into microtiter tissue culture plates at 1 x 10^5 cells per well and incubated at 37°C in 7% CO_2. Medium was changed every four days and replenished with fresh HAT growth medium. Hybridomas were grown for a total of 14 days in HAT medium and gradually adapted to hypoxanthine-thymidine (HT) medium and further passaged for 7 days. Hybridomas were monitored daily for growth or contamination under an inverted microscope (Olympus CK2). The confluent hybridomas were primarily screened against diphtheria toxoid by indirect ELISA.Three rounds of limiting dilution were performed to establish the monoclonality of the progeny hybridomas.

Binding of hybridomas by Indirect ELISA: Diphtheria toxoid, diphtheria toxin and non-toxic mutant of diphtheria toxin (CRM-197) were dissolved in carbonate bicarbonate buffer (0.1 M), pH 9.6, at a final concentration of 5 µg/ml respectively and subsequently, 100 µl of each antigen was coated in respective wells in Maxisorp 96-well micro titer plates. These plates were incubated overnight at 4°C. The wells were washed thrice with phosphate buffered saline (PBS) containing 0.05% (v/v) Tween-20 (PBST) to remove any unbound antigen and the remaining active surfaces in the wells were blocked with 2% (w/v) skimmed milk powder in PBST for 1 hour at 37°C. The plates were again washed with PBST and 100 µl of hybridoma culture supernatants, negative controls (PBST, unimmunized mouse serum, myeloma culture fluid) and the positive control (immunized mouse serum) were added to respective wells and incubated at 37°C for 1 hour. After completion of the incubation step, the plates were washed thoroughly with PBST and goat anti-mouse IgG Fc specific HRPO conjugate (1:25,000) was added to each well (100 µl/well) and incubated for 1 hour at 37°C. The unbound secondary antibody was removed by washing with PBST and 3, 3', 5, 5'-Tetramethylbenzidine (TMB) with H_2O_2 (0.03% v/v) was added to the wells as a

chromogenic substrate. The reaction was stopped after 10 minutes with 1.25M sulfuric acid. Absorbance was recorded at 450 nm using ELISA plate reader (Molecular Devices).

Purification of mAbs by Affinity chromatography: The mAbs were affinity purified employing Protein G Sepharose™ 4 Fast Flow as per manufacturer's recommendations. All the buffers required for the purification were prepared and filtered using 0.45 µm bottle top filter units and stored at 2-8°C until use. Briefly, the resin was packed into a suitable column (XK 16/20) and equilibrated with 5-10 column volumes of 10mM Tris, pH 7.5 (Buffer A) at a flow rate of 2 ml/ minute. The filtered TCF was prediluted with the equilibration buffer, maintained on ice bath and passed through the resin at a flow rate of 1ml/ minute to ensure higher residence time and a maximum binding of the IgG to the resin. The unbound proteins were washed with 5-10 column volumes of Buffer A at a flow rate of 2 ml/minute. The bound mAbs were eluted in small fraction volumes of 10 ml using 5-10 column volumes of 0.1M Glycine, pH 2.5-3.0 (Buffer B) at a flow rate of 1ml/minute. The eluted fractions were neutralized with 1M Tris, pH 9.0 by adding 1/10th volume of the fraction. The eluted fractions were analyzed by SDS-PAGE and immunoblotting. Elution fractions containing the MAb were pooled and dialyzed against PBS, and were concentrated using PEG-4000. The protein concentration was estimated by bicinchoninic acid (BCA) method. The sample was stored at 20 °C till further analysis.

Immunoblot analysis of purified mAbs with diphtheria toxin: SDS-PAGE was performed as previously described (20). Diphtheria toxin(10µg) were loaded onto a 12% sodium dodecyl sulphate polyacrylamide gel electrophoresis under denaturing conditions. The proteins were electrophoretically transferred onto polyvinylidene fluoride (PVDF) membrane (Immobilon-P, Millipore) using standard techniques. Western blot analysis of diphtheria toxin using purified monoclonal antibodies was performed as described (21). The unbound active surfaces of the PVDF membrane were blocked with 5% (w/v) skimmed milk powder in PBST at 37 °C for 2 hours. The membrane was washed and incubated with the purified mAbs at 37 °C for 2 hours. After incubation, membrane was washed and incubated with anti- mouse IgG HRPO conjugate (1:10,000) (Sigma-Aldrich) at 37 °C for 1 hour. The reaction was visualized with diaminobenzidine tetra hydrochloride (DAB) (Sigma- Aldrich) chromogen.

Binding specificity of mAbs toward unrelated antigens by Indirect ELISA: *Clostridium septicum*, *Clostridium perfringens* type B, *Clostridium perfringens* type D and *Clostridium sordelli* toxin were dissolved in carbonate bicarbonate buffer (0.1 M), pH 9.6, at a final concentration of 5 µg/ml respectively and subsequently, 100 µl of each antigen was coated in respective wells in Maxisorp 96-well micro titer plates. These plates were incubated overnight at 4°C. The wells were washed thrice with PBST to remove any unbound antigen and the remaining active surfaces in the wells were blocked with 2% (w/v) skimmed milk powder in PBST for 1 hour at 37°C. The plates were again washed with PBST and respective purified antibodies, negative controls (PBST, unimmunized mouse serum, myeloma culture fluid) and the positive control (immunized mouse serum) were added to respective wells and incubated at 37°C for 1 hour. After completion of the incubation step, the plates were washed thoroughly with PBST and goat anti-mouse IgG Fc specific HRPO conjugate (1:25,000) was added to each well (100 µl/well) and incubated for 1 hour at 37°C. The unbound secondary antibody was removed by washing with PBST and TMB substrate was added to the wells. The reaction was stopped after 10 minutes with 1.25M sulfuric acid and absorbance was recorded at 450 nm using an ELISA plate reader (Molecular Devices).

Isotyping of mAbs: Isotyping analysis of the mAbs was performed to identify the monoclonality of the clones using isostrip method as per the manufacturer's instructions (Roche, Germany). Briefly, 150 µl of MAb culture supernatant was added into individual tubes with colored latex beads and agitated. The isostrips were positioned

in each tube for 5 minutes and then observed for the blue bands at the places indicated for light chain type and different sub-classes of heavy chain.

Biotinylation of mAbs: Antibodies were biotin labeled as previously described (22). Briefly, mAbs were dialyzed against 0.1 M Sodium bi carbonate buffer and incubated overnight at 4°C. Biotin solution (EZ-Link™Sulfo-NHS-SS-Biotin) was added to each antibody as per manufacturer instructions. The mixtures were incubated at room temperature for 1 hour and dialyzed against PBS to remove free biotin. Biotinylated mAbs were aliquoted and stored at - 20°C for further studies.

Competitive ELISA: Competitive ELISA was performed to identify the antibodies binding to the same epitope by an indirect ELISA. Diphtheria toxoid was dissolved in carbonate bicarbonate buffer (0.1 M), pH 9.6, at a concentration of 5 µg/ml and coated at 100 µl/well in Maxisorp 96 well microtiter plates. After overnight incubation at 4°C and subsequent blocking with 2% (w/v) skimmed milk powder in PBST for 1 hour at 37°C, equal volumes of purified antibodies (native and biotin conjugated) were added to respective wells and incubated for 1 hour at 37°C. After completion of the incubation step, these plates were washed thoroughly with PBST and streptavidin HRPO conjugate (1:25,000) was added to each well and incubated for 1 hour at 37°C and finally the reaction was developed using TMB substrate. The reaction was stopped after 10 minutes with 1.25M sulfuric acid. Absorbance was recorded at 450 nm using an ELISA plate reader (Molecular Devices).

Determination of sub fragments of diphtheria toxin: To determine the binding of mAbs to sub fragments of diphtheria toxin by western blot analysis.Diphtheria toxin (10 µg) was treated with 50 µg/ml of trypsin and incubated at 25°C for 30 minutes. Dithiothreitol (DTT) of 0.1 M solution was added to the mixture and further incubated at 37°C for 90 minutes (23).

Quantification of diphtheria toxoid by Immunocapture ELISA: Quantification of diphtheria toxoid was performed by immunocapture ELISA. MAb 2C4.1C was dissolved in carbonate bicarbonate buffer (0.1 M), pH 9.6, at a final concentration of 5 µg/ml respectively. Subsequently, 50 µl of each antibody was coated in respective wells in Maxisorp 96-well micro titer plates. The wells were washed thrice with PBS containing 0.05% (v/v) Tween-20 (PBST) to remove any unbound antibody and the remaining active surfaces in the wells were blocked with 2% (w/v) skimmed milk powder in PBST for 1 hour at 37°C. Diphtheria toxoid was dissolved in PBS at a final concentration of 5 µg/ml respectively. Subsequently, 100 µl of each antigen was added in respective wells in micro titer plates. These plates were incubated at 37°C for 1 hour. The wells were washed thrice with PBST to remove any unbound antigen and the remaining active surfaces in the wells were detected with biotinylated MAb 3B5.1C dissolved in PBST were added to respective wells and incubated at 37°C for 1 hour. After completion of the incubation step, the plates were washed thoroughly with PBST and streptavidin HRPO conjugate (1:10,000) was added to each well (100 µl/well) and incubated for 1 hour at 37°C. The unbound avidin was removed by washing with PBST and TMB substrate was added to the wells. The reaction was stopped after 10 minutes with 1.25M sulfuric acid and absorbance was recorded at 450 nm using ELISA plate reader (Molecular Devices).

Determination of cytotoxic dose of diphtheria toxin: To determine the cytotoxic dose on Vero cells the assay was performed according to the method described (24). Briefly, diphtheria toxin (1 Lf/ml) was added to 96 well tissue culture plate and serially diluted in Dulbecco's modified Eagles medium (DMEM). A suspension of Vero cells were prepared in complete medium with approximately 2×10^5 cells/ml, 2.5×10^5 cells/ml and 3×10^5 cells/ml and 50 µl of each cell suspension was added to the wells of three micro titer plates respectively. The plates were incubated at 37°C in the presence of 5% CO_2 for 96 hours. The cytotoxic effect was observed under inverted microscope. Cell debris was removed by washing the wells with PBS for three times. Crystal violet

Vol. 12 (4) 318-333, October 2018, ISSN 0973-8916 (Print), 2230-7303 (Online)

dye (0.03%) was added to each well and incubated the plate at room temperature for 40 minutes. Subsequently, post washing the stained cells were eluted from the wells by adding 70% ethanol (200 µl/well) and incubated at room temperature for 20 minutes. The absorbance of the eluted cells was measured at 595 nm using an ELISA plate reader (Molecular Devices).

In vitro neutralization assay: Neutralizing ability of selected mAbs was evaluated by cytotoxicity assay. Briefly, 1µg of purified MAb was serially diluted (50µl/well) then diphtheria toxin 0.062 Lf/ml (cytotoxic dose) was added in 1:1 ratio. Plates were incubated at 37°C for 1 hour. Vero cells were added to each well at a density of 2.5 x 10^5 cells/ml and incubated at 37°C in 5% CO_2 for 96 hours. The cytotoxic effect was observed under inverted microscope. The cell debris was removed by washing the cells with PBS for three times. The crystal violet dye (0.03%) was added to each well and incubated the plate at room temperature for 40 minutes. Subsequently, post washing the stained cells were eluted from the wells by adding 70% ethanol (200 µl/well) and incubated at room temperature for 20 minutes. The absorbance of the eluted cells was measured at 595 nm.

Receptor-blocking ELISA:ELISA plates were coated with 1 µg/ml (100 µl/well) of recombinant human Heparin binding epidermal growth factor (rhHB-EGF, R&D Systems), and incubated overnight at 4°C. 1 Lf/ml of diphtheria toxin and different concentrations of mouse monoclonal antibodies were added in a 96-well round-bottom plate and incubated for 1 hour at 37°C. Antigen-antibody mixture was transferred to the rhHB-EGF coated ELISA plate and incubated for 1 hour at 37°C. The plates were washed thoroughly with PBST and binding activity was detected by addition of Diphtheria anti-toxin (Equine polyclonal serum, NIBSC Standard 0.01 IU/ml). Plates were incubated for 1 hour at 37°C and washed thoroughly with PBST followed by incubation with Anti-Equine IgG HRPO conjugate (1:10,000) for 1 hour at 37°C. Finally the reaction was developed using TMB substrate. The reaction was stopped after 10 minutes with 1.25M sulfuric acid. Absorbance was recorded at 450 nm using an ELISA plate reader (Molecular Devices) (25).

Results:

Development of mAbs against diphtheria toxoid: The mAbs were generated and developed from mouse hybridomas according to standard techniques, as detailed in Materials and Methods. The hybridomas were developed by fusion of spleenocytes from mouse showing good seroconversion to diphtheria toxoid by indirect ELISA, with mouse myeloma partner Sp2/mIL-6. A total of 960 clones were selected on HAT medium and screened against diphtheria toxoid

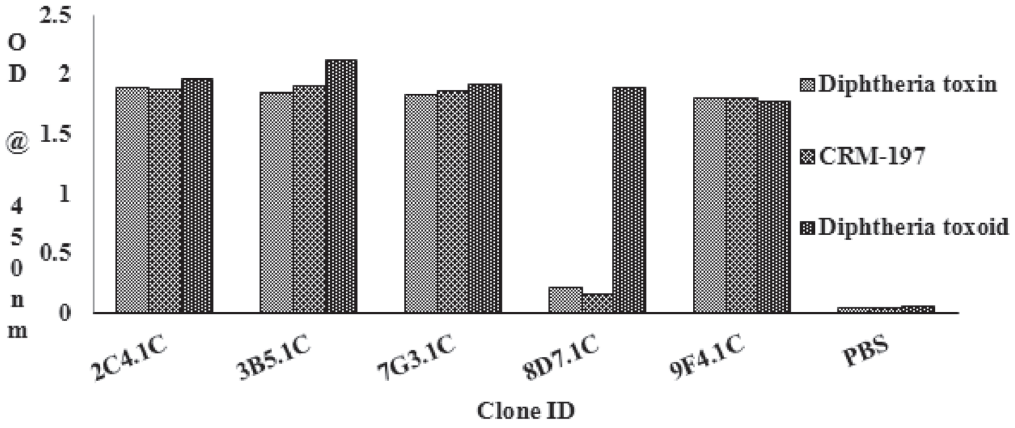

Fig. 1. Determination of cross reactive mAbs with diphtheria toxin, CRM-197 and diphtheria toxoid by indirect ELISA.

Vol. 12 (4) 318-333, October 2018, ISSN 0973-8916 (Print), 2230-7303 (Online)

by indirect ELISA. Selected five clones (2C4.1C, 3B5.1C, 7G3.1C, 8D7.1C and 9F4.1C) that shown high binding activity with diphtheria toxoid by indirect ELISA. These were cloned for three rounds of limiting dilution for the establishment of monoclonality.

Binding of mAbs to diphtheria toxoid, toxin and CRM-197 by indirect ELISA: The selected mAbs were tested for cross reactivity towards diphtheria toxin, toxoid and CRM-197. Out of five selected mAbs, four mAbs (2C4.1C, 3B5.1C, 7G3.1C, and 9F4.1C) were found to cross react with diphtheria toxin and CRM-197, while one MAb 8D7.1C showed specific binding towards diphtheria toxoid as shown in Fig. 1.

Purification of monoclonal antibodies: The matured culture supernatants of the selected clones were affinity purified by Protein-G Sepharose column (26) as discussed in Materials and methods section. The purified mAbs was analysed under 12% reduced SDS-PAGE gel which showed bands at ~50 and ~25 kDa (Fig.2). These purified mAbs were used for further studies.

Binding of mAbs with diphtheria toxin: Immunoblotting analysis of the five selected purified mAbs against diphtheria toxin revealed that 2C4.1C, 3B5.1C, 7G3.1Cand 9F4.1C showed binding to diphtheria toxin whereas 8D7.1C showed no binding (Fig. 3).

Binding of mAbs with diphtheria toxin sub fragments: Diphtheria toxin was trypsinized as mentioned in methods section and tested purified mAbs against fragments A and B of diphtheria toxin.MAbs viz. 2C4.1C, 7G3.1C and 9F4.1C recognized the subunit fragment B, whereas, 3B5.1C reacted with subunit fragment A diphtheria toxin and 8D7.1C showed no binding towards fragment A or B (Table 1).

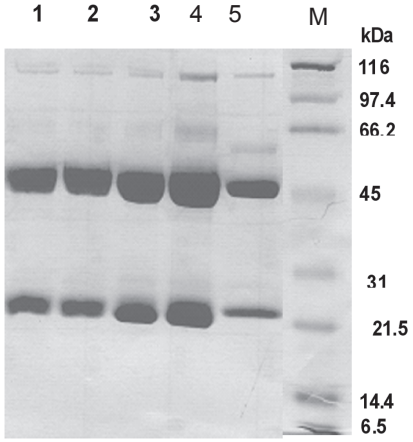

Fig. 2. Detection of purified mAbs on 12% sodium dodecyl sulfate-polyacrylamide gel electrophoresis. Lane 1 to 5 represents the mAbs 2C4.1C, 3B5.1C, 7G3.1C, 8D7.1C, 9F4.1C respectively and Lane M: protein molecular size standard.

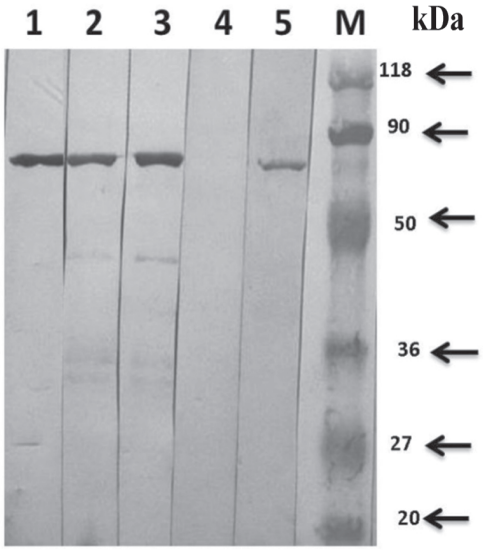

Fig. 3. Binding of mAbs against intact diphtheria toxin by western blot analysis. Lane 1 to 5 represents the mAbs 2C4.1C, 3B5.1C, 7G3.1C, 8D7.1C, 9F4.1C respectively and Lane M is molecular weight marker.

Vol. 12 (4) 318-333, October 2018, ISSN 0973-8916 (Print), 2230-7303 (Online)

S. No	Clone ID	Fragment B (37 kDa)	Fragment A (21 kDa)
1	2C4.1C	+	
2	3B5.1C	-	+
3	7G3.1C	+	
4	9F4.1C	+	
5	8D7.1C	-	-

Table. 1. Analysis of binding of mAbs against diphtheria toxin fragments A and B.

Isotype analysis of mAbs: The isotyping of the monoclones were analyzed to identify the sub-class of immunoglobulin of the antibodies. All the tested monoclones were identified as sub-class of IgG. The purified monoclonal antibodies 2C4.1C, 3B5.1C, 7G3.1C, 8D7.1C and 9F4.1C on isotyping showed that all of them were IgG_1 heavy chain with kappa light chain.

Specificity of mAbs: MAbs specificity were tested against toxin produced by different *clostridial* species (*Clostridium septicum*, *Clostridium perfringens* Type C) by indirect ELISA. Varying concentrations of the purified monoclonal antibodies (2C4.1C, 3B5.1C, 7G3.1C, 8D7.1C and 9F4.1C) were evaluated for binding against *clostridial* toxins. The mAbs did not show any cross reactivity with *clostridium* toxins as shown in Fig.4.

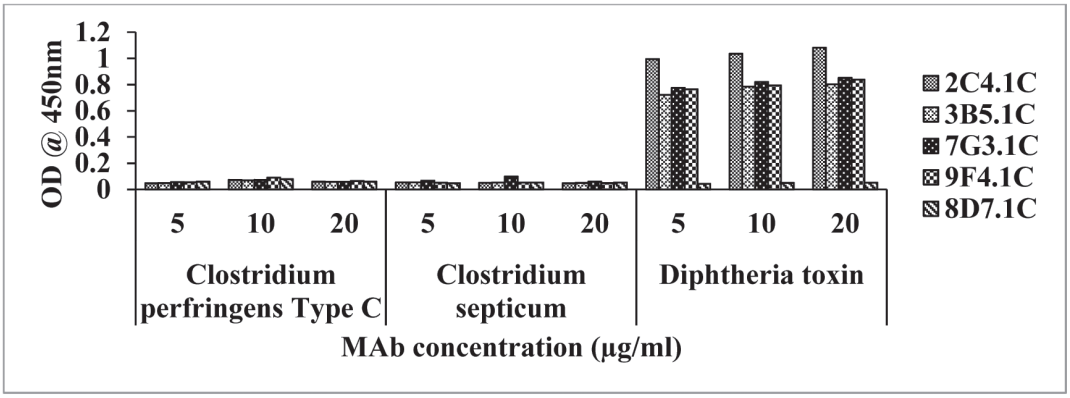

Fig. 4. Specificity of mAbs (2C4.1C, 3B5.1C, 7G3.1C, 9F4.1C and 8D7.1C) were tested against diphtheria toxin, *Clostridium septicum* and *Clostridium perfringens* Type C by Indirect ELISA.

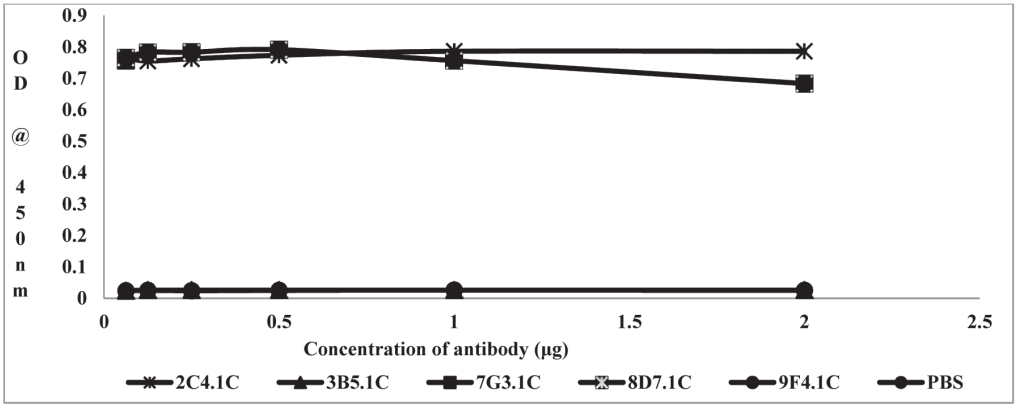

Fig. 5. Competition assay between Biotin labelled 3B5.1C and developed mAbs against diphtheria toxoid.

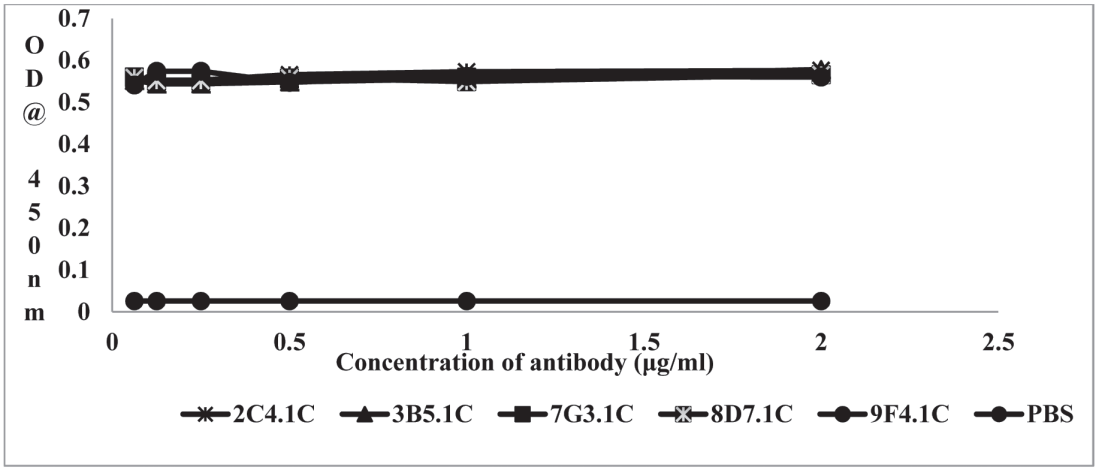

Fig. 6. Competition assay between Human mAb (16MF10, ATCC) and in house developed mAbs against diphtheria toxoid.

Competitive ELISA: The purified mAbs were tested for competition against diphtheria toxoid by a competitive ELISA (27). Purified monoclonal antibodies 2C4.1C, 3B5.1C, 7G3.1C, 8D7.1C and 9F4.1C were biotinylated as described in methods. No competition was observed between the mAbs 2C4.1C and 3B5.1C and also with the biotinylated mAb 3B5.1C .The results indicates that mAbs are binding to different epitopes on diphtheria toxoid (Fig.5). Similarly, no competition was observed between Human mAb 16M3F10.1C (ATCC) and the in house developed mAbs (Fig. 6).

Immunocapture ELISA: Immunocapture ELISA was developed to quantify the antigen in bulk diphtheria toxoid vaccine samples. Two non-competing mAbs were selected, one mAb (mAb 2C4.1C) as capture and mAb 3B5.1C which was biotinylated as an antigen detection. The optimal dilutions of the monoclonal antibodies to be used for developing a sandwich ELISA were selected based on the checker board titration calibrated with the standard antigen. The mAbs were able to quantify the diphtheria toxoid of different lots and showed a linear regression (r^2=0.99) as shown in Fig.7. The repeatability of the assay was established using six different standard concentrations, and repeated four times as per the standard qualification guidelines. The assay linearity at six different concentrations showed good curve fit and % of CV was less than 20% at each standard concentration. The recovery rate of the developed sandwich ELISA method with coefficient of variation of 5.88–16.43% indicates that the method possesses good sensitivity and provides a reliable quantitative rate (Table 2).

Cytotoxic effect of diphtheria toxin: Vero cells were seeded at the rate of 2.5 x 10^5 cells/ml were found suitable for monolayer cell sheath formation

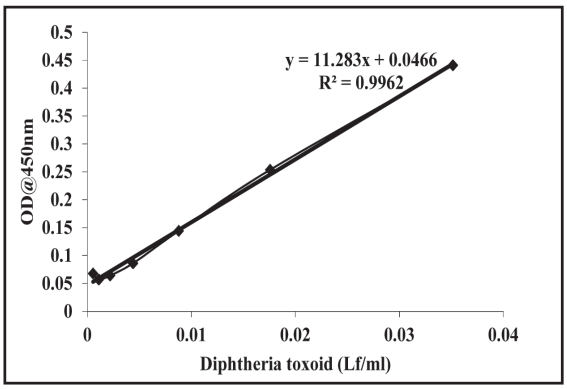

Fig. 7. Validation of sensitivity of diphtheria toxoid (Lf/ml) on Immunocapture ELISA.

Table. 2. Repeatability of the sandwich ELISA was assessed by inter-test variances of four Independent tests with five experimental blends.

S.No.	Description	Test-1	Test-2	Test-3	Test-4	Mean Lf/ml	Standard deviation	% Coefficient of variance
1	Standard	3446	3143	3130	3596	3328.75	233.47	6.9
2	Sample-A	4010	4241	3312	2760	3580.75	585.5	16.43
3	Sample-B	3724	4175	3572	3907	3844.5	225.55	5.88
4	Sample-C	3359	4030	3022	3110	3380.25	430.02	13.01
5	Sample-D	2644	3684	3368	2612	3077	518.57	16.3
6	Sample-E	3300	3860	3657	3025	3460.5	322.71	9.36

(28). Cytotoxic effect of diphtheria toxin was tested on Vero cells at varying concentrations of the toxin (Lf/ml). Results indicated that minimum cytotoxicity effect of diphtheria toxin on Vero cells was found to be 0.0625 Lf/ml as shown in Fig. 8.

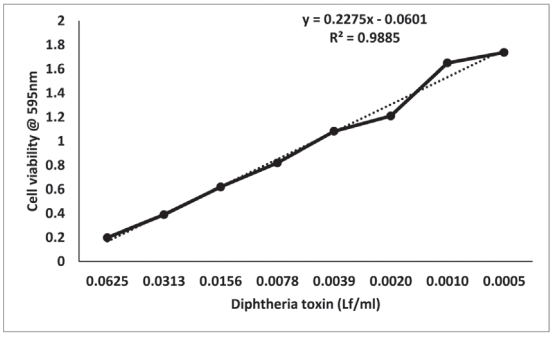

Fig. 8. Validation of sensitivity of diphtheria toxin (Lf/ml) on Vero cells assay.

In vitro neutralization assay: The purified monoclonal antibodies (2C4.1C, 3B5.1C, 7G3.1C, 8D7.1C and 9F4.1C) were tested for neutralizing activity against diphtheria toxin by cytotoxicity assay. Results revealed that mAbs 2C4.1C, 7G3.1C and 9F4.1C were able to neutralize the cytotoxic effect of diphtheria toxin in a concentration dependent manner, whereas, mAbs 3B5.1C and 8D7.1C did not neutralized the toxin (Fig. 9).

Receptor-blocking ELISA: Receptor blocking ELISA was performed to identify whether mAbs were recognizing receptor domain of diphtheria toxin and inhibit its binding to the receptor (29). The mAbs at varying concentrations were pre-incubated with 1 Lf/ ml of diphtheria toxin and then the solution was allowed to bind HB-EGF

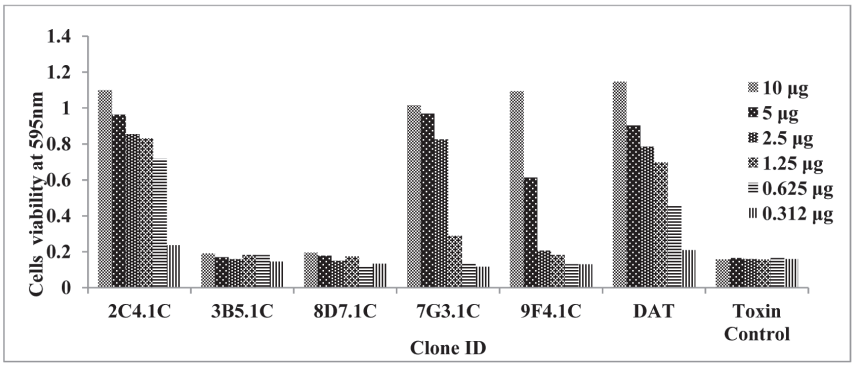

Fig. 9. Neutralizing activity of mAbs by *In vitro* Vero cell cytotoxicity assay.

Vol. 12 (4) 318-333, October 2018, ISSN 0973-8916 (Print), 2230-7303 (Online)

receptor. ELISA results indicated that mAbs 2C4.1C, 7G3.1C and 9F4.1C shown inhibition of binding of diphtheria toxin to the receptor in a concentration dependent manner, further no blocking was observed for mAbs 3B5.1C and 8D7.1C (Fig.10).

Discussion:

Diphtheria is known to be a localized infection of mucous membranes or skin caused by toxigenic strains of *Corynebacterium diphtheriae* and it is characterized by the presence of a pseudomembrane at the site of infection. A massive release of toxin into the body will cause lethal necrosis of the heart and liver.Vaccination essentially remains effective in elimination of infection, however the individuals are known to infectedby bacteria and becoming asymptomatic carriers and possibility of transmitting to others.Diphtheria anti- toxin (DAT) has been the focus for the treatment of diphtheria infection for several years. The global incidence of disease has decreased constantly though it remains endemic in many parts of the globe and resulting in outbreaks. Due to limitations in availability and shortage in supply globally, an alternative to diphtheria anti-toxin which is safe and more readily available would be desirable to meet the need of DAT. Monoclonal antibodies have the potential to replace the anti-toxin and it can circumvent the adverse effects like hypersensitivity reactions,risk of contamination due to blood derived products etc. (30). As the discovery of hybridoma technology by Kohler and Milstein (1975) brought a new dimension in the diagnosis and therapeutic usage of monoclonal antibodies for several diseases which includes in inhibition of angiogenesis, cancer treatment and as an immune suppressor after organ transplantations etc.(27,31, 32, 33). The monoclonal antibodies have many potential applications and do not depend upon the polyclonal serum. Monoclonal antibodies are more specific and sensitive when compared to the polyclonal serum. Hence monoclonal antibodies are being used in therapeutics and in development of diagnostics (34).

In the present paper, we describe the monoclonal antibody generation, expression, purification and immunological characterization of an anti-diphtheria antibodies and their application for the quantification of antigen in in-process samples during vaccine production by ELISA. Monoclonal antibodies for diphtheria toxoid have been screened for their activity by ELISA. Based

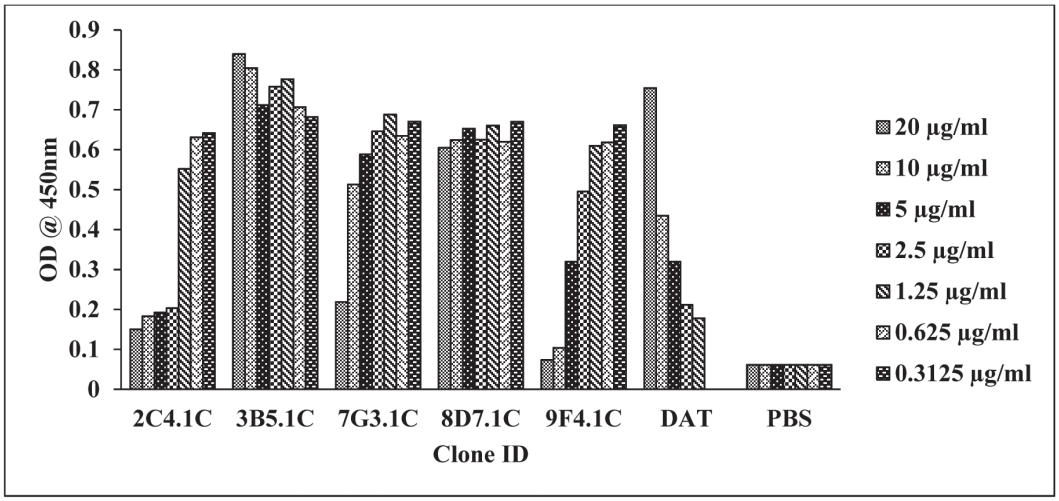

Fig. 10. Receptor binding inhibition assay of mAbs by ELISA. 2C4.1C, 7G3.1C and 9F4.1C mAbs are shown to block diphtheria receptor (HB-EGF) binding with diphtheria toxin.

Vol. 12 (4) 318-333, October 2018, ISSN 0973-8916 (Print), 2230-7303 (Online)

on the reactivity, five mAbs were selected for further studies. The lack of cross reactivity with other bacterial antigens confirmed the specificity of the mAbs for the defined antigen.Further, the mAbs did not compete with each other and with the commercial mAb as well.This indicates that both in house developed mAbs and commercial mAb bound to different epitopes on diphtheria toxoid as shown by competitive ELISA. Immunoblot analysis revealed that mAbs 2C4.1C, 7G3.1C and 9F4.1C bound to the fragment B whereas 3B5.1C bound to the fragment A (35).

Among the five mAbs developed, four mAbs were shown cross reactive to diphtheria toxin, diphtheria toxoid and CRM-197. Our results are in complete agreement with the results reported (36), where the mAbs developed against diphtheria toxoid have shown cross reactivity with CRM-197. However, one mAb 8D7.1C showed high specificity towards diphtheria toxoid and did not show cross reactivity with diphtheria toxin and CRM-197. These mAbs can be used for assessing the complete inactivation of diphtheria toxin (37). The combination of mAbs helps in determination of the vaccine quality i.e.,one mAb that binds to diphtheria toxoid but not toxin (8D7.1C) while other detect both toxin and toxoid which can be used as a positive control (2C4.1C, 3B5.1C 7G3.1C and 9F4.1C) during inactivation process. Isotyping analysis demonstrated that, the developed clone belongs to IgG1 heavy chain and Kappa light chain isotype.

Diphtheria toxoid vaccination has been included as a part of the regular national vaccination program (38). The production of diphtheria toxoid is relatively easier but to ensure consistency of batches and to maintain appropriate quality is found to be critical. Diphtheria toxoid is not a well-defined biological agent and routine testing requires both in vitro and in vivo assays (39). In vitro testing would be more beneficial as it helps in reduction and replacement of animal usage for batch release criteria. However this assay needs to be validated and correlated well with in vivo assays (40). During the process of vaccine development, it is essential to establish vaccine characteristics as good quality and protective levels of antigen in the batches (41).

Quantification of antigen is essential for blending of antigen in vaccine batches, and these quantifications are being performed through the ELISA based methods (42).The mAbs developed were used in the development of an in-house ELISA for the quantification of antigen in in-process samples during manufacture of vaccine. The ELISA showed a perfect linear fit with R^2 value of >0.98.Quantitation of diphtheria toxoid antigen in vaccine preparations using mAbs offers a cheap, simple and convenient way of estimation of antigen by immunocapture ELISA without the loss of antigen (43).Similar antigen assays utilizing antibodies to capture and quantify tetanus toxoid have been described (44,45) and their value for quality control testing continues to be explored (46).

Diphtheria pathogenicity is caused by binding to the R domain of diphtheria toxin B-sub unit to the cell receptor (47, 48). Blocking or interfering with R region plays a significant role in preventing diphtheria toxin to bind to the cells. Three of the mAbs in our study recognized fragment B and thus further studies to evaluate their neutralization potential in an *in vitro* neutralization assay were studied as described earlier (15). Indeed, the neutralization test using cell culture as an alternative to *in vivo* method were also recommended by World Health organization (WHO) and the European Pharmacopoeia to reduce the animal usage (49). These *in vitro* assays are found to be specific and sensitive when compared to the conventional methods like flocculation test and neutralization test performed in rabbits and guinea pigs. Though the animal neutralization test considered as the golden standardand it involves cumbersome and limitations for large scale screening and ethical reasons (50).The mAbs were tested for neutralizing capability using Vero cell based assay (51). MAbs 2C4.1C, 7G3.1C and 9F4.1C were found to exhibit neutralization potential and competed with almost same degree of DAT blocking diphtheria toxin to the cells (52). This

was further substantiated when preincubation of mAbs with Vero cells also inhibited the toxicity of diphtheria toxin suggesting the blocking of diphtheria toxin binding to the receptor by mAbs (53).

Furthermore the receptor blocking ELISA reaffirmed the binding of mAbs (2C4.1C, 7G3.1C and 9F4.1C) to HB-EGF receptor. On the contrary, 3B5.1C (specific to fragment A of toxin) and 8D7.1C (specific to diphtheria toxoid) were unable to inhibit the diphtheria toxin activity as expected.

Conclusion:

Diphtheria was an infectious disease and spread worldwide even in the vaccination era. There are several reports where the disease was more susceptible to children and adults. Disease can be treated with antibiotics along with the antibiotics and diphtheria polyclonal produced in Equine. Due to the low production of diphtheria anti-toxin, monoclonal antibodies can act as an alternate for treatment of disease. Developed monoclonal antibodies are capable for neutralizing and in quantification of diphtheria toxoid. The epitope mapping of the mAbs to be further established. These antibodies needs to be further characterized for a possible application in the development of therapeutics and diagnostics.

Abbreviations:

mAbs, monoclonal antibodies; CRM -197, Cross reactive material, a non-toxic mutant of diphtheria toxin; IC-ELISA, immune capture Enzyme linked immunosorbent assay; FBS, fetal bovine serum; PAGE, polyacrylamide gel electrophoresis; WHO,World Health Organization.

References:

1. Coyle, M. B., and Lipsky, B. A. (1990). Coryneform bacteria in infectious diseases: Clinical and laboratory aspects. Clin Microbial Rev, 3(3): 227-246.

2. Uchida, T., Gill, D, M. and Pappenheimer Jr. A. M. (1971). Mutation in the structural gene for diphtheria toxin carried by temperate phage. Nat New Biol,233(35): 8-11

3. Stratton, K. R., Howe, C. J. and Johnston, R. B. Jr. (1994). Adverse events associated with childhood vaccines other than pertussis and rubella. Summary of a report from the Institute of Medicine. JAMA, 271(20): 1602-1605.

4. Drazin, R., Kandel, J. and Collier, R. J. (1971). Structure and activity of diphtheria toxin. II. Attack by trypsin at a specific site within the intact molecule. J Biol Chem, 246:1504-1510.

5. Galazka, A. (2000). The changing epidemiology of diphtheria in the vaccine era. J Infect Dis, 181 (1):S2-9.

6. Gidding, H. F., Burgess, M. A. and Gilbert, G. L. (2000). Diphtheria in Australia, recent trends and future prevention strategies. Commun Dis Intell, 24(6):165-167.

7. Chitkara, A., ShyamKukreja, J., Raju, C. and Shah.(2008). Pertussis and Diphtheria Immunization. Indian Pediatrics, 45:723-727.

8. WHO. Manual or Quality control of diphtheria, tetanus and pertussis vaccines, WHO/IVB/11.11, 2013; 54-59.

9. Olga, R., Povitzky., Minnie Eisner. and Erla Jackson. (1933). Effectiveness of Standard Diphtheria Antitoxin against All Types of Diphtheria Infection. J Infect Dis, 52(2):246-252.

10. Stiehm, E, R.(2013). Adverse effects of human immunoglobulin therapy. Transfus. Med Rev, 27(3):171-178.

11. Both, L., Banyard, A, C., van Dolleweerd, C., Wright, E., Ma, J, K. and Fooks, A, R. (2013). Monoclonal antibodies for prophylactic and therapeutic use against viral infections. Vaccine, 31:1553-1559.

12. Sgouris, J. T., Volk, V. K., Angela, F., Portwood, L. and Gottshall, R. Y.(1969). Studies on diphtheria immune globulin

prepared from outdated human blood. Vox Sang, 16: 491–495.

13. Galazka, A, M. (1993). Expanded programme on immunization: the immunological basis for immunization. Module 2: diphtheria. WHO document WHO/ EPI/GEN/93.12. World Health Organization, Geneva, Switzerland.

14. Both, L., White, J., Mandal, S., Efstratiou, A. (2014). Access to diphtheria antitoxin for therapy and diagnostics. Euro. Surveill, 19(24): 20830.

15. Hendriksen, C, F. (2009). Replacement, reduction and refinement alternatives to animal use in vaccine potency measurement. Expert. Rev. Vaccines, 8(3):313-322.

16. Metz, B., Jiskoot, W., Hennink, W. E., Crommelin, D. J. and Kersten, G. F. (2003). Physicochemical and immunochemical techniques predict the quality of diphtheria toxoid vaccines. Vaccine, 22(2): 156-167.

17. Winsnes, R., Sesardic, D., Daas, A. and Behr-Gross, M. E. (2004). Collaborative study for the validation of serological methods for potency testing of diphtheria toxoid vaccines-part 1. Pharmeuropa. Bio, 2003(2): 35-68.

18. Waldmann, T, A. (1991). Monoclonal antibodies in diagnosis and therapy. Science, 252(5013): 1657-1662.

19. Kohler, G. and Milstein, C. (1975). Continuous cultures of fused cells secreting antibody of predefined specificity. Nature, 256:495-497.

20. Laemmli. (1970). Cleavage of structural proteins during the assembly of the head of bacteriophage T4. Nature, 227: 680-685.

21. Towbin, H., Staehelin, T., and Gordon, J. (1979). Electrophoretic transfer of proteins from polyacrylamide gels to nitrocellulose sheets: procedures and some applications. Proc. Natl. Acad. Sci, 76:4350-4354.

22. Rolf, J, M. and Eidels, L. (1993). Structure-function analyses of diphtheria toxin by use of monoclonal antibodies. Infect. Immun, 61:994-1003.

23. Suwanthim, K., Pootong, A., Chaisri, U., Tongtawe, P. and Tapchaisri, P. (2008). Murine Monoclonal Antibodies Neutralizing the Cytotoxic Activity of Diphtheria Toxin. Asian. Pac. J. Allergy. Immunol, 26:47-55.

24. Miyamura, K., Nishio, S., Ito, A., Murata, R.and Kono, R. (1974). Micro cell culture method for determination of diphtheria toxin and antitoxin titres using VERO cells. I. Studies on factors affecting the toxin and antitoxin titration. J. Biol. Stand, 2:189-201.

25. Sevigny, L. M., Booth, B. J., Rowley, K. J., Leav, B. A., Cheslock, P. S. and Garrity, K. A., et al.(2013). Identification of a Human Monoclonal Antibody to Replace Equine Diphtheria Anti-toxin for the Treatment of Diphtheria Intoxication. Infect. Immun. 81(11): 3992-4000.

26. Harlow E. and Lane, D. (1988). Antibodies-A Laboratory Manual. Cold Spring Harbor Laboratories, New York.

27. Yalow, R, S. and Berson, S, A. (1996). Immunoassay of endogenous plasma insulin in man. Obes Res, 4(6):583-600.

28. Kumar, S., Kanwar, S., Bansal, V. and Sehgal, R. (2009). Standardization and validation of Vero cell assay for potency estimation of diphtheria antitoxin serum. Biologicals, 37(5): 297-305.

29. Gretch, D. R., Suter, M. and Stinski, M. F. (1987). The use of biotinylated monoclonal antibodies and streptavidin affinity chromatography to isolate herpes virus hydrophobic proteins or glycoproteins. Anal. Biochem, 163(1):270-277.

30. Huygen, K. (2016). Development of human monoclonal antibodies to diphtheria toxin:

A solution for the increasing lack of equine DAT for therapeutic use. Virulence, 7:613-615.

31. Koch, M., Niemeyer, G., Patel, I., Light, S. and Nashan, B.(2002). Pharmacokinetics, pharmacodynamics, and immunodynamics of daclizumab in a two-dose regimen in liver transplantation. Transplantation, 73: 1640-1646.

32. Byrd, J. C., Murphy, T., Howard, R. S., Lucas, M. S., Goodrich, A., Park, K., Pearson, M., Waselenko, J. K., Ling, G., Grever, M. R., Grillo-Lopez, A. J., Rosenberg, J., Kunkel, L. and Flinn, I. W.(2001). Rituximab using a thrice weekly dosing schedule in B-cell chronic lymphocytic leukemia and small lymphocytic lymphoma demonstrates clinical activity and acceptable toxicity. J Clin Oncol, 19(8):2153-2164.

33. Sparano, J. A., Gray, R., Giantonio, B., O'Dwyer, P.and Comis, R. L. (2004). Eastern Cooperative Oncology Group Portfolio of Clinical Trials. Evaluating antiangiogenics agents in the clinic: the Eastern Cooperative Oncology Group Portfolio of Clinical Trials. Clin Cancer Res, 10(4): 1206-1211.

34. Thirumeni Nagarajan., Wilfred, E., Marissen Charles. and Rupprecht, E. (2014). Monoclonal antibodies for the prevention of rabies: theory and clinical practice, Antibody Technology Journal, 4: 1–12.

35. Efstratiou, A., Engler, K. H., Dawes, C. S.and Sesardic, D.(1998). Comparison of phenotypic and genotypic methods for the detection of diphtheria toxin among isolates of pathogenic corynebacteria. J Clin Microbiol, 36:3173– 3177.

36. Bigio, M., Rossi, R., Nucci, D., Antoni, G., Rappuoli, R. and Ratti, G.(1987). Conformational changes in diphtheria toxoids. Analysis with monoclonal antibodies. FEBS. Lett, 218: 271-276.

37. Hallas, G., Harrison, T, G., Samuel, D. and Colman, G. (1990). Detection of diphtheria toxin in culture supernates of Corynebacterium diphtheriae and C. ulcerans by immunoassay with monoclonal antibody. J Med Microbiol, 32:247–253.

38. Galazka, A., Susan, E., and Robertson. (1995). Diphtheria: Changing patterns in the developing world and the industrialized world, European. Journal of Epidemiology, 11:107-117.

39. Kersten, G., Jiskoot, W., Hazendonk, T., Spiekstra, A., Westdijk, J. and Beuvery, C.(1999). Characterization of diphtheria toxoid. Pharm. Pharmacol Commun, 5: 27–31.

40. Hendriksen, C., Spieser, J. M., Akkermans, A., Balls, M., Bruckner, L., Cussler, K., Daas, A., Descamp, J., Dobbelaer, R., Fentem, J., Halder, M., Van der Kamp, M., Lucken, R., Milstien, J., Sesardic, D., Straughan, D. and Valadares, A. (1998).Validation of alternative methods for the potency testing of vaccines. The Report and Recommendations of ECVAM Workshop 31. ATLA, 26: 747-761.

41. Griffiths, E. (1996). Assuring the quality of vaccines. Regulatory requirements for licensing and batch release. Methods in Molecular Medicine. Vaccine [10], Protocols. Totowa, NJ: Humana Press ,269–288

42. Engler, K. H., Efstratiou, A., Norn, D., Kozlov, R. S., Selga, I.and Glushkevich, T. G. (2002). Immunochromatographic strip test for rapid detection of diphtheria toxin: description and multicenter evaluation in areas of low and high prevalence of diphtheria. J Clin Microbial, 40: 80-83.

43. Metz, B., Jiskoot, W., Mekkes, D., Kingma, R., Hennink, W.E., Crommelin, D.J.A. and Kersten, G.F.A.(2007b). Quality control of

routine, experimental and real- time aged diphtheria toxoids by in vitro analytical techniques. Vaccine. 25, 6863-6871.

44. Prieur, S., Broc, S., Gal, M., Poirier, B. and Fuchs, F.(2002). Development of an in vitro potency test for tetanus vaccines. Dev Biol (Basel), 111: 37-46.

45. Xing, D.K.L., McLellan, K., Corbel, M.J. and Sesardic, D.(1996). Estimation of antigenic tetanus toxoid extracted from biodegradable microspheres. Biologicals, 24: 57-65.

46. Coombes, L., Stickings, P., Tierney, R., Rigsby, P. and Sesardic, D. (2009). Development and use of a novel in vitro assay for testing of diphtheria toxoid in combination vaccines. J Immunol Methods, 350: 142.

47. Naglich, J. G., Matherall, J. E., Russel, D. W. Q. and Eidels, L. (1992). Expression cloning of a diphtheria toxin receptor: identity with a hairpin-binding EGF-like growth factor precursor. Cell, 69:1051-1061.

48. Mitamura, T., Iwamoto, R., Umata, T., Yomo, T., Urabe, I., Tsuneoka, M. and Mekada, E. J. (1992). The 27-kD diphtheria toxin - receptor associated protein (DRAP27) from Vero cell is the monkey homologue of human CD9 antigen: expression of DRAP27 elevates the number of diphtheria toxin receptors on toxin sensitive cells. Cell Biol, 118:1389-1399.

49. Paolo Di Giovine., Antonella Pinto., Rose-Marie Ölander., Dorothea Sesardic., Paul Stickings., Guy Berbers., Shona Neal., AndroullaEfstratiou., RutaPaberza., SnieguoleDauksiene., Marina Bujko., AntoanetaDetcheva., Unna Joks., BelkisLevent. and Christina von Hunolstein. (2010). External Quality Assessment for the Determination of Diphtheria Antitoxin in Human Serum. Clin Vaccine Immunol, 17(8): 1282-1290.

50. Leenaars, P. P. A. M., Kersten, G. F. A., de Bruijn, M. L. H. and Hendriksen, C. F. M.(2001). An in vitro approach in quality control of toxoid vaccines. Vaccine, 19:2729-2733.

51. WHO, 1997.Vero cell method for testing the potency of diphtheria toxoids. Pact 3. In: Manual of laboratory methods. Geneva: WHO; WHO/VSQ/97.04.

52. Wahby, A. I. N., El-kady, E. and Hamdi, M.(1998). Determination of antibodies to the fragments A and B of diphtheria toxin. Egypt J Immunol, 6:41-48.

53. Gilliland, D. G., Steplewski, Z., Collier, R. J., Mitchell, K. F., Chang, T. H.and Koprowski, H. (1980). Antibody-directed cytotoxic agents: use of monoclonal antibody to direct the action of toxin A chains to colorectal carcinoma cells. Proc Natl Acad Sci, 77(8):4539-4543.

Current Trends in Biotechnology and Pharmacy
Vol. 12 (4) 334-341, October 2018, ISSN 0973-8916 (Print), 2230-7303 (Online)

Purification of Foot and mouth disease virus non-structural protein 3ABC from vaccine in-process samples and their characterization

Anil Kumar Jangam[1], Sridevi V Nimmagadda[1] , Premalatha Dasari[†] and Rajendra Lingala [1*]

[1]Indian Immunologicals Limited, Rakshapuram, Gachibowli, Hyderabad- 500032, Telangana, India.
[†]Department of Biotechnology, Jawaharlal Nehru Technological University, Kukatpally, Hyderabad- 500085
*Corresponding author - Email: rajendra.lingala@indimmune.com

Abstract

Foot and mouth disease is a highly contagious disease that affects the cloven hoofed animals which includes livestock and can impact on nation's economy. Adjuvanted inactivated whole virus (140s) is used as vaccine to protect animals and control the disease. The vaccine production process is well established by many commercial manufacturers by culturing the virus on BHK cell line. The development of vaccine requires partial purification of the antigen batches to eliminate unwanted proteins along with virus non structural protein 3ABC to claim as a marker vaccine in differentiating vaccinated from infected animals (DIVA) and also to improve the quality of the vaccine thus enhancing the levels of protection. In the current study, we have shown the process of eliminating 3ABC protein from the antigen batches by size exclusion chromatography using Sephacryl S-400 and Toyopearl HW 65F columns. We have demonstrated the removal of 3ABC protein in various antigen batches of FMDV Serotype O by each of the above chromatographic media and quantifying the 3ABC protein by ELISA during the chromatographic process.The process involving the treatment of sample with the buffer containing Triton X -100 has shown a minimum NSP levels in the final antigen purified by both the chromatographic media. We also suggest that the method could also be applied for other serotypes of FMDV. The present method has the potential for a large scale production of marker vaccine which can be used in differentiating vaccinated from infected animals (DIVA).

Keywords: FMDV, NSP, Chromatography, ELISA.

Introduction

FMDV is a highly contagious disease affecting the domestic and wild cloven hoofed animals like sheep, cattle, goat, pig, deer, bison etc. It is causing severe economic loss to the developing countries, as majority of them are farming animals contributing to the nation's economical integrity. The virus belongs to the genus Apthovirus and family *picornaviridae*. It is prevalent and confined to a specific region with seven serotypes viz. Type O, A, C, Asia-1, SAT-1, SAT-2 and SAT-3 (1) and the spread of the disease can be prevented by vaccination.Till date the vaccine produced against FMD is a cell cultured derived and an inactivated whole virus.The potency of inactivated virus vaccines that are routinely used as a part of elimination of the disease are majorly dependent on virus integrity (2 and 3).

Vol. 12 (4) 334-341, October 2018, ISSN 0973-8916 (Print), 2230-7303 (Online)

The virus is a non-enveloped, icosahedral symmetry with 30nm diameter and composed of 60 copies of four structural proteins (VP3, VP1, VP4 and VP2) and a copy each of non-structural proteins L, 2A, 2B, 2C, 3A, 3C, 3D and three copies of 3B with their precursor forms 2AB, 3AB and 3ABC (4, 5, 6 and 7). Vaccine component against FMD is the inactivated intact whole virus, 140s particle with a molecular weight of 8200 KDa (8).The sucrose based density gradient fractionation method was considered as gold standard for the quantification of virus and determining the vaccine payload (9). Vaccine payload is determined by the quantity of the virus required to protect the animals from infection (10). Countries like India, endemic to the disease have national mass vaccination program to prevent and eliminate the disease. For a successful vaccination program and to export the vaccine to the FMD free countries, it is required to have a protective low dose PD_{50} value and the presence of lower NSPs (Non - Structural Proteins) level in the vaccine (11). Among NSPs, 3ABC is most immune dominant and hence can be used as the marker protein in differentiating infected from affected animals (DIVA) (12). The unavailability of a consistent method to estimate the active component present in vaccines is a vital factor to sustain the cost and to replace the complex tests that are involving the usage of large animals as a batch release criteria.

The chromatographic techniques are the traditional and conventional process being used in separation of the bio macromolecules (11). Advancement in the column chromatography has allowed the purification of diversified class of biomolecules including viruses in less time. There are evidences for purification and quantification of viruses based on ion exchange chromatography (12, 13, 14 and 15) and affinity chromatography (16, 17 and 18). FMDV has been purified and quantified by affinity chromatography (19) and receptor ligand binding of FMDV has been studied extensively (20). The virus can also be quantified using Size exclusion chromatography (SEC) as described by Yang, 2015 (21). To date preparative columns with pore size of stationary phase above 100 nm are commercially available, making it possible to analyze most of large molecules within the range of 10–100 nm. Moreover, SEC requires a mild operation unlike ion exchange or hydrophobic chromatography, wherein latter case there could be strong interaction between the antigen and the chromatographic media. Such a strong interaction may break up the virus integrity. As reported earlier, FMDV was quantified by SEC from clarified harvested virus culture in serum free media (22).

In the present study, we demonstrated the process of eliminating the virus non-structural proteins (NSPs) from the FMD inactivated and concentrated vaccine antigen batches by the application of size exclusion chromatography technique that has the potential to act as a marker vaccine in differentiating vaccinated from infected animals (DIVA). The presence of NSPs at various stages of purification is done by detecting and quantifying 3ABC protein.

Materials and Methods:

FMDV vaccine strain of serotype O was cultured on BHK cell line with MEM (Hi Media GmbH, Germany) containing 1% adult bovine serum (GIBCO, USA).The harvested virus was inactivated and concentrated using 500 KDa cut-off Hydrosart ultra-filtration cassettes (Sartorius stedim, USA), Ribonuclease A (Sigma, R 4875-100 mg), Hiprep Sephacryl S – 400 HR 16/60 (GE Healthcare, USA), Toyopearl HW65F(Tosoh biosciences, Japan) packed in XK 16/70 column (GE Healthcare, USA), Gradient maker (BIO-RAD, USA) and all other inorganic chemicals were procured from Merck, USA.

Preparation of Sample: The harvest and concentrated vaccine antigen batches of serotype O were centrifuged at 8000xg for 15 min and treated with equal volume of 0.25% v/v triton X 100 in 100mM Tris buffer (pH 7.6). Alternatively, the antigen were mixed with Triton X 100 with a final concentration of 0.125% v/v. The treated sample is then incubated at 4ºC for 2-3 h by gentle mixing.

Vol. 12 (4) 334-341, October 2018, ISSN 0973-8916 (Print), 2230-7303 (Online)

Size Exclusion Chromatography: The treated and untreated cultures were used for purification by column chromatography. The column was pre equilibrated with two column volumes of 50mM Tris and 150mM NaCl, pH 7.6 as mobile phase and both the virus batch preparations were incubated with 0.1% v/v of 1M RNase at room temperature (RT) for 30 min prior to loading onto the column. The sample was then loaded with 5mL loop volume (4% of total column volume) at 30cm/hour linear flow rate and a pressure limit of 0.15 MPa on Akta purifier chromatographic system (GE Healthcare, USA). The peak resolution was observed as absorbance (mAU) at 254nm with volume (mL) as baseline. The running conditions were kept similar for both the media i.e. Sephacryl S-400 and Toyopearl HW65F.

Quantification of the whole virus by Sucrose density gradient: The whole virus was quantified based on the conventional method by separating on sucrose density gradient centrifugation as described earlier (9).The excluded chromatographic fractions from the column were pooled and treated with ribonuclease A and the samples were overlaid on a 25–45% (v/v) sucrose concentration gradient prepared with a gradient maker (Model 485, BIO-RAD). The overlaid sample was centrifuged at 40000 rpm for 2 hrs. on HITACHI ultracentrifuge. Post centrifugation the fractionated gradients were scanned at 254 nm using UA-6 absorbance detectors (Teledyne Isco, USA) by pushing with 60% (v/v) sucrose solution.

Immunoblotting of the chromatographic fractions: The eluted fractions from the column chromatography samples were also analyzed by immunoblotting. The fractions along with the load sample were run on 12% denaturing polyacrylamide gels. Western blotting was done using nitrocellulose membrane (Immobilon, Amersham, USA) and probing with the bovine convalescent sera. 5% (w/v) skimmed milk (Difco, USA) in PBSA was used as blocking agent. Anti-bovine IgG conjugated with HRPO was used as secondary antibody (Sigma, USA). The blot is developed by activating the chromogen DAB substrate(3, 3'-diaminobenzidine tetrahy drochloride) with hydrogen peroxide.

Quantification of the 3ABC protein by ELISA: 3ABC content in the eluted fractions from the column chromatography were measured by in-house developed ELISA method.The 3ABC content in the sample will be captured between immobilized 3ABC specific mAb (8C4) and biotin labeled 8C4 in sandwich format. Bacterial expressed r3ABC antigen was used as the internal reference standard to estimate 3ABC content in the unknown samples.

Results:

Purification of antigen samples by Size Exclusion Chromatography:

The chromatography was carried out independently with six different antigen batches (Serotype O) in triplicates. Batch 1 and batch 2 refers to untreated ones, batch 3 and batch 4 refers to antigen batches that were treated with buffer containing Triton X100 and batch 5 batch 6 refers to the antigen batches that were directly treated with Triton X100.The chromatographs showed peak profile with a symmetrical peak corresponding to the column void volume at 42 and 52 mL when run with a volumetric flow rate of 1mL/min for Sephacryl S 400 and Toyopearl HW 65F respectively.The elution of the chromatography was collected as fractions with 2 mL each (Fig. 1-3). The fractions were then analyzed by western blot using 12% SDS- PAGE under denaturing conditions for both virus structural proteins and non-structural proteins.

Immunoblot analysis of the void volume fractions: The eluted fractions from the void volume were collected and analyzed by immunoblotting using bovine convalescent sera**.** We have pooled the eluted peak fractions into two halves prior to testing. The blot depicted the presence of band corresponding to virus structural protein VP1 at 34 KDa and no 3ABC specific band at 56 KDa detected in the fractions collected from batch 3 and 4 respectively, as shown in figure 4.

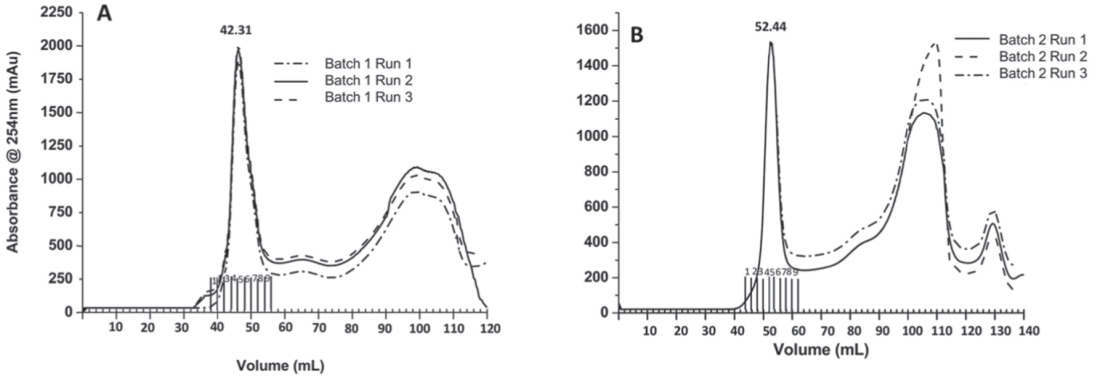

Fig. 1. Chromatogram showing three independent runs of the antigen batches loaded without treatment. A. Sephacryl S 400 and B. Toyopearl HW 65F. Note: The extended tick labels on X-axis indicates the fractions of the respective peak.

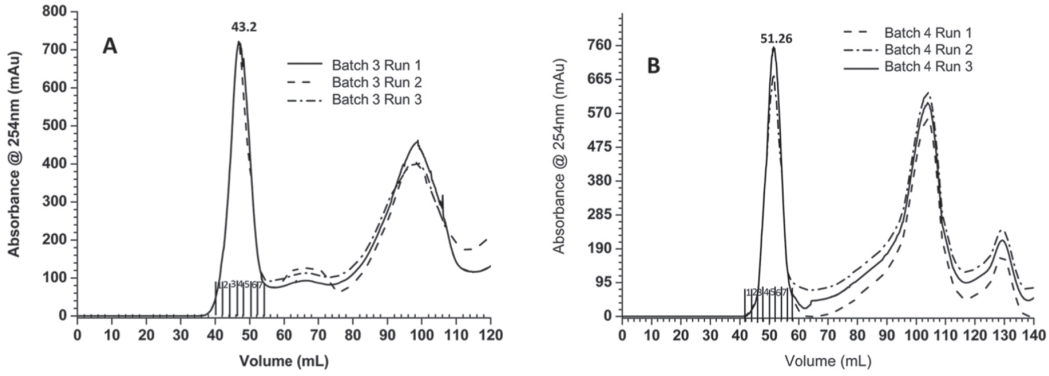

Fig. 2. Chromatogram showing three independent runs of the antigen batches loaded after treating with buffer containing 0.25% v/v Triton X 100. A. Sephacryl S 400 and B. Toyopearl HW 65F. Note: The extended tick labels on X-axis indicates the fractions of the respective peak.

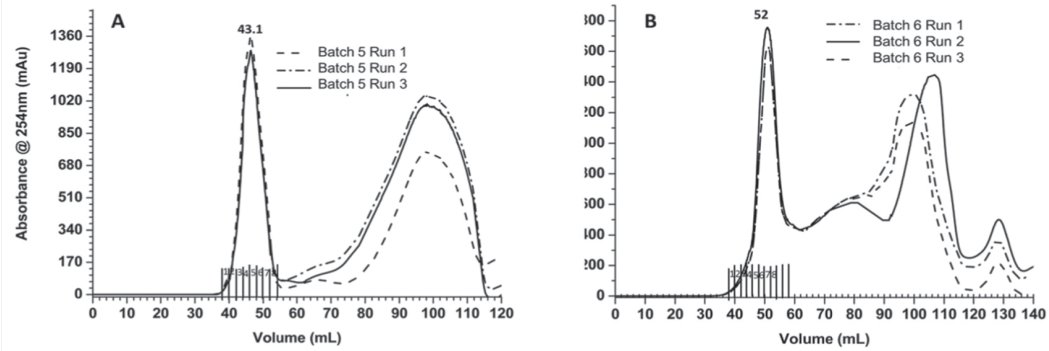

Fig. 3. Chromatogram showing three independent runs of the antigen batches loaded after treating with 0.25% v/v Triton X 100. A. Sephacryl S 400 and B. Toyopearl HW 65. Note: The extended tick labels on X-axis indicates the fractions of the respective peak.

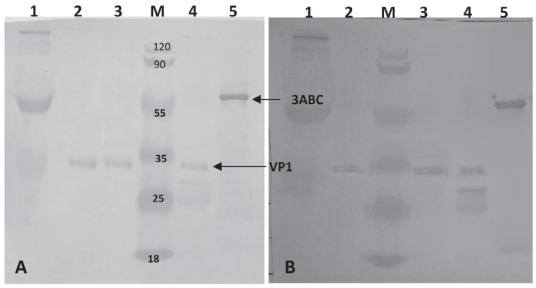

Fig. 4. Western blot analysis of the eluted fractions probed with bovine convalescent sera A. Batch 3 and B. Batch 4, Lanes: 1. Load 2. First half pooled fractions 3. Second half pooled fractions 4. Purified 140s 5. r3ABC.

Quantification of the 3ABC protein by ELISA:

The eluted void volume fractions were analyzed by quantifying 3ABC protein through sandwich ELISA method developed earlier in our lab. All the fractions from all the three repeat runs were analyzed. Figure 5, a multi curve double Y axis plot (drawn using Origin version 8.5 data analysis software), indicates percentage removal of 3ABC in micrograms before and after chromatography. The percentage removal of 3ABC from batches 3 and 4 were found to be 94% and 100 % respectively.

Quantification of the whole virus by Sucrose density gradient: The aliquots from each eluted fractions were pooled that would represent the entire void volume. The 140s (whole virus) content in the pooled fraction were quantified by separating on density based sucrose gradient. Treated sample (Batch 3, 4, 5 and 6) and untreated samples (Batch 1 and 2) did not show any significant loss.The recovery values after chromatography were above 80% for all the runs with relatively higher recoveries (Table 1) for the batch 1 and batch 2 samples.

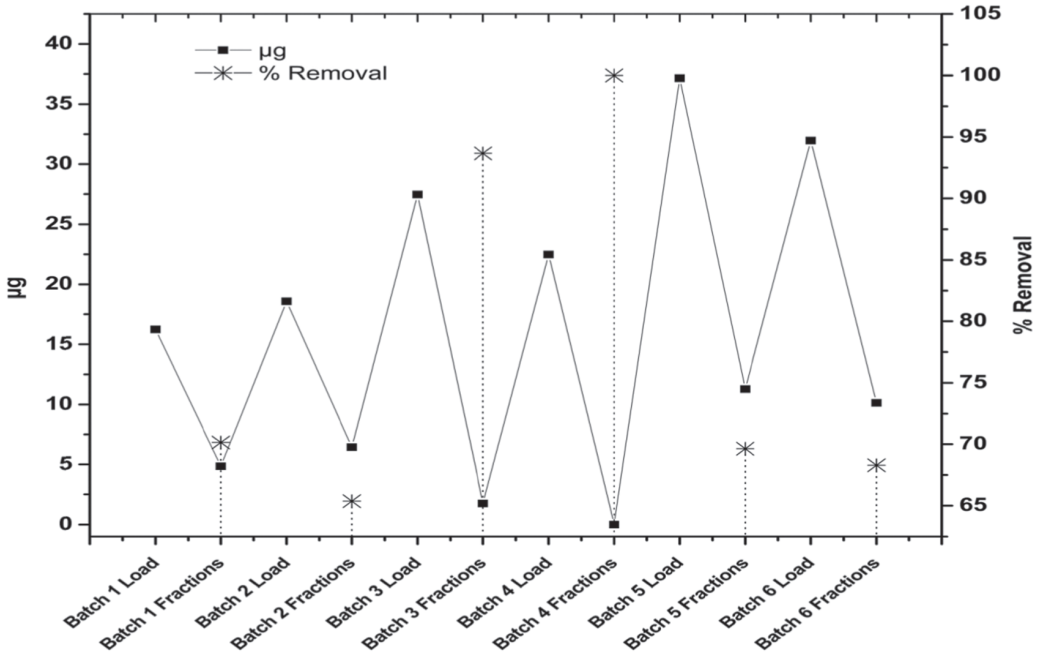

Fig. 5. Double Y-axis plot showing the quantity of 3ABC on the left Y-axis and their percentage removal of the respective runs on the right Y-axis.

Table 1: 140s quantification of the in process samples showing percentage recoveries

Pre-treatment of sample	Run	140s value (µg/mL) post sample treatment	140s value (µg/mL)	Total 140s injected (µg/5mL)	Eluted void volume (mL)	140s value (µg/mL) after chromato graphy	Total 140s (µg) after chromato graphy	% Re-covery
Untreated	Batch 1	65	NA	325	18	15	270	83.1
	Batch 2	51.6	NA	257.8	18	12	216	83.8
Treated	Batch 3	44	22	110	14	6.4	89.6	81.4
	Batch 4	50	25	125	14	7.2	100.8	80.6
	Batch 5	42	42	210	16	11.3	180.8	86.1
	Batch 6	54	54	270	16	13.6	217.6	80.6

Discussion:

Foot-and-mouth disease (FMD) is one of the known devastating viral disease of cloven-hoofed animals. It shows significant socio economic consequences worldwide, from national livestock industries declining due to international trade restrictions, affecting the stock productivity and livelihood. The primary method of controlling the disease in endemic areas is only by way of regular vaccination with inactivated vaccine. However, there are many limitations in the manufacturing of NSP free vaccine thus interfere in sero diagnosis of animals in differentiating infected from vaccinated animals (11 and 23).

Attempts are being made to standardize the production process of a vaccine that is operator independent and can be automated. One such approach is the use of separation and purification techniques like chromatography in vaccine manufacturing process. Since FMDV is a pH labile virus (24 and 25) and there is no reported PI of the whole virus (26). Purification of virus from the concentrated cell culture harvest becomes strenuous by Ion-exchange chromatography. The affinity purification of FMDV though reported earlier (19), has limitations in distinguishing the intact antigens from disassembled small particles and the large aggregates.The method reported also involves sensitive procedure involving FMDV labile parameters and difficult to adopt in large scale.The method described by Spitteler, 2011 (22), showed that concentration of inactivated FMDV could be estimated by SEC in vaccine manufacturing process.

In the current study, we have optimized the process for removal of viral NSPs along with other discrete proteins in the concentrated virus culture. The purified virus is eluted in the void volume using two different size exclusion chromatographic separation media, Sephacryl S-400 and Toyopearl HW65F. We have selected the chromatographic media based on their exclusion limit of 9000 KDa and more than 5000 KDa for Sephacryl S-400 and Toyopearl HW 65F respectively. The estimation of 140s through sucrose density gradient has shown a total recovery of more than 80% and the content of 3ABC protein in the purified virus concentration were reported to contain less than 6% w/w. The purification process can be validated further by immunizing animals and testing for the sero conversion against 3ABC NSP according to the OIE guidelines. This strategy will be a useful tool for other serotypes also and this method has the potential for a large scale manufacturing of NSP free FMD vaccine.

Conclusion:

Currently available conventional FMD vaccine prepared with virus grown on mammalian cells consists of unwanted moieties which interferes in production of quality vaccine. With an objective of developing a quality FMD vaccine,

we have come up with the method of partial purification of the antigen batches by chromatography. We have incorporated chromatography step in the purification process either by using Toyopearl HW 65F or Sephacryl S 400 as chromatographic media, which has effectively contributed in the removal of FMDV NSP (3ABC) at 95% and 100% respectively. The process also involved treatment of the sample with Triton X-100 for solubilization of the membrane proteins prior to chromatography. Presently developed method has the potential in production of NSP free quality vaccine that could act as marker vaccine in DIVA.

Reference:

1. Marvin, J. Grubman and Barry Baxt. (2004). Foot-and-Mouth Disease. Clinical Microbiology reviews, 17(2):465-493.

2. Cartwright, B., Chapman, W.G. and Brown, F. (1980). Serological and immunological relationships between the 146S and 12S particles of foot-and-mouth disease virus. Journal of General Virology, 50:369-75.

3. Doel, T.R. and Chong, W.K.T. (1982). Comparative immunogenicity of 146S, 75S and 12S particles of foot-and-mouth disease virus. Archives Virology, 73(2):185-91.

4. Mercedes García-Briones., María, F. Rosas., Mónica González-Magaldi., Miguel, A. Martín-Acebes., Francisco Sobrino and Rosario Armas-Portela. (2006). Differential distribution of non-structural proteins of foot-and-mouth disease virus in BHK-21 cells. Virology, 349:409-421.

5. Graham, J.Belsham. (1993). Distinctive features of Foot and Mouth disease virus, a member of the picornavirus family; aspects of virus protein synthesis, protein processing and structure. Progress in biophysics and molecular biology, 60(3):241-60.

6. Mohana Subramanian,B., Madhanmohan,M., Rajan Sriraman., Chandrasekhar Reddy,R.V., Yuvaraj,S., Kankipati Manikumar., Rajalakshmi,S., Nagendrakumar,S.B., Samir Kumar Rana and Srinivasan,V.A. (2012). Development of foot-and-mouth disease virus (FMDV) serotype O virus-like-particles (VLPs) vaccine and evaluation of its potency.Anti viral Research, 96:288-295.

7. Neeta Longjam., Rajib Deb., Sarmah,A. K., Tilling Tayo., Awachat,V. B. and Saxena,V. K. (2011). Brief Review on Diagnosis of Foot-and-Mouth Disease of Livestock: Conventional to Molecular Tools. Veterinary Medicine International, 11:1-17.

8. Anke, K.Trilling., Michiel, M. Harmsen., Vincent, J. B. Ruigrok., Han Zuilhof and Jules Beekwilder. (2013). The effect of uniform capture molecule orientation on biosensor sensitivity: Dependence on analyte properties. Biosensors and Bioelectronics, 40:219-226.

9. Barteling, S.J., and Meloen, R.H. (1974). A simple method for the quantification of 140S particles of foot-and-mouth disease virus (FMDV). Archive fur die gesamte virusforschung, 45(4):362-364.

10. Sarah, J. Cox and Paul, V. Barnett. (2009). Experimental evaluation of foot-and-mouth disease vaccines for emergency use in ruminants and pigs: a review. Veterinary research, 40(13):1-30.

11. Bo Zhu and Ying, Y. Chen. (2017). Development and Application of Liquid Chromatography in Life Sciences. Journal of Chromatography & Separation Techniques, 8(2):1-4.

12. King,D.P., Ludi,A., Wilsden,G., Parida,S. and Paton,D.J. (2015). The use of Non-Structural Proteins to differentiate between vaccinated and infected animals. OIE Annual regional Commission bulletin, Middle East, Kaslik, Lebanon, 1-4.

13. Julia Transfiguracion., Aziza, P. Manceur., Emma Petiota., Christine, M. Thompsona

and Amine, A. Kamena. (2015). Particle quantification of influenza viruses by high performance liquid chromatography. Vaccine, 33:78-84.

14. Petra Kramberger., Matja¡z Peterka., Jana Bobenb., Maja Ravnikar and Ales Strancar. (2007). Short monolithic columns-A breakthrough in purification and fast quantification of tomato mosaic virus. Journal of Chromatography A, 1144:143-149.

15. Nikola Kaludov., Beverly Handleman and John, A. Chiorini. (2002). Scalable Purification of Adeno-Associated Virus Type 2, 4, or 5 Using Ion-Exchange Chromatography. Human Gene Therapy, 13:1235-1243.

16. Vadim Klyushnichenko., Alice Bernier., Amine Kamen and Eef Harmsen. (2001). Improved high-performance liquid chromatographic method in the analysis of adenovirus particles. Journal of Chromatography B, 755:27-36.

17. Zolotukhin,S., Byrne,B.J., Mason,E., Zolotukhin,I., Potter,M., Chesnut,K., Summerford,C., Samulski,R.J. and Muzyczka,N. (1999). Recombinant adeno-associated virus purification using novel methods improves infectious titer and yield. Gene Therapy, 6:973–985.

18. Oka., Tetsuya Kotoh and Kumamoto-shi Kumamoto-ken. (1988). A method for purification of Influenza virus. European patent No. 0171086A2, 1-22.

19. Kuniaki Sakamoto., Kunio Ohkuma., Tetsuo Kawahara Ohzu and Mitsuo Sakoh, Kumamoto. (1988). A method for purification of Rabies Virus.United states patent No. US4725547A, 1-4.

20. Agustin, A. Navarro Del Cai-iizo., Marcela Mazza., Rodolfo Bellinzonis and Osvaldo Cascone. (1996). Foot and Mouth Disease Virus Concentration and Purification by Affinity Chromatography. Applied Biochernistry and Biotechnology, 61(3):399-409.

21. Vivian O'Donnell., Michael LaRocco., Hernando Duque and Barry Baxt. (2005). Analysis of Foot-and-Mouth Disease Virus Internalization Events in Cultured Cells. Journal of Virology, 79(13): 8506-8518.

22. Yanli Yanga., Hao Li., Zhengjun Li., Yan Zhanga., Songping Zhanga., Yi Chena., Mengran Yua., Guanghui Maa and Zhiguo Sua. (2015). Size-exclusion HPLC provides a simple, rapid, and versatile alternative method for quality control of vaccines by characterizing the assembly of antigens. Vaccine, 33:1143-1150.

23. Marcelo, A. Spitteler., Ignacio Fernándeza., Erika Schabesa., Alejandro Krimerb., Emmanuel, G. Réguliera., Mariela Guinzburga., Eliana Smitsaarta and Susana Levya,M. (2011). Foot and mouth disease (FMD) virus: Quantification of whole virus particles during the vaccine manufacturing process by size exclusion chromatography. Vaccine, 29(41):7182-7187.

24. Cao, Y., Lu Z and Liu Z. (2016). Foot-and-mouth disease vaccines: progress and problems. Expert Rev Vaccines, 15(6):783-789.

25. Andrea, C. Oliveira., Daniella Ishimaru, Rafael, B. Goncalves., Thomas, J. Smith., Peter Mason., Daniel Sa Carvalho and Jerson, L. Silva. (1999). Low Temperature and Pressure Stability of Picornaviruses: Implications for Virus Uncoating. Biophysical Journal, Volume 76: 1270-1279.

26. Michen,B., and Graule,T. (2010). Isoelectric points of viruses. Journal of Applied Microbiology, 109:388-397.

Current Trends in Biotechnology and Pharmacy
Vol. 12 (4) 342-348, October 2018, ISSN 0973-8916 (Print), 2230-7303 (Online)

An *In silico* Structural study on Bacterial Sulfite Reductase

Rajeswara Reddy Erva[1]*, Rinku.P.Varghese[2], A.L.Prasanna[2], G.Madhunika[2], K.S.Ravi Teja[2], V.S.Santosh[2], Satish Babu Rajulapati[3]

[1] Department of Biotechnology, National Institute of Technology Andhra Pradesh, Tadepalligudem, Andhra Pradesh, India.

[2] School of Biotechnology, VFSTR (Deemed to be University), Vadlamudi, Andhra Pradesh, India.

[3]Department of Biotechnology, National Institute of Technology Warangal, Warangal, Telangana, India.

*Corresponding author: rajeshreddy.bio@gmail.com

Abstract

Sulfur is amongst the most profuse elements on the globe and a vital component for life maintenance. Sulfite reductase plays a key role in sulfur pathway. It converts sulfite to sulfide. Reductase enzyme is present in sulfur reducing bacteria. Three organisms from *Desulfovibrio* species namely, *D. alaskensis, D. vulgaris, Desulfovibrionaceae* are used in this study. The computational analysis has been done out on the sulfite reductase enzyme form the above listed sulfur reducing bacteria using *in silico* tools. The study focused on mainly structural analysis, structural determination and structural validation as well. Structure of *D. vulgaris* is present in PDB and it is used as template for analyzing the structures of *D.alaskensis* and *Desulfovibrionaceae* using different structural validation and modelling online tools. Among the homology modeling tools used, based on the validation of structures using RAMPAGE tool, Swissmodel server gave the best models upon which the scientific community can be relayed. These modeled structures can be further used in molecular docking and molecular dynamics and simulation studies.

Keywords: Sulfite Reductase. Sulfur reducing bacteria. structure analysis. homology modeling and structural validation.

Introduction

Sulfur is an essential nutrient for living organisms being a vital component of certain amino acids, enzymes and proteins. Plants convince their nutritional requirements for sulfur by incorporating simple mineral compounds from the environment. Sulfur is cycled in the earth's crust biologically on such a profound scale that the effects are evident globally. Sulfur also has an obligatory existence in living constitution, majorly as protein component (S-containing amino-acids with sulfur), in coenzymes (e.g. biotin, coenzyme A, thiamine) and also in metallo-proteins as iron-sulfur clusters, with considerable responsibilities in the electron transport, enzymatic, and structural components of every biological cell. The sulfur cycle (Fig. 1.) is the compilation of actions by which sulfur travel to and from minerals (including the living systems and the waterways) (1). Steps in sulfur cycle are conversion of organic sulfur into inorganic forms (like sulfide minerals, elemental sulfur, as well as hydrogen sulfide [H_2S]), sulfides and elemental sulfur oxidation into sulfates (SO_4^{2-}), sulfate reduction to sulfides and sulfide assimilation to organic compounds.

Sulfite Reductase

Sulfate serves as the terminal electron acceptor in Dissimilatory Sulfate Reduction (DSR) which is an anaerobic respiration process. This kind of metabolism is observed in some kinds of archaea and bacteria which are called sulfate-reducing organisms. DSR is a three step process (2) namely, switch of sulfate to Adenosine 5'-phosphosulfate (APS), APS reduction into sulfite and sulfite reduction into sulfide which consumes one ATP with an the input of 8 electrons. Sulfite

Vol. 12 (4) 342-348, October 2018, ISSN 0973-8916 (Print), 2230-7303 (Online)

reductase performs major function in metabolism of sulfur by catalyzing the sulfite reduction to hydrogen sulfide and water.

SO_3^{2-} (sulfite) + electron donor $H_2S \rightarrow$ (hydrogen sulfide) + oxidized donor + $3H_2O$

Sulfite reductase belongs to oxidoreductases and is observed in bacteria, archaea, plants and fungi. They are categorized as dissimilatory or assimilatory type based on the function, catalytic properties and spectroscopic properties. It takes part in assimilation of sulfur. The process of sulfate reduction is a two phase process; sulfate reduction into sulfite followed by sulfite reduction into sulfide. But for microorganisms sulfate is not a favorable electron acceptor. The process of reducing sulfite to sulfide (Fig. 2.) is pervasive in nature, that is executed by many kinds of sulfite reductases like assimilatory (aSiR) and dissimilatory sulfite reductase (dSiR), anaerobic sulfite reductase (asrC) (for example Salmonella typhimurium and Clostridium species), assimilatory sulfate reductase type alSiR and nitrite reductases (3).

Desulfovibrio cells have mesophilic growth patterns with an ideal growth rate between the temperatures of twenty-five to forty degrees Celsius (NCBI). This family of bacteria has the ability to reduce the sulfite to sulfide, which can be used by the living organisms further. For any enzyme structure plays key role in its function. Out of the *Desulfovibrio* species the structure of sulfite reductase from *Desulfovibrio vulgaris* is present in PDB and is used as template for structural analysis of *Desulfovibrio desulfuricans* and *Desulfovibrionaceae* whose structures are yet to be determined. So, this study aimed at determination of sulfite reductase structures by different *in silico* tools and the structural validation of modelled structures for further study.

Methodology

Retrieval of Sequences and Structures: Crystal structure of Sulfite reductase from *D. vulgaris* is readily available in Protein Data Bank (PDB) with the ID number 1UCR. The same was retrieved in PBD format and the same was used for further studies. As no crystal structures are determined and deposited for *D. alaskensis* and *Desulfovibrionaceae* in any of the biological data bases yet, the available sequences were retrieved from NCBI with the ID numbers gi|499685910 and gi|518844986 respectively.

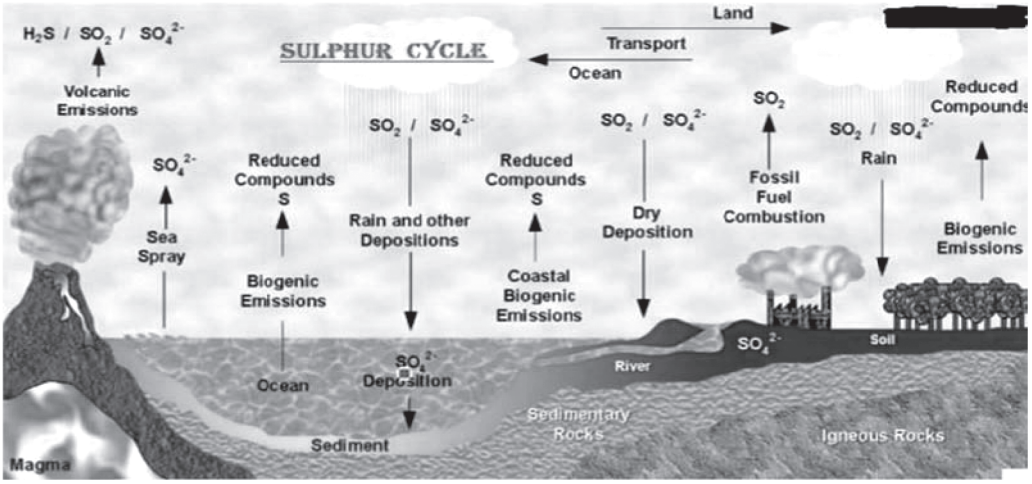

Fig. 1. The Sulfur Cycle

Vol. 12 (4) 342-348, October 2018, ISSN 0973-8916 (Print), 2230-7303 (Online)

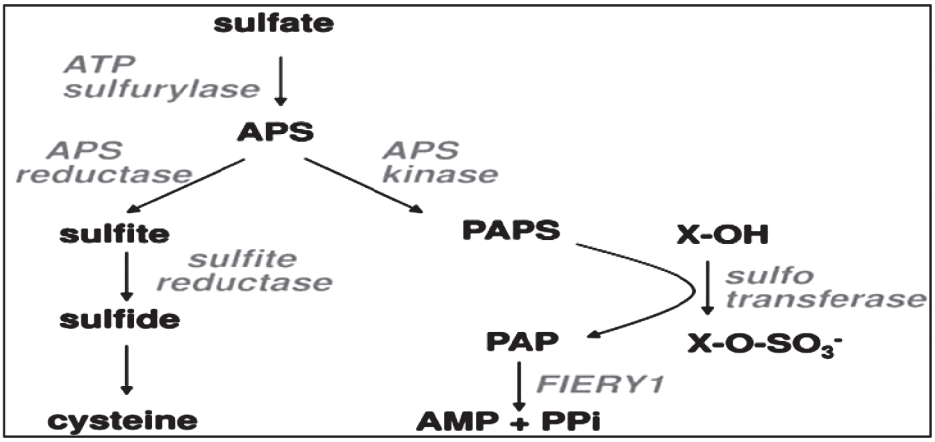

Fig. 2. Sulfate Reduction Pathway

Protein Structural Analysis

Primary and Secondary structural analysis : Primary structural analysis of sulfite reductase enzyme in *D. vulgaris, D. alaskensis* and *Desulfovibrionaceae* was done to compute various physico-chemical properties from a protein sequence like amino acid composition, aliphatic index and grand average of hydropathicity (GRAVY) etc. using PROTPARAM online tool (4). Secondary structural analysis of sulfite reductase enzyme in D.alaskensis, Desulfovibrionaceae and D. vulgaris was done using SOPMA (self-optimized prediction method) (5) tool to predict the formation of protein structures such as alpha helices and beta strands. Secondary structural analysis was also done using GOR (Garnier-Osguthorpe-Robson) IV (6) computational tool which is an information theory-based method for the prediction of secondary structures in proteins.

Table 1. Primary Structure Analysis by PROTPARAM

S.No	Properties	*D. vulgaris*	*D.alaskensis*	*Desulfovi brionaceae*
1	Number of amino acids	78	437	437
2	Molecular weight	8829.93	49057.44	48837.08
3	Theoretical pI	5.30	5.29	5.15
4	Aliphatic index	61.28	72.52	70.11
5	Grand average of hydropathicity (GRAVY)	-0.656	-0.484	-0.437
6	Instability index	25.14	43.33	40.94
7	Total number of atoms	1229	6791	6720
8	Total no of negatively charged residues (Asp + Glu)	13	65	64
9	Total no of positively charged residues (Arg +Lys)	11	49	44

Tertiary Structural Modelling

PHYRE2 (Protein Homology/analogy Recognition Engine) : Tertiary structural modeling was done by using PHYRE2 (Protein Homology/analogy Recognition Engine) (7) – an online server for the predicting protein tertiary structure. Phyre 2 uses hidden Markov models alignment via H search to extensively improvise the alignment accuracy and rate of detection in every case. The tool also integrates Poing, a new *ab initio* folding simulation for modelling regions of proteins without homology.

CPHmodels-3.0 : An online web-server, CPHmodels-3.0 (8) uses single template homology modelling approach for obtaining protein tertiary structure. It utilizes hybrid of a novel remote homology-modelling algorithm and CPHmodels-2.0 (9) scoring functions. Initially a query sequence is attempted for modelling using the fast CPHmodels-2.0 profile-profile scoring function appropriate for nearby homology modelling.

Swiss Model Server : Tertiary structural modelling was also done by using Swiss model, a web-server devoted to protein homology modelling which is the most precise method now-a-days to produce reliable 3D models of protein structure. This type of methods uses experimentally derived protein structures (called templates) to generate protein models (called targets) (10-14).

Structure Validation : Structure validation is a course of assessing the reliability for 3D atomic models of nucleic acids and proteins which are large biomolecules. These biological models, providing 3D coordinates for every atom of molecule, comes from x-ray nuclear magnetic resonance (NMR) or crystallography. The structure validation has the following aspects; checking on the validity of the thousands to millions of measurements in the experiment, checking how consistent the atomic model is with those experimental data and checking consistency of the model with known physical and chemical properties. Some of the other structure validation tools are Rampage (15), Prosess (16), Procheck (17) and Harmony (18).

Results and Discussion

Structural analysis was done using various online protein structure analysis tools.

Primary and Secondary Structural Analysis : Primary structural analysis of sulfite reductase enzyme in *D. alaskensis* was performed using PROTPARAM tool. PROTPARAM is an online tool that computes various physico-chemical properties from a protein sequence. The protein can be specified as accession number or ID in form of a raw sequence. The accession number or ID number is retrieved from NCBI database and entered into PROTPARAM tool and the computed results are displayed. Protparam results displayed that sulfite reductase in all three organisms is highly hydrophilic as the values is less than 0.05. Results show that the protein in *D.vulgaris* is stable and in remaining two organisms are predicted to be highly unstable having higher instability index values. Having more number of negatively charged residues than positively charged ones the enzyme remains acidic in the three organisms. Other information computed is as follows (table 1).

SOPMA analysis revealed that the percentage of alpha helix is more compared to other forms of secondary structural elements in sulfite reductase from all the three organisms. Random coils proportion is almost near to alpha helix in *D.alaskensis* and *Desulfovibrionacea* (table 2). On the other hand, as per GOR IV the percentage of alpha helix is close to percentage of beta sheets. But, in contrast to SOPMA results, random coils percentage is high in all the three organisms i.e., 44.87%, 53.09% and 56.75% in *D.vulgaris, D.alaskensis* and *Desulfovibrionaceae* respectively (table 3).

Tertiary Structural Modeling and Validation

Crystal Structure of *D.vulgaris* was retrieved from PDB (ID: 1UCR) and the same was shown in figure 3a. Tertiary structural modelling of *D. alaskensis* and *Desulfovibrionaceae* was done

Vol. 12 (4) 342-348, October 2018, ISSN 0973-8916 (Print), 2230-7303 (Online)

Table 2. Secondary Structure Analysis by SOPMA

S.No	Properties	*D. vulgaris*	*D. alaskensis*	*Desulfovibrionaceae*
1	Sequence length	78	437	437
2	Window width	17	17	17
3	Similarity threshold	8	8	8
4	No of states	4	4	4
5	Alpha helix	58.97%	35.70%	37.07%
6	Beta strands	15.38%	18.99%	18.54%
7	Beta turns	3.85%	12.81%	13.96%
8	Random coils	21.79%	32.49%	30.43%

Table 3. Secondary Structure analysis by GOR IV

S.No	Properties	*D.vulgaris*	*D.alaskensis*	*Desulfovibrionaceae*
1	Sequence length	78	437	437
2	Alpha helix	25.64%	21.51%	24.49%
3	Beta strands	29.49%	25.40%	18.76%
4	Beta turns	0.00%	0.00%	0.00%
5	Random coils	44.87%	53.09%	56.75%

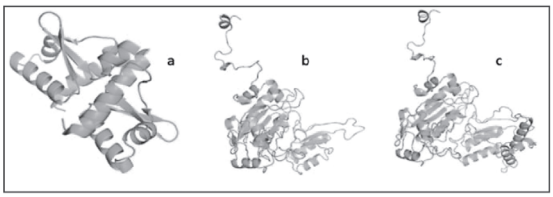

Fig. 3. Structural Modelling by PHYRE 2.0

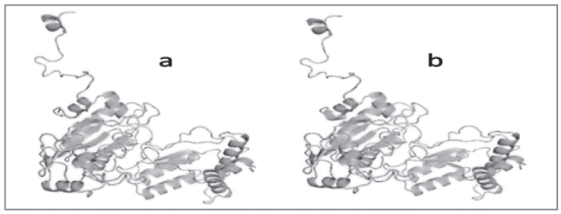

Fig. 4. Modelled Structures of (a) *D. alaskensis* and (b) *Desulphovibrionaceae* using CPHmodels

using PHYRE 2.0 (Fig.3b, 3c), CPHmodels-3.0 (Fig. 4a, 4b) and Swiss model server (Fig. 5a, 5b).

Templates were identified by performing the BLAST search tool of NCBI. Based on the BLAST analysis the best template identified was 2V4J Chain A with the sequence identity score of 86% and 85% against *D. alaskensis* and *Desulfovibrionaceae* respectively. Similarly structures of the enzyme from *D. alaskensis* and *Desulphovibrionaceae* were also modeled using Swissmodel Web-server.

In order to assess the best predicted model, structural validation was performed by using RAMPAGE online tool (fig. 6). In *D. alaskensis* amino acids falling in favored region is 97%, allowed region is 2.5%, outlier region is 0.3% using Swiss model where as in *Desulfovibrionaceae* they are 96.9%, 2.8% and 0.3%. RAMPAGE analysis using PHYRE 2.0 models shows that percentage of favored region

Vol. 12 (4) 342-348, October 2018, ISSN 0973-8916 (Print), 2230-7303 (Online)

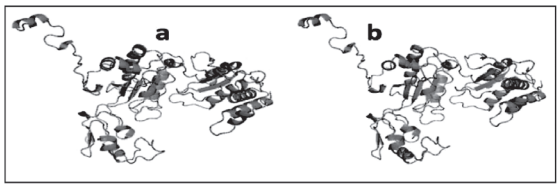

Fig. 5. Modelled Structures of (a) *D. alaskensis* and (b) *Desulphovibrionaceae* using Swissmodel Server

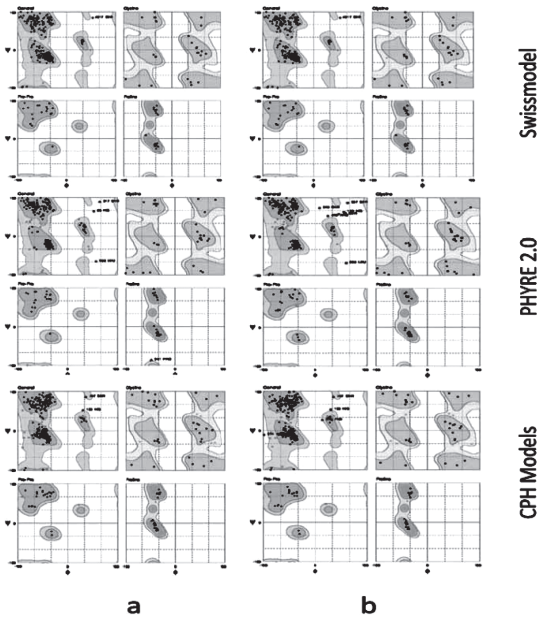

Fig. 6. Structural validation of modeled structures by RAMPAGE tool

amino acid residues in *D. alaskensis* is 95.3%, allowed region is 3.6% and outlier region is 1.2%, where as in *Desulfovibrionaceae* the percentages ranges as 95.2%, 3.4% and 1.4%. For the models generated by CPH models, % of residues in favored regions is 93.5%, allowed region is 6% and outlier region is 0.5% in case of *D. alaskensis* and on the other hand in *Desulfovibrionaceae* favored the same are 92.2%, 6.9% and 0.9% respectively. Based on the RAMPAGE analysis the structures modelled by Swiss model tool are the best models.

Conclusion

Structural modelling, validation and analysis was done for sulfite reductase enzyme in sulfite reducing bacteria namely *D.alaskensis* and *Desulfovibrionaceae* by using *D.vulgaris* as a template whose structure is already present in PDB using different online modelling, validation and analysis tools. Structural analysis revealed that the enzyme is acidic in nature in all the three organisms, is stable only in *D. vulgaris*. After the structural validation by Ramachandran plot analysis by RAMPAGE tool, out of the three homology modeling tools used for 3D structure prediction, Swissmodel web server gave the most reliable model, which can be further used in computational studies.

References

1. Canfield, D. E., and Raiswell, R. (1999). The evolution of the sulfur cycle. *American Journal of Science*, *299*(7-9), 697-723.

2. Crane, B. R., Siegel, L. M., and Getzoff, E. D. (1995). Sulfite reductase structure at 1.6 Å: evolution and catalysis for reduction of inorganic anions. *Science*, *270*(5233), 59-67.

3. Dhillon, A., Goswami, S., Riley, M., Teske, A., and Sogin, M. (2005). Domain evolution and functional diversification of sulfite reductases. *Astrobiology*, *5*(1), 18-29.

4. Gasteiger, E., Hoogland, C., Gattiker, A., Wilkins, M. R., Appel, R. D., and Bairoch, A. (2005). Protein identification and analysis tools on the ExPASy server. In *The proteomics protocols handbook* (pp. 571-607). Humana press.

5. Geourjon, C., and Deleage, G. (1995). SOPMA: significant improvements in protein secondary structure prediction by consensus prediction from multiple alignments. *Bioinformatics*, *11*(6), 681-684.

6. Garnier, J. (1998). GOR secondary structure prediction method version IV. *Meth. Enzym., RF Doolittle Ed.*, *266*, 540-553.

7. Kelley, L. A., Mezulis, S., Yates, C. M., Wass, M. N., and Sternberg, M. J. (2015). The Phyre2 web portal for protein modeling, prediction and analysis. *Nature protocols*, *10*(6), 845.

8. Nielsen, M., Lundegaard, C., Lund, O., and Petersen, T. N. (2010). CPHmodels-3.0-remote homology modeling using structure-guided sequence profiles. *Nucleic acids research*, *38*(suppl_2), W576-W581.

9. Lund, O., Nielsen, M., Lundegaard, C., and Worning, P. (2002, January). CPH models 2.0: X3M a computer program to extract 3D models. CASP CONFERENCE.

10. Waterhouse, A., Bertoni, M., Bienert, S., Studer, G., Tauriello, G., Gumienny, R., and Lepore, R. (2018). SWISS-MODEL: homology modelling of protein structures and complexes. *Nucleic acids research*.

11. Bienert, S., Waterhouse, A., de Beer, T. A., Tauriello, G., Studer, G., Bordoli, L., and Schwede, T. (2016). The SWISS-MODEL Repository—new features and functionality. *Nucleic acids research*, *45*(D1), D313-D319.

12. Guex, N., Peitsch, M. C., and Schwede, T. (2009). Automated comparative protein structure modeling with SWISS MODEL and Swiss PdbViewer: A historical perspective. *Electrophoresis*, *30*(S162-173).

13. Benkert, P., Biasini, M., and Schwede, T. (2010). Toward the estimation of the absolute quality of individual protein structure models. *Bioinformatics*, *27*(3), 343-350.

14. Bertoni, M., Kiefer, F., Biasini, M., Bordoli, L., and Schwede, T. (2017). Modeling protein quaternary structure of homo-and hetero-oligomers beyond binary interactions by homology. *Scientific reports*, *7*(1), 10480.

15. Lovell, S. C., Davis, I. W., Arendall, W. B., De Bakker, P. I., Word, J. M., Prisant, M. G., and Richardson, D. C. (2003). Structure validation by Cá geometry: Õ, ø and Câ deviation. *Proteins: Structure, Function, and Bioinformatics*, *50*(3), 437-450.

16. Berjanskii, M., Liang, Y., Zhou, J., Tang, P., Stothard, P., Zhou, Y., and Wishart, D. S. (2010). PROSESS: a protein structure evaluation suite and server. *Nucleic Acids Research*, *38*(Web Server issue), W633–W640.

17. Laskowski, R. A., MacArthur, M. W., Moss, D. S., and Thornton, J. M. (1993). PROCHECK: a program to check the stereochemical quality of protein structures. *Journal of applied crystallography*, *26*(2), 283-291.

18. Pugalenthi, G., Shameer, K., Srinivasan, N., and Sowdhamini, R. (2006). HARMONY: a server for the assessment of protein structures. *Nucleic acids research*, *34* (suppl_2), W231-W234.

Current Trends in Biotechnology and Pharmacy
Vol. 12 (4) 349-354, October 2018, ISSN 0973-8916 (Print), 2230-7303 (Online)

Insilico Studies of FOR20 - A Centrosomal Protein

A. Ranganadha Reddy[1*], N. Madhan Sai[1], S. Krupanidhi[1], P. Sudhakar[2], and T. C. Venkateswarulu[1]

[1*.] Department of Biotechnology, VFSTR (Deemed to be University) Guntur - 522213, India
[2.] Department of Biotechnology, Acharya Nagarjuna University Guntur - 522 510, India
Corresponding author : rangaaluri@gmail.com

Abstract

There is enough scientific evidence on microtubule playing important role in various functions, one such is chromosomal segregation, which made them as primary targets in the cancer treatment. Centrosomal proteins plays vital role in maintaining microtubule dynamics that having significant effect on various functions involving microtubule such as chromosomal segregation, intracellular transport and cell polarity. There are diverse centrosomal proteins that are involved in this biological functions inside the cell system, to name a few EB1, EB2, tau, FOR20.We aim to characterize the regulation of microtubule dynamics by FOR20 and its implication in cellular processes like mitotic cell division, apoptosis, and cell migration. We worked on FOR20 specifically with its enough facts about involvement in maintaining microtubule dynamics and in cell migration and to find whether FOR20 regulate dynamic properties of microtubules by performing computational studies. The evidence of interaction of FOR20 with microtubule is poorly understood at molecular level.

FOR20 protein structure was modeled by using SWISS MODEL and the model was validated by using PROCHECK.

Keywords: FOR20 protein, Centrosomal protein, SWISS MODEL, PROCHECK.

Introduction

This report depicts the result of various interactions between FOR20 with tubulin. Instead of concentrating on a single biological process it uses computer simulations to understand the effects of these interactions at molecular level. Both prokaryotic and eukaryotic cells have cytoskeleton. It helps in maintenance of internal organization and shape of cells by providing mechanical support. It also plays important roles in muscle contractions, cell motility, axonal growth, cell migration, cell division and platelet formation and also helps in providing transport and communication within the cell [1]. Cytoskeleton is built up with three components microfilaments (actin Filaments), microtubules and intermediate filaments. Networks are formed by filamentous components. In prokaryotes microtubules and microtubules are present in cytoskeleton and only in animal cells intermediate filaments are found [2]. Microtubules are hollow rigid rods that are 25nm in diameter. Microtubules are vital formations it has repeated assemblage and breakdown [3]. Cell locomotion, intracellular transport and separation of chromosomes during mitosis all these require cytoskeleton and also determination of the shape of cells [4]. Microtubules unlike intermediate filaments that contain different types of fibrous proteins, it has a single tubulin protein. The protein is a dimer protein and it contains two 55-kd polypeptides they are á-tubulin and â-tubulin. Small families of similar genes encode á- and â-tubulin similar to actin.Another type of tubulin is ã- tubulin its present in the centrosome and plays an important role in initiation of microtubule assembly [5]. Polymerization of tubulin results in the formation of microtubules that contains 13 linear protofilaments that are assembled to a hollow core

[6]. Parallely head to tail arrays of tubulins make up protofilaments. Microtubules are polar structures it has two ends a positive end that grows fast and a minus end that has a slow growth rate. Direction along microtubules is determined by polarity, similar to how direction of myosin is determined by polarity of actin filaments. The tubulin protein dimers can both polymerize and depolymerize. Microtubules go through repeated phases of assembly and disassembly. á- and â-tubulin bind GTP that is analogous to ATP bound to actin to regulate polymerization. During or after polymerization GTP that is bound only to â-tubulin is hydrolyzed to GDP. Binding affinity of tubulin is weakened by hydrolysis of GTP and depolymerization takes place and results in the vital behaviour of microtubules [7]. Similar to actin microtubules also undergo tread milling that makes tubulin molecules to bind to GDP are lost from minus end and are replaced by the molecules that are bound to the plus end of the same microtubule [8]. Dynamic instability is caused due to GTP hydrolysis in which microtubules alternate between cycles of growth and shrinkage [9]. Rate of tubulin addition determines the growth or shrinkage of microtubule with respect to hydrolysis of GTP. GTP is hydrolyzed and the microtubules are retained only when new tubulin molecules that are GTP bound are added fastly to the positive end and the growth of microtubule continues. When the rate of polymerization slows down the GTP that has bound to tubulin on the positive end will be hydrolyzed to GDP. If this process takes place then dissociation of tubulin takes place that results in fast depolymerization and the microtubule shrinks. Continuous and fast turnover of the microtubules is caused due to dynamic instability that has been described by Tim Mitchison and Marc Kirschner in 1984 [10] it has half life of minutes in the cell. This turnover is important for the remodeling of cytoplasm that takes place during the mitosis process. As microtubules play an important role in mitosis the drugs that affect the microtubule assembly can also be used for treating cancer. Some of the frequently used drugs that bind to the protein tubulin which causes polymerization of microtubules and this causes blockage of mitosis process. [11]. Vincristine and Vinblastin are the two drugs that are used for cancer treatment cause the stop the cells division. Taxol instead of inhibiting the assembly of microtubules helps in stabilizing it [12]. Cell division gets blocked due to stabilization and hence its used as anticancerous drug and also as an experimental tool. Katanin, motor protein kinesin and dynein, and other centrosomal proteins are basically molecular motor proteins that interacts with microtubules and it changes the dynamics of microtubules like FOR20 [13]. Actin protein makes microfilaments or actin filaments and these filaments are 5 nm diameter and they are particular filaments. One of the most dynamic and smallest elements of cytoskeleton is actin. The filaments are type of polymers that are flexible, linear and can hold the resistance to multi-pico newton whereas they unravel upon nano newton tensile forces [14]. These filaments are either bundled up or are in the form of networks. These actin filaments can be seen in two orientations either in polar or non polar filamentous arrays that are bristly ends that pinpoint to the same ending of the bundle whereas in non polar filaments some of the bristle ends are pointed at one side and some are pointed to the other end [15]. Intermediate filaments are 10 nm in size and built up of tetrameric units [16]. They are found in cell of animals. They are formed from proteins that have alike features and structure and are said to be family protein.

Methodology

The primary sequence of FOR20 (Acc.ID. NP_653201.1) was retrieved from Swiss Prot. BLAST software was used for homology search of FOR20.

FOR20 crystal structure was modeled by using the SWISS MODEL [17] server with (PDB ID: 4BTJ) as structural template.

Stereo-chemical quality of all the chains in a protein within the given PDB structure can be done by PROCHECK analysis [18]. The regions that have unusual geometry are highlighted and the overall structural estimation is also provided.

Homology modeling

The steps to creating a homology model are as follows:

- Identify homologous proteins and determine the extent of their sequence similarity with one another and the unknown.
- Align the sequences.
- Identify structurally conserved and structurally variable regions
- Generate coordinates for core (structurally conserved) residues of the unknown structure from those of the known structure(s).
- Generate conformations for the loops (structurally variable) in the unknown structure.
- Build the side-chain conformations.
- Refine and evaluate the unknown structure.

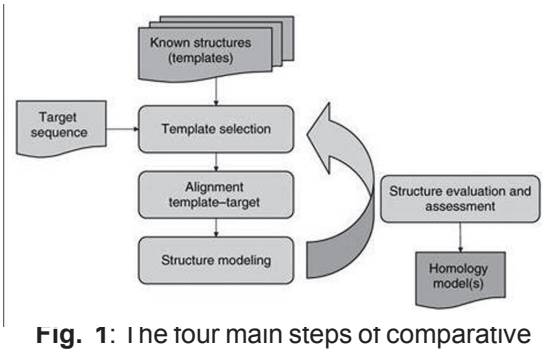

Fig. 1: The four main steps of comparative protein structure modeling: template selection, target–template alignment, model building and model quality evaluation [19-21].

Results and Discussion

Sequence Retrieval and Data Collection By using UniProtKB/Swiss-Prot database the details of FOR20 (Acc No. NP_653201.1**) the information such as** helix lengths, N-and C-terminus amino acid lengths etc., was retrieved. The sequence information is provided below.

Query sequence of FOR20

>sp|Q96NB1|FOPNL_HUMAN LisH domain-containing protein FOPNL OS=Homo sapiens OX=9606MATVAELKAVLKDTLEKKG VLGHLKARIR AEVFNAL DDDRE PRPSLSHE NLLINE LIREY LEFNKYKYTAS VLIAESG QPVVPLDRQFLIHELNAFEESKDNTIPLL YGILAHFLRGT KDGIQNAFL KGPSLQPSDP SLGRQPSRRKPMD DHLRKEEQKST NIEDLHV SQAVNR

BLAST tool helps to search the regions of similarity between nucleotide or protein sequences by using local alignment algorithm. Statistical significance of the matches is calculated by comparing the protein or nucleotide query to the sequences in the database. By using the BLAST tool the target sequence i.e., FOR20 (UniProt ID: NP_653201.1) was searched against the sequences of protein in the database. By analyzing the BLAST results it can be seen that maximum identity with target sequences are shown by three different proteins (PDB IDs: 1T11.1.A, 1Q1V.1.A, 2D68.1.B).For further use out of these three sequences 1T11.1.A is selected (Figure 2.).

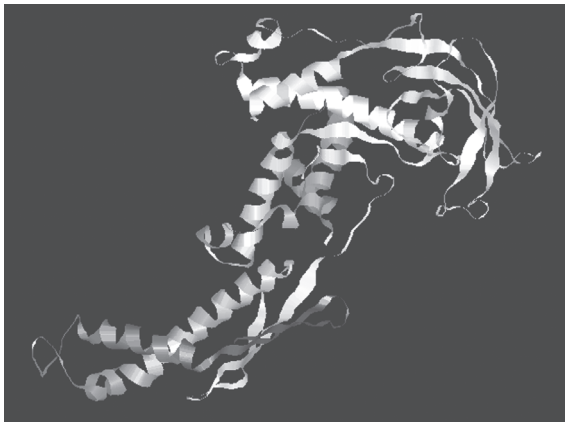

Fig. 2. Crystal structure of ribosomal chaperone trigger factor (PDB ID: 1T11) as structural template

Three-Dimensional Structure Prediction by SWISS MODEL

1T11 was retrieved through BLAST results and was taken as template, NP_653201.1 was taken as query sequence and Protein BLAST was performed, the 3D structure of FOR20 (NP_653201.1) was predicted by using the tool

SWISS MODEL and can be seen in Figure 3. Taking 1T11_1_A chain as templates that are homologous to query sequence tau-protein kinase the 3D structure of the FOR20 (NP_653201.1) was predicted. A model with RMS deviation is 0.75 after superimposition of FOR20 structure with templates 1T11 was obtained.

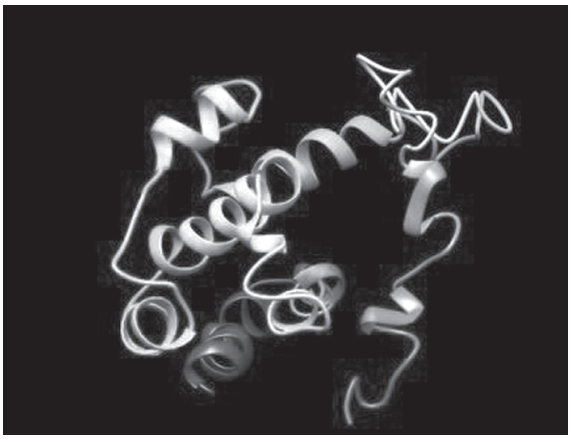

Fig. 3. Homology model of FOR20 protein structure built by SWISS MODEL server

Ramachandran Plot

PROCHECK checks the stereochemical quality of a protein structure, producing a number of PostScript plots analysing its overall and residue-by-residue geometry. It includes PROCHECK-NMR for checking the quality of structures solved by NMR and the results of procheck for protein structure after energy minimization is as follows (Figure 4).

PROCHECK is used for stereochemical assessment of the model. Ramachandran plot was developed by Gopalasamudram Narayana Ramachandran and Viswanathan Sasisekharan. Iit is used to visualize dihedral angles Psi and Phi of amino acid residues in protein structure. It is commonly known as Ramachandran map or a Ramachandran diagram or a [Psi and Phi] plot. It depicts the possible conformations of Psi and Phi angles for a polypeptide. The model developed by

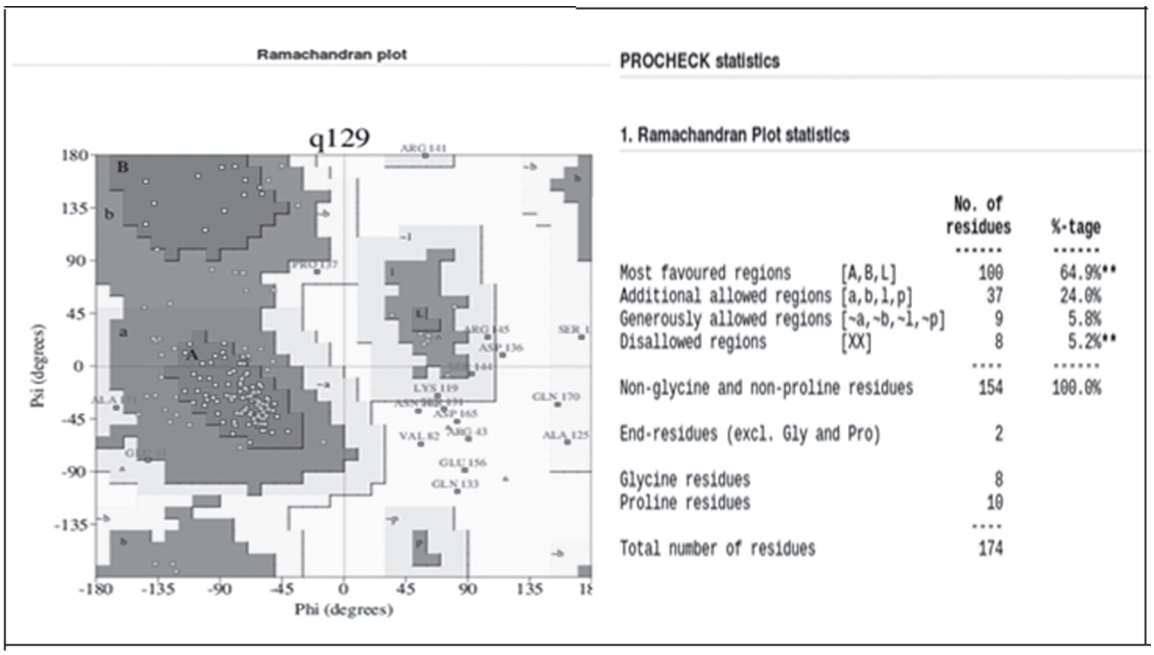

Fig. 4. Ramachandran plot analysis of the generated model

PROCHECK was checked with the Ramachandran plot, FOR20 protein had 100 (64.9 %) residues in the most favored region, 37 (24.0 %) residues in allowed region, 9 (5.8 %) generously allowed region and 8 (5.2 %) residues in disallowed region and it can be seen in the Figure 4.

Conclusion

In the current study we have modeled FOR20, an important centrosomal protein aids to investigating in different cellular functions like cell signaling. By using BLASTP the template 1T11 was found. SWISS MODEL was used for building the homology model of FOR20; by using PROCHECK the protein structure validation was done.

References

1. Bray, D. Cell movements from molecules to motility. Garland Science (2001).
2. Alberts, B. Molecular Biology of the Cell. Garland Science (2008).
3. Howard, J., Hyman, A.A. Microtubule polymerases and depolymerases. Current opinion in cell biology. 19, 31-35 (2007).
4. Kirschner, M., Mitchison, T. Beyond self-assembly: From microtubules to morphogenesis. Cell. 45, 329-342 (1986).
5. Vandecandelaere,A., Brune,M., Webb,M.R., Martin,S.R., Bayley, P.M.: Phosphate release during microtubule assembly: What stabilizes growing microtubules. Biochemistry. 38, 8179-8188 (1999).
6. Tilney, W.G., Bryan, J., Bush, D.J., Fujjiwara, K., Mooseker, M.S., Murphy, D.B., Snyder. D.H. Microtubules: evidence for 13 protofilaments. Journal of Cell Biology. 59, 267–275(1973).
7. Stewart, R.J., Farrell, K.W., Wilson, L. Role of GTP hydrolysis in microtubule polymerization: evidence for a coupled hydrolysis mechanism. Biochemistry. 29, 6489-6498 (1990).
8. O'Brien, E.T., Voter, W.A., Erickson, H.P. GTP hydrolysis during microtubule assembly. Biochemistry. 26, 4148-4156 (1987).
9. Simon, J.R., Salmon, E.D. The structure of microtubule ends during the elongation and shortening phases of dynamic instability examined by negative-stain electron microscopy. *Journal* of *Cell Science*. 96, 571-582 (1990).
10. Mitchison, T., Kirschner, N. Dynamic instability of microtubule growth 123. Nature. 312, 237-242 (1984).
11. Akhmanova,A., Hoogenraad,C. C.,Drabek, K., Stepanova,T.,D ortland,B.,Verkerk,T., Vermeulen, W., Burgering, B.M., De Zeeuw, C.I., Grosveld, F., Galjart, N. Clasps are CLIP-115 and -170 associating proteins involved in the regional regulation of microtubule dynamics in motile ftbroblasts. Cell. 104, 923-935 (2001).
12. Giannakakou, P., Sackett, D., Fojo, T.: Tubulin/microtubules: still a promising target for new chemotherapeuticagents *Journal* of the *National Cancer Institute.* 92, 182–183 (2000).
13. Ligon, L. A., Shelly, S. S., Tokito, M., Holzbaur, E. L.: The microtubule plus-end proteins EB1 and dynactin have differential effects on microtubule polymerization. *Molecular Biology* of the *Cell.* 14, 1405–1417 (2003).
14. Letourneau, P. C., Shattuck, T. A. Ressler, A.H. 'Pull' and 'push' in neurite elongation: observations on the effects of different concentrations of cytochalasin B and taxol. *Cell Motility* and the Cytoskeleton 8, 193–209 (1987).
15. Lin, C. H., Forscher, P. Cytoskeletal remodeling during growth cone-target interactions. Journal of Cell Biology. 121, 1369–1383 (1993).

16. Franke, W.W. Differentiation-related patterns of expression of proteins of intermediate-size filaments in tissues and cultured cells. Cold Spring Harbor Symposia on Quantitative Biology. Vol. 46. Cold Spring Harbor Laboratory Press, 1982.

17. Benkert, P., Biasini, M., Schwede, T. Toward the estimation of the absolute quality of individual protein structure models. Bioinformatics. 27, 343-350 (2011).

18. Laskowski, R.A., Malcolm, W.M., David, S.M., Janet, M.T. PROCHECK: a program to check the stereochemical quality of protein structures. Journal of applied crystallography. 26, 283-291 (1993).

19. Bordoli, L., Kiefer, F., Arnold, K., Benkert, P., Battey, J., Schwede, T. Protein structure homology modelling using SWISS-MODEL workspace. Nature Protocols. 4, 1-13 (2009).

20. Kopp, j., Schwede, T. Automated protein structure homology modeling: a progress report. Pharmacogenomics. 5, 405-416 (2004).

21. Marti-Renom, M.A., Stuart, A.C., Fiser, A., Sánchez, R., Melo, F., Sali, A. Comparative protein modeling of genes and genomes. Annual review of biophysics and biomolecular structure. 29, 291-325 (2000).

Current Trends in Biotechnology and Pharmacy
Vol. 12 (4) 355-366, October 2018, ISSN 0973-8916 (Print), 2230-7303 (Online)

Evaluation of Antimicrobial Activity of *Emblica officinalis* against Skin Associated Microbial Strains

Lovey Sharma[1*] and Ram Kumar Pundir[1]
[1]Department of Biotechnology, Ambala College of Engineering and Applied Research, Devsthali (near Mithapur), P.O. Sambhalkha-133101, Ambala (Haryana)-India
*For Correspondence: lovey.sharma92@gmail.com

Abstract

The present study was undertaken to access antimicrobial activity of fruit extracts of Amla (*Emblica officinalis*) against skin associated microorganisms. The antimicrobial activity of five different solvents viz. methanol, ethanol, distilled water, chloroform and petroleum ether against Gram positive, Gram negative bacteria and yeast namely *Propionibacterium acne*, *Staphylococcus aureus*, *Pseudomonas aeruginosa*, *Escherichia coli* and *Candida albicans* was assessed by using agar well diffusion method. The methanolic extract of *Emblica officinalis* showed maximum zone of inhibition, aqueous extract was most effective against *S. aureus* and ethanolic extract was most effective against *C. albicans.* Comparison of antimicrobial activity of *Emblica officinalis* extracts with antibiotics revealed that *Emblica officinalis* methanolic extract had maximum effective antimicrobial activity against all tested microorganisms. MIC and MBC of methanolic extract of *Emblica officinalis* against the microbial strains was ranged between 0.50 to 0.03125mg/ml. The synergistic interaction of *Emblica officinalis* with antibiotics (Gentamicin, Amikacin and Clotrimazole) indicated much better results as compared to antibiotics susceptibility pattern alone. Phytochemicals analyses showed the presence of Alkaliods, Saponins, Glycosides, Proteins, Phenols and Phytosterols. The compounds identified by GC-MS analysis had been useful as skin conditioning agent. The present study reflects a hope for the development of novel agents of biomedical importance.

Keywords: Antimicrobial activity, *Emblica officinalis* fruit, GC-MS analysis, Phytochemicals, Skin disease.

Introduction

Human skin is one of the largest organ of the body. It is a very complex tissue consisting of several distinct layers and components. The most obvious function is to protect the body against external influences. The skin is a highly organized, stratified structure consisting of three main layers, called the epidermis, dermis and hypodermis (1). Normal microflora of skin is dominated by Gram-positive bacteria such as *Staphylococcus, Micrococcus, Corynebacteria* (*Corynebacterium*) and Diptheroids (*Propionibacterium acne*). In addition to resident skin flora, the dust particles may also carry Fungi and Bacilli. *Aspergillus, Penicillium, Cladosporium* and *Mucor* are the major types of fungi found under the nails (2). Multidrug resistant bacteria including nosocomial pathogens have become important cause for higher skin care costs. A novel compound, with difference in mode of activity of antibiotics against microbes, is an attractive alternative against multidrug resistant microorganisms. Plant kingdom is a gold mine for novel and affordable skin care acting through novel mechanisms against skin pathogen (3).

Amla which is known as *Emblica officinalis* is an Indian herb which is extensively used in ayurvedic system of medicine. *Amla* is a prestigious herb finds it mention in Charak Samhita

Vol. 12 (4) 355-366, October 2018, ISSN 0973-8916 (Print), 2230-7303 (Online)

as a Rasayan. The herb is also aphrodisiac, haemostatic, nutritive tonic and rejuvenative. It increases red blood cell count. It improves complexion and removes wrinkles. *Amla* is also used to treat constipation and is used as a cooling agent to reduce the effects of sun strokes and sun burns. It is the main ingredient used in the shampoo (4). *Amla* fruit is widely used in the Indian system of medicine as diuretic, laxative, liver tonic, refrigerant, stomachic, restorative, anti-pyretic, hair tonic and ulcer preventive and for common cold, fever; as alone or in combination with other plants. Phytochemical studies on amla disclosed major chemical constituents including tannins, alkaloids, polyphenols, vitamins and minerals. It is used as analgesic, anti-tussive, antiatherogenic, adaptogenic; cardio, gastro, nephro and neuro protective, chemopreventive, radio and chemo-modulatory and anticancer properties. *Amla* is also reported to possess potent free radical scavenging, antioxidant, anti-inflammatory, anti-mutagenic, immune-modulatory activities, which are efficacious in the prevention and treatment of various diseases like cancer, atherosclerosis, diabetes, liver and heart diseases (5).

Materials and methods

Collection of plant materials and solvent extraction: The fruits of the Amla (*Emblica officinalis)* were washed thoroughly 2-3 times with running tap water and then with sterile water followed by shade-dried, powdered and used for extraction. Five gram of shade dried powder of Amla was put in 50 ml each of chloroform, distilled water, ethanol, methanol and petroleum ether in separate conical flasks. The solutions were placed in shaker for 24hrs so as to shake them properly. All these five extracts were filtered through Whatman filter paper no. 44 and evaporated in the water bath at 65º C. The extracts were dissolved in 2% DMSO to make the final concentration (1mg /ml), which kept in refrigerator till further use (6).

Test Microorganisms used: The total five test organisms were used in the present study, which included Gram positive bacteria (*Staphylococcus aureus (isolate)* and *Propionibacterium acne (isolate))*, Gram negative bacteria (*Pseudomonas aeruginosa* MTCC 741 and *Escherichia coli*-MTCC 483*)* and yeast (*Candida albicans*- MTCC 183).

Preparation of the microbial inoculums: The density of test bacteria and yeast was adjusted equal to that of the 0.5 McFarland standards (1.5×10^8 CFU/ml) by adding sterile distilled water. McFarland standards were used as a reference to adjust the turbidity of microbial suspensions so that the number of microorganisms may be within a given range. For the preparation of the 0.5 McFarland standard, 0.05 ml of 0.17%w/v $BaCl_2.2H_2O$ was added to 9.95 ml of 0.18M H_2SO_4 (1.0% w/v) with constant stirring. The McFarland standard tube was tightly sealed to prevent loss by evaporation and stored for up to 6 months (7).

Antimicrobial Activity: The antimicrobial activity of five different extracts of Amla (*Emblica officinalis*) against five test microorganisms was evaluated by using Agar well diffusion method.

Antibiotic susceptibility pattern of test microorganisms used: Antibiotic susceptibility testing against test strains was done according to Kirby-Bauer Disc Diffusion assay. Autoclaved medium (Nutrient Agar for gram negative bacteria i.e. *E. coli* and *P. aeruginosa*, Brain Heart Infusion Agar (BHI) for *Propionibacterium acne*, Mannitol Salt Agar medium for *S. aureus* and Malt extract Agar medium for *C. albicans*) was poured in sterile Petri plates thereafter the antibiotic disk diffusion assay was carried out after 24 hours.100µl standardized culture was spread on these agar plates. Antibiotic Hexa discs of Hi-Media were placed on the inoculums seeded plates. After incubation for 24 hrs at 37ºC, the plates were observed. If antimicrobial activity was present on the plates; it was indicated by an inhibition zone surrounding the disc. The zone of inhibition was measured and expressed in millimeters (8).

Determination of MIC, MBC and MFC of most potent plant extract: For MIC (Minimum Inhibitory Concentration), the macro-dilution agar method, a two-fold serial dilution of the plant extract was prepared in sterile distilled water to achieve a decreasing concentration ranging from 1mg/ml to 0.03125mg/ml in different tubes. Sterile cork borer

of 6.0 mm diameter was used to bore well in pre-solidified medium agar plates and 50-100µl volume of each dilution was added aseptically into the wells made in agar plates in triplicate that had test bacteria and yeast seeded with the standardized inoculums (1.5× 10^8 CFU /ml). 50-100µl solvent was introduced into the well used as control. All the test plates were incubated at 37ºC for bacteria and 35ºC -37ºC for yeast and were observed for the growth after 24 hrs. The lowest concentration of an extract showed a clear zone of inhibition was considered as the MIC. The MIC plates were further incubated for 24-48hrs (9). The lowest concentration that yields no growth following this further incubation was the MBC (Minimum Bactericidal Concentration). The same method was used for antifungal activity. The standardized fungal inoculum was used. The inoculated plates were incubated at 35ºC-37ºC for the *Candida albicans* growth. The above mentioned procedure was done for the fungal strain. The lowest concentration that yields no growth following further incubation of MIC plates was considered as the MFC (Minimum Fungicidal Concentration).

Synergistic activity of plant extract/s and commercially available antibiotic: The bacterial cultures were grown in culture broth at 37ºC. After growth, each bacterium was inoculated on the surface of MHA agar plates. Subsequently, the antibiotic disk of 6 mm diameter was placed on the surface of each inoculated plate and then added 20µl of plant extract (at a concentration of 1mg/ml), to identify synergistic effect between the plant extract and antibiotic used. The plates were incubated at 37ºC for 24 hrs .The diameter of clearing zones was measured (9).

Phytochemical analysis of most potent plant extract: Freshly prepared extract was subjected to standard phytochemicals analysis to find the presence of the following phytoconstituents phenols, flavonoids, alkaloids, glycosides, tannins, saponins, carbohydrates, phytosterols, proteins and steroids by using Mayer's test, Molisch's test, Modified Borntrager's Test**,** Foam Test, Salkowski's Test, Ferric chloride test, Lead acetate test, Ninhydrin test and copper acetate test (9).

Partial characterization of most potent plant extract: It was done by GC-MS (Gas Chromatography-Mass Spectroscopy). The plant extract was analyzed with the help of GC-MS analyzer (GC Clarius 500 Perkin Elmer).

- On Elite-1 column the data was generated. The carrier gas helium (99.99%) was used at flow rate of 1ml per min in split mode (10: 1). Methanolic sample (2 µl) was injected to column at 250ºC injector temperature.
- Temperature of oven starts at 110ºC and hold for 2 min and then it was raised at rate of 10ºC per min to 200ºC without holding. Holding was allowed for 9 min at 280ºC at program rate of 5ºC per min. Temperature of ion source was maintained at 200ºC.
- The injector temperature was set at 250ºC and detector temperature was set at 280ºC.The mass spectrum of compounds present in samples was obtained by electron ionization at 70 eV and detector operates in scan mode from 45 to 450 Da atomic mass units. A 0.5 seconds of scan interval and fragments from 45 to 450 Da was maintained.
- Total running time was 36 minutes (10). The electron gun of mass detector liberated electrons having energy of about 70eV.The column employed there for the separation of components was Elite 1(100% dimethyl poly siloxane).
- The identity of the components in the extracts was assigned by the comparison of their retention indices and mass spectra fragmentation patterns with those stored on the computer library and with published literatures.NIST08 LIB9, WILEY8 LIB10 library sources were also used for matching the identified components from the plant material (11).

Result

The present study revealed the scientific validation of natural products as an antibacterial and antifungal agent. The five solvents viz. Ethanol, methanol, chloroform, distilled water and petroleum ether were used for the extraction from Amla (*Emblica officinalis*) and used for antimicrobial activity against tested microbial strains. Methanolic extracts of *Emblica officinalis* showed maximum zone of inhibition i.e. 27 mm, while aqueous extract of *Emblica officinalis* was most effective against *S. aureus* (28 mm). Ethanol extract of *Emblica officinalis.* was most effective against *C. albicans* (29 mm). Antimicrobial activity of *Emblica officinalis* extracts was compared with antibiotics and *Emblica officinalis* methanolic extract was the most promising plant having maximum effective antimicrobial activity against all tested microorganisms as shown in Table-1 and Fig.-1. For the antibiotic susceptibility pattern, Gentamicin was the most effective for Gram positive test bacteria, whereas Amikacin was the most effective antibiotic for Gram negative test bacteria and Clotrimazole for test fungal strain as shown in Table-2.

MIC and MBC of methanolic extract of *Emblica officinalis* against the microbial strains was ranged between 0.50 to 0.03125 mg/ml as shown in Table-3 and Fig.-2.

Synergistic effect of methanolic extracts of *Emblica officinalis* with antibiotics against tested microorganisms showed that the zone of inhibition was found to be greater when compared to zone of inhibition of different antibiotics used alone. As shown in Table-4, for Gram positive bacteria *S. aureus*, the methanolic extract of *Emblica officinalis.* with Gentamicin showed the synergism of zone of inhibition of 29 mm. For *P. acne,* the synergism between *Emblica officinalis* with Gentamicin was observed with zone of inhibition of 30 mm. In case of Gram negative bacteria *E. coli,* the methanolic extract of *Emblica officinalis* with Amikacin showed the synergism of zone of inhibition of 30 mm. For *P. aeruginosa*, the synergism between *Emblica officinalis* with Amikacin was observed with zone of inhibition of 30 mm. In case of *C. albicans,* there was no synergism effect observed for *Emblica officinalis* to the Clotrimazole as shown in Table-4.

Phytochemicals analysis of *Emblica officinalis* included Alkaliods, Saponins, Glycosides, Proteins, Phenols and Phytosterols respectively as shown in Fig.-3.

Major Phytocompounds along with their uses present in the methanol extract of the *Emblica officinalis* included Cyclopentasiloxane, decamethyl (deodorants, sunblocks and skin

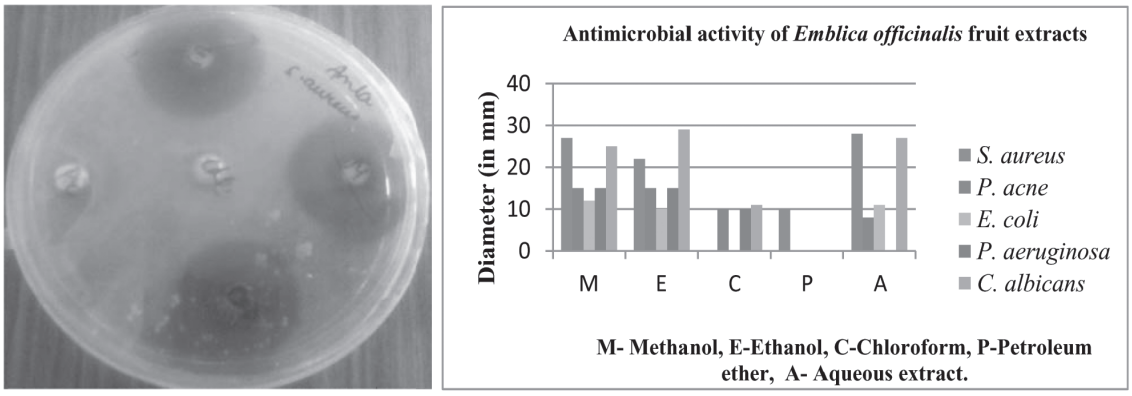

Fig. 1. Antimicrobial activity of *Emblica officinalis* extracts against test microorganisms with Graphical representation.

Table 1. Antimicrobial activity of *Emblica officinalis* fruit extracts

Microorganisms	Diameter of zone of inhibition(mm)				
	Methanolic	Ethanolic	Chloroform	Petroleum ether	Aqueous
S. aureus	27	22	NA	10	28
P. acne	15	15	10	NA	8
E. coli	12	10	NA	NA	11
P. aeruginosa	15	15	10	NA	NA
C. albicans	25	29	11	NA	27

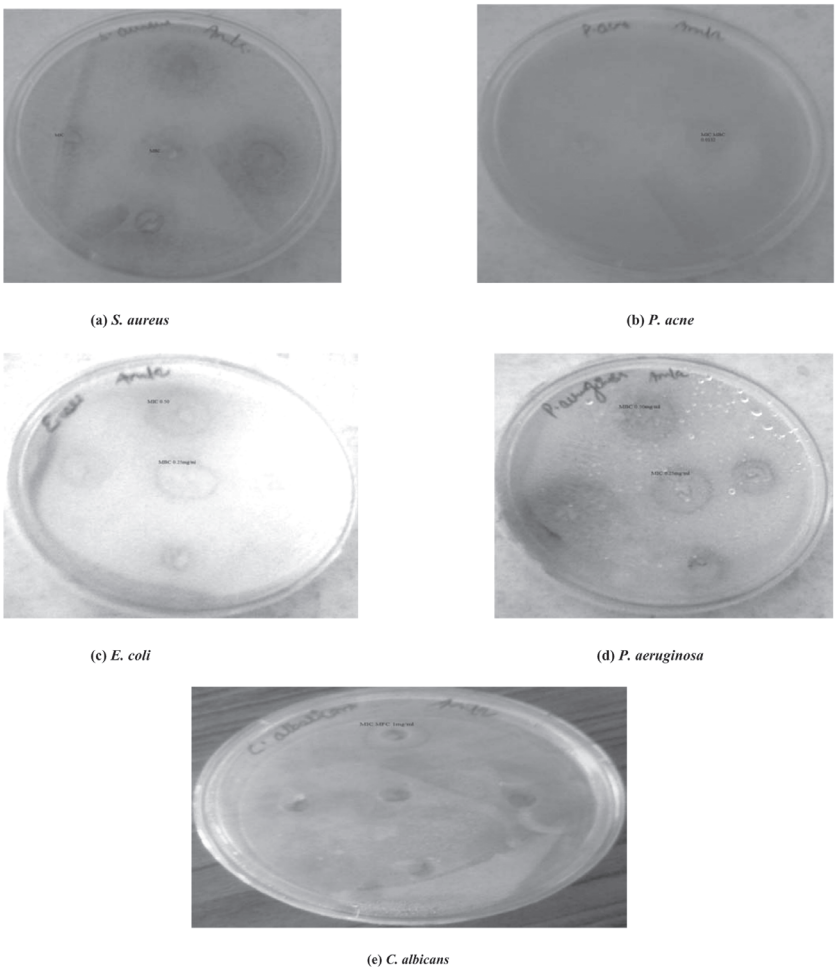

(a) *S. aureus* (b) *P. acne* (c) *E. coli* (d) *P. aeruginosa* (e) *C. albicans*

Fig. 2. MIC, MBC and MFC of methanolic extract of *Emblica officinalis* against test micro-organisms (a) *S. aureus* (b) *P. acne* (c) *E. coli* (d) *P. aeruginosa* and (e) *C. albicans*

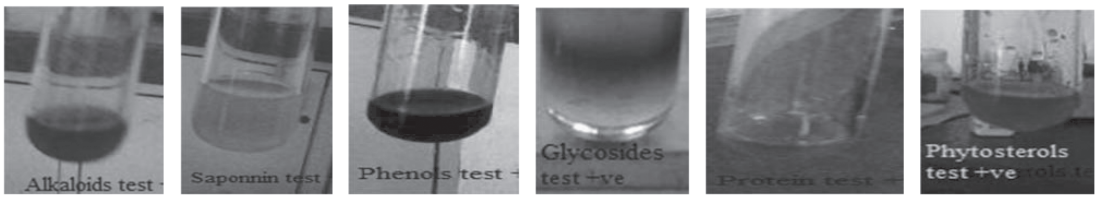

Fig. 3. Phytochemical analysis of methanolic extracts of *Emblica officinalis* (a) Alkaloids test (b) Saponin Test (c) Phenol Test (d) Glycosides Test (e) Protein Test (f) Phytosterols test

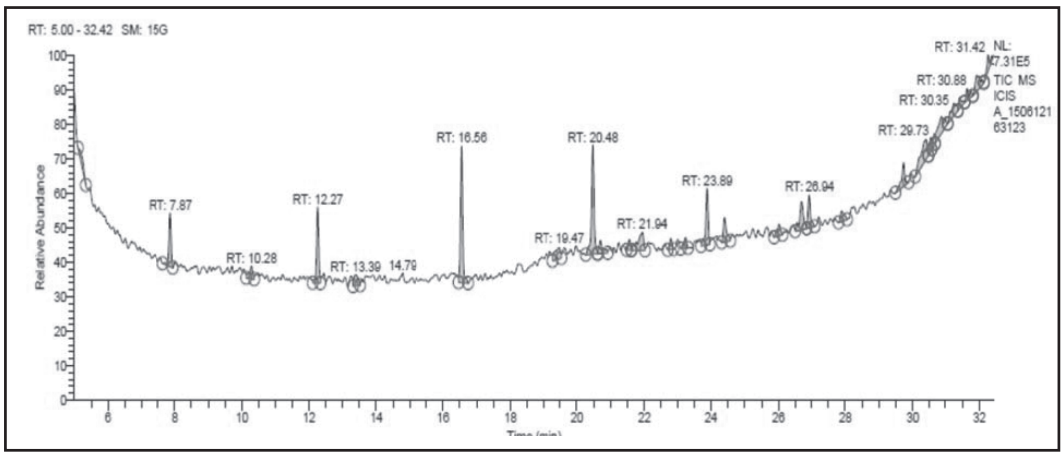

Fig. 4. Total Ion Chromatogram (TIC) of methanol extract of *Emblica officinalis*

care), 3,4 Dihydroxy mandelic acid, ethyl ester, tri TMS(antioxidant), Rhodopin (Carotenoid), Hyocholic acid (precursor for steroid synthesis), Cyclohexasiloxane, dodecamethyl12 (Conditioning agent, emollient, defoaming agent and lubricant.), 6,9,12,15 Docosatetraenoic acid, methyl ester (essential fatty acid and abundant in retina and brain), Cycloheptasi-loxane, tetradecamethyl Anti-caking agent and Skin-Conditioning agent), Cycloocta-siloxane, hexad ecamethyl (skin conditioning agent), Tetradecanoic acid, 9a (acetyloxy) 1a,1b,4,4a, 5,7a, 7b, 8,9,9a decahydro 4a, 7b dihydroxy3 (hydroxymethyl) 1,1,6,8tetramet Hyl5oxo1 Hcyclopropa [3,4] benz [1,2e] azulen9yl ester (Cosmetic and topical medicinal preparations where good absorption through the skin is desired, Cyclonanosiloxane,octadecamethyl(Textile,polishes and waxes, electronics manufacture, monomer in the production of polysiloxanes and laboratory reagent),Heptasiloxane,1 ,1,3,3,5, 5,7,7,9,9,1 1, 11, 13, 13 tetradecamethyl(bioaccumulative), Hexasiloxane, 1,1,3,3,5,5,7,7,9,9,11,11 dodecamethyl (Lubricant and de-foaming agent), 9,12,15 Octadecatrienoic acid,2,3bis [(trimethylsilyl)oxy] propyl ester,(Z,Z,Z) (tumor growth suppressor), Ethyl isoallocholate (Antimicrobial, Diuretic Anti-inflammatory, Antiasthma), 1Heptatriacotanol (Antimicrobial) and 2[4methyl6 (2,6,6 tri methyl yclohex1enyl) hexa1,3,5trienyl] cyclohex 1en1carboxaldehyde (cosmetic products soaps, eaudetoilettes, after shaves and deodorants allergen) and 1Monolinoleoylglycerol trimethylsilyl ether (Ether compound antimicrobial, antioxidant, antiinflammatory). The compounds identified by GC-MS analysis of methanolic extract of *Emblica officinalis* are useful as the conditioning agent,

emollient, defoaming agent, lubricant, antimicrobial, diuretic anti-inflammatory, antiasthma, lubricant, de-foaming agent and skin conditioning agent (Fig-4).

Discussion

The result of the aqueous extract of *Emblica officinalis* in terms of zone of inhibition diameter against *S. aureus* were better than the findings of (12), perhaps due to the fact that they demonstrated the antimicrobial activity of *Emblica officinalis* on the basis of phytochemicals constituents of seeds extracts of *Emblica officinalis*. For *C. albicans*, the result was better for the ethanolic extracts of *Emblica officinalis* than the findings of (13). They demonstrated the antimicrobial and anticandidal activity of *Emblica officinalis* by taking 100 g of powered plant sample, extracted with 200 ml of ethanol using the Soxhlet apparatus whereas 5g sample in 50 ml of ethanol using water bath apparatus was taken in this study and even then obtained better results.

The reason for different sensitivity between Gram positive and Gram negative bacteria could be ascribed to the morphological differences between these microorganisms; Gram negative bacteria having an outer polysaccharide membrane carry the structural lipopolysaccharide components. As discussed by (14), this makes cell wall impermeable to lipophilic solutes, the Gram positive are more susceptible having only an outer peptidoglycan layer which is not effective permeability barrier.

The results of screening revealed that the most of the plant extracts were active against

Table 2. Antibiotic susceptibility pattern of test microorganisms

Antibiotic- Symbol (concentration)	Zone of inhibition (in mm)				
	Gram positive bacteria		Gram negative bacteria		Fungus
	P. acne	*S. aureus*	*E. coli*	*P. aeruginosa*	*C. albicans*
Ciprofloxacin- CIP(5mcg)	32mm	19 mm	—	—	—
Gentamicin-GEN(10 mcg)	28 mm	24 mm	19 mm	20mm	—
Vancomycin-VA(30 mcg)	26 mm	23 mm	—	—	—
Linezolid- LZ(30mcg)	11 mm	39 mm	—	—	—
Ampicillin- AMP 10 10 mcg	10 mm	8 mm	25 mm	22 mm	—
Streptomycin-S10(10 mcg)	15 mm	18 mm	—	—	—
Amikacin- AK(30 mcg)	26 mm	30 mm	—	—	—
Tetracycline-TE(30 mcg)	—	—	21 mm	25 mm	—
Chloramphenicol-C(30 mcg)	—	—	26 mm	16 mm	—
Cotrimoxazole-CO(25 mcg)	—	—	21 mm	22 mm	—
Clotrimazole- CC (10mcg)	—	—	—	—	15mm
Micanazole- MIC(30mcg)	—	—	—	—	No zone
Nystatin- NS(50mcg)	—	—	—	—	No zone

Table 3. Minimum Inhibitory Concentration (MIC), Minimum Bactericidal Concentration (MBC) and Minimum Fungicidal Concentration (MFC) values of methanol extract of *Emblica officinalis*

S. No.	Microorganisms	Plant Extract	MIC (mg/ml)	MBC (mg/ml)	MFC (mg/ml)
1.	*S. aureus*	*Embliica officinalis*	0.50	0.25	-
2.	*P. acne*	*Emblica officinalis*	0.0312	0.0312	-
3.	*E. coli*	*Emblica officinalis*	0.25	0.50	-
4.	*P. aeruginosa*	*Emblica officinalis*	0.25	0.50	-
5.	*C. albicans*	*Emblica officinalis*	1	-	1

Table 4. Synergistic activity of methanolic extract of *Emblica officinalis* with antibiotics

S. No.	Microorganisms	Plant extract + Antibiotic	Zone of inhibition (mm)	Comparative Effect on zone of inhibition
1.	*S. aureus*	*Emblica officinalis* + Gentamicin	29 mm	Activity increases
2.	*P. acne*	*Emblica officinalis* + Gentamicin	30 mm	Activity increases
3.	*E. coli*	*Emblica officinalis* + Amikacin	30 mm	Activity increases
4.	*P. aeruginosa*	*Emblica officinalis* + Amikacin	30 mm	Activity increases
5.	*C. albicans*	*Emblica officinalis* + Clotrimazole	NA	Activity decreases

Gram positive bacteria (*S. aureus and P. acne*) than Gram negative bacteria (*E. coli* and *P. aeruginosa*). In case of antibiotic susceptibility pattern, our results were in agreement with the findings of (15), for the susceptibility test of ciprofloxacin and ampicillin against *S. aureus*, (16), for the susceptibility test of amikacin against *E. coli*, (17), for the susceptibility test of amikacin against *P. aeruginosa* and (18) and for the susceptibility test of clotrimazole against *C. albicans*.

Gupta *et al*. studied the antimicrobial activity of *Emblica officinalis* and found that the MIC values of methanolic extract ranged between 0.025 mg/ml to 0.050 mg/ml against *P. aeruginosa, E. coli* and *S. aureus* which might be due to change in methodology followed and concentration of *Emblica officinalis* extract considered by them (12).

Synergistic effects of extracts of *Emblica officinalis* with antibiotics against tested microorganisms showed that the Zone of inhibition found to be greater when compared to zone of inhibition of different antibiotics used alone i.e ranges from 0.25 mg/ml to 0.50 mg/ml (Table-4). Such synergistic effects could not be traced in the available literature.

Phytochemicals analysis was done by (9) and (19) for methanolic extract of *Emblica*

Table 5: Phytocompounds present in the methanolic extract of the *Emblica officinalis* GC-MS Peak Report TIC

Peak	Retention Time	Chemical formula	Compound	Uses	Cas#
1	7.87	C10H30O5Si5	Cyclopentasiloxane, decamethyl	deodorants, sunblocks and skin care	541026
1	7.87	C16H30O4Si3	Benzoicacid, 2,6-bis[(trimethylsilyl)oxy],trimethylsilyl ester	Not found	3782852
1	7.87	C19H36O5Si3	3,4-Dihydroxymandelic acid, ethyl ester, triTMS	antioxidant	NA
2	10.28	C40H58O	Rhodopin	Carotenoid	105920
2	10.28	C24H40O5	Hyocholic acid	precursor for steroid synthesis	547751
3	12.27	C12H36O6Si6	Cyclohexasiloxane, dodecamethyl12	Conditioning agent, emollient, defoaming agent and lubricant.	540976
4	13.39	C20H13N5O2	2,7- Diphenyl1,6-dioxopyridazino[4,5:2',3'] pyrrolo[4',5'd] Pyridazine	Undergo direct nucleophilic addition and substitution reactions	91757061
4	13.39	C23H38O2	6,9,12,15-Docosatetraenoic acid, methyl ester	essential fatty acid and abundant in retina and brain.	17364340
5	16.56	C14H42O7Si7	Cycloheptasiloxane, tetradecamethyl	Antimicrobial Agents in Cosmetics	107506
6	19.47	C25H42N4O4	2-Nonadecanone 2,4-dinitrophenylhydrazine	sensitive to shock and friction	28813618
7	20.48	C16H48O8Si8	Cyclooctasiloxane, hexadecamethyl	Antimicrobial Agents in Cosmetics	556683
7	20.48	C14H42O5Si6	Hexasiloxane, tetradecamethyl	Antioxidants	107528
8	21.94	C36H56O8	Tetradecanoic acid, 9a(acetyloxy)1a,1b,4,4a,5,7a,7b,8,9,9adecahydro4a,7b dihydroxy3(hydroxymethyl) 1,1,6,8 tetramet Hyl 5-oxo,1-Hcyclopropa[3,4]benz[1,2e] azulen9yl ester.	Cosmetic and topical medicinal preparations where good absorption through the skin is desired	16561298

9	23.89	C18H54O9Si9	Cyclononasiloxane, octadecamethyl	Textile, polishes and waxes, electronics manufacture, monomer in the production of polysiloxanes and laboratory reagent.	556718
10	26.94	C14H44O6Si7	Heptasiloxane, 1,1,3,3,5,5,7,7,9,9,11,11,13,13-tetradecamethyl	bioaccumulative	19095239
10	26.94	C12H38O5Si6	Hexasiloxane,1,1,3,3,5,5,7,7,9,9,11,11dodecamethyl	Lubricant and de-foaming agent.	995824
11	29.73	C27H52O4Si2	9,12,15Octadecatrienoic acid,2,3bis[(trimethylsilyl)oxy]propyl ester,(Z,Z,Z)	tumor growth suppressor	55521227
11	29.73	C20H13N5O2	2,7Diphenyl1,6dioxopyridazino[4,5:2',3']pyrrolo[4',5'd] Pyridazine	Pipeline	91757061
12	30.35	C20H13N5O2	2,7Diphenyl1,6dioxopyridazino[4,5:2',3']pyrrolo[4',5'd] Pyridazine	pipeline	91757061
12	30.35	C26H44O5	Ethyl isoallocholate	Antimicrobial, Diuretic Anti-inflammatory, Antiasthma	NA
13	30.88	C37H76O	1Heptatriacotanol	Antimicrobial	105794589
14	31.42	C23H32O	2[4methyl6(2,6,6trimethylcyclohex1enyl)hexa1,3,5trienyl] cyclohex1en1carboxaldehyde	cosmetic_products soaps, eaude toilettes, after_shaves and deodorants and allergen.	NA
14	31.42	C27H54O4Si2	1Monolinoleoylglycerol trimethylsilyl ether	Antimicrobial Antioxidant Antiinflammatory Antiarthritic Antiasthma, Diuretic	54284456

Vol. 12 (4) 355-366, October 2018, ISSN 0973-8916 (Print), 2230-7303 (Online)

officinalis. All the prepared plant extract were subjected to preliminary screening for the presence of alkaloids,tannins, saponins, glycosides, proteins, phenols, carbohydrate, diterpenes, phytosterols and Flavonoides. The methanolic extract of *Emblica officinalis* includes alkaliods, saponins, glycosides, proteins, phenols and phytosterols, respectively. (20) also studied the phytochemicals present in *Emblica officinalis* and found the presence of quercetin, phyllaemblic compounds, gallic acid, tannins, flavonoids, pectin, and vitamin C and also contain various polyphenolic compounds. The results may be varied due to the solvent selection and the methodology followed.

GC-MS analysis was used for the analysis and identification of the bioactive compounds present in the *Emblica officinalis*. GC-MS analysis for *Emblica sp.* revealed the presence of the octasiloxane, hexadecamethyl, cyclononasiloxane, octadecamethyl, heptasiloxane, tetradecamethyl**,** octadecatrienoic acid, ethyl isoallocholate, phthalic acid, 2-cyclohexylethyl butyl ester**,** rhodopin, benzoic acid and hyocholic acid. (21) also studied the GC-MS analysis of methanolic extract of *Emblica officinalis* and found the presence of flavonoids, carbohydrates and saponins. The results were slightly varied because of the GC-MS analyzing methodology.

Conclusion

In this way, this study revealed the methodology and identification of the bioactive compounds present in the *Emblica officinalis* which were responsible for their antimicrobial activity against skin associated microorganisms. The use of crude drugs of *Emblica officinalis* as an agent to control microbial strains needs further extensive research for their better economic and therapeutic utilization. Thus, the present study reflects a hope for the development of novel agents of biomedical importance.

Acknowledgements

The authors are thankful to the Chairman, Director and Principal of the Ambala College of Engineering and Applied Research (ACE, Devsthali, Ambala, Haryana, India) for providing excellent facility to carry out this research project. The authors are very grateful to Dr. P. K. Singh, Principal Scientist, ICAR-National Bureau of Animal Genetic Resources, Karnal, Haryana, India for encouraging us to write this research article.

References

1. Hendriks, F.M. (2005). Mechanical behaviour of human epidermal and dermal layers in vivo, 1st edn, (Eindhoven: Technische Universiteit Eindhoven, The Netherlands).
2. Aneja, K.R., Jain, P. and Aneja, R. (2008). A textbook of Basic and Applied Microbiology, 1st edn, (New Age International (P) Ltd.).
3. Jagtap, S.D., Deokule, S.S., Pawar, P.K., Kuvalekar, A.A. and Harsulkar, A.M. (2010). Antimicrobial Activity of some crude herbal drugs used for skin diseases by Pawra tribes of Nandurbar district, Indian J Nat Prod Resour, 1(2): 216-220.
4. Kumar, K.P.S., Bhowmik, D., Amitsankar, D., Yadav, A.P., Paswan, S., Srivastava, S. and Deb, L. (2012). Recent trends in potential traditional Indian herbs *Emblica officinalis* and its medicinal importance, J Pharmacogn Phytochem, 1(1): 24-32.
5. Dasaroju, S. and Gottumukkala, K.M. (2014). Current trends in the research of *Emblica officinalis* (*Amla*):A Pharmacological perspective, Int J Pharm Sci Rev Res, 24(2): 150-159.
6. Harborne, J.B. (2008). Phytochemical methods: A guide to modern techniques of plant analysis, 3rd Indian edition (Springer, New Delhi).
7. Andrews, J.M. (2001). Determination of minimum inhibitory concentration, J Antimicrob Chemother, 48: 5.

8. Bauer, R.W., Kirby, M.D.K., Sherris, J.C. and Turck, M. (1966). Antibiotic susceptibility testing by standard single Disk-Diffusion method, A J Clinical Pathol, 45: 493-496.

9. Tiwari, P. Kumar, B. Kaur, M. Kaur, B. and Kaur, H. (2011). Phytochemical screening and Extraction: A Review, Internationale Pharmaceutica Sciencia,1(1):98-106.

10. Manickam, D. and Latha, P. (2014). GC-MS analysis of methanol extract of Analysis of *Decalepis Hamiltonii root (*Wight & Arn), W J P P S, 3(4): 983-989.

11. Sen, A. and Batra, A. (2012). Chemical composition of methanol extract of the leaves of Melia *Azedarach L,* Asian J Pharm Clin, 5(3): 42-45.

12. Gupta, P., Nain, P. and Sidana, J. (2012). Antimicrobial and antioxidant activity of *Emblica officinalis* seed extract, Int J Res Ayurveda Pharm, 3(4): 591-96.

13. Aggrawal, M.K., Goyal, S.K., Varma, A.K. and Varma, A. (2014). Antibacterial and anticandidal screening of certain traditionally used Indian medicinal plants against Multidrug resistant human pathogens, I J S N, 5(3): 423-432.

14. Scherrer, R. and Gerhardt, P. (1971). Molecular sieving by the Bacillus megaterium cell wall and protoplast, Journal of Bacteriology, 107: 718-735.

15. Jahan, F., Lawrence, R., Kumar, V., and Junaid, M. (2011). Evaluation of Antimicrobial Activity of Plant Extracts on Antibiotic Susceptible and Resistant *Staphylococcus aureus* Strains, J Chem Pharm Res, 3(4): 777-789.

16. Mos, I., Micle, O., Zdranca, M., Dranca, Muresan M. and Vicas, L. (2015). Antibiotic Sensitivity of the *Escherichia coli* Strains Isolated from Skin Wounds, *Farmacia*, 58 (5): 637-645.

17. Nagma, F.S., Prabhu, N., Jeevitha, T., Rithik, R. and Uma, A. (2014). Noscomial Bacteremia Caused by *Pseudomonas aeruginosa:* Sensitive to Antibiotics and Risk Factors, *Pharmacophore*, 5(1): 69-76.

18. Saranya, S.A., Moorthy, K., Malar, S.S.A.S., Punitha, T., Vinodhini, R., Bhuvaneshwari M. and Kanimozhi, C. (2014). Prevalence and Antifungal Susceptibility Pattern of *Candida albicans* from Low Socio-economic Group, Int J Pharm Pharm Sci, 6(2): 158-162.

19. Tiwari, P., Kumar, B., Kaur, M., Kaur, G. and Kaur, H. (2011). Phytochemical screening and Extraction: A Review, Internationale Pharmaceutica Sciencia, 1(1): 98-106.

20. Singh, E., Sharma, S., Pareek, A., Dwivedi, J., Yadav, S. and Sharma, S. (2011). Phytochemistry, traditional uses and cancer chemo-preventive activity of Amla (*Phyllanthusembllica*): The Sustainer, J App Pharm Sci, 02(01): 176-183.

21. Singh, N., Mathur, C., Sase, N.A., Rai, S. and Abraham, J. (2015). Pharmaceutical Properties of *Emblica officinalis*and *Phyllanthusembllica* extracts, R J P B C S, 6(1): 1008.

Current Trends in Biotechnology and Pharmacy
Vol. 12 (4) 367-370, October 2018, ISSN 0973-8916 (Print), 2230-7303 (Online)

Protein Characterization at atomic level: A Novel approach for sequence analysis

Parul Johri[1*], Mala Trivedi[1], Drishti Srivastava[1], Aman Kumar Singh[1] and Mohammed Haris Siddiqui[2]

[1]Amity Institute of Biotechnology, Amity University Uttar Pradesh,
Lucknow Campus, Malhaur, Gomti Nagar Extension, Lucknow, Uttar Pradesh, India
[2]Department of Bioengineering, Integral University Lucknow Uttar Pradesh, India
* Corresponding Author: pjohri@lko.amity.edu; +91 9838144680

Abstract

Carbon being the most omnipresent element in all the organic compounds is of great importance with regards to its structure and function. The fundamental structure of protein is composed of amino acids arranged in linear chain and folded to a globular form. All twenty amino acids consist of combination of only five different atoms that are Carbon, Nitrogen, Oxygen, Hydrogen and Sulphur. Depending on the property of their side chain the amino acids are classified as hydrophobic and hydrophilic. The allocation of the hydrophobic residue in a protein contributes majorly towards protein folding, protein interaction , active site formation and other biological functions. As carbon is the most important element which contributes to hydrophobic interaction in proteins, the hydrophobic amino acids characteristically have greater number of carbon atoms. In the present study, we have analyzed 4,306 protein sequences of *Escherichia coli,* a gram negative, facultative anaerobic, rod shaped bacterium. All the protein sequences of *Escherichia coli* were scanned to get a profound view on carbon content and its distribution. The sequences were retrieved from proteome section of UniprotKB (http://www.uniprot.org/uniprot/) database and atomic percentages were calculated with the aid of a dynamic programming algorithm and Microsoft Excel. The analysis of the atomic percentages calculated for the proteins revealed that there is a precise range of carbon percentage for all the *Escherichia coli* proteins (30%-33% carbon) .Also the different categories of protein like transport protein, repressor protein , catalytic protein, inhibitory protein etc have discrete range of carbon percentages which could be further linked to their exact activity

Keyword : *Carbon, E. Coli, dynamic programming, proteins.*

Introduction:

Proteins make almost 50% of the dry weight of the cells and are present in profound amount, than any other biomolecules. Proteins are basically organic compounds composed of amino acids arranged in linear chain and folded to a globular form (1). All 20 amino acids consist of combinations of only five different atoms Carbon, Nitrogen, Hydrogen, Sulphur, Oxygen. Depending on the properties of their side chains, the amino acids are classified as hydrophobic and hydrophilic (2; 3; 4). The distribution of hydrophobic residues in a protein contributes majorly towards protein folding, protein interactions, formation of core, active side formation and other biological functions (5).

Materials and Methods:

A hydropathy plot maps the hydrophobic regions against the hydropathy indices of the amino acids in the protein. It gives a clear idea of level of hydrophobicity in a protein. The hydrophobicity and carbon distribution profile of a protein is studied with help of a hydropathy plot (Fig. 1 and Fig. 2). In the carbon distribution profile

obtained, it was possible to locate the hydrophobic, hydrophilic and also the active sites in the protein. The hydropathy plot does not give information on the active sites of a protein (6; 7; 8; 9). So it was postulated that the carbon distribution profile is a better alternative to hydropathy plot.

Escherichia coli, a gram negative, facultative anaerobic, rod shaped bacterium was the model organism used by us in our study. The entire project commenced by the retrieval of protein sequences of *Escherichia coli* from the public repository of protein sequences i.e UniprotKB database(http://www.uniprot.org/uniprot/). There were 4,306 protein sequences of *Escherichia coli(*strain K12) present in the proteome section of the database. Each and every sequence was scanned by us using the script written in perl

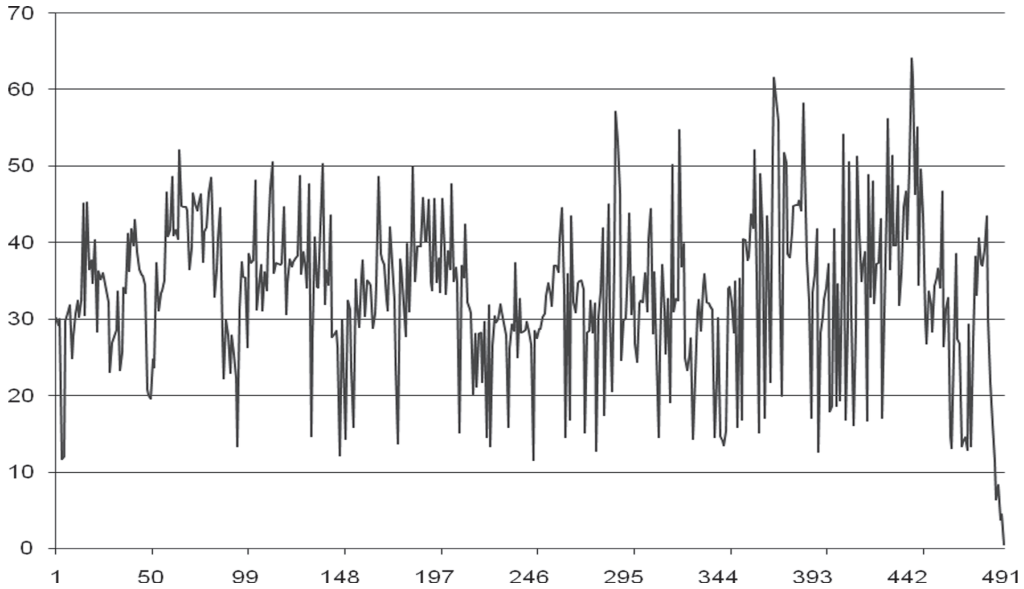

Fig. 1: Carbon distribution plot for GLUT1

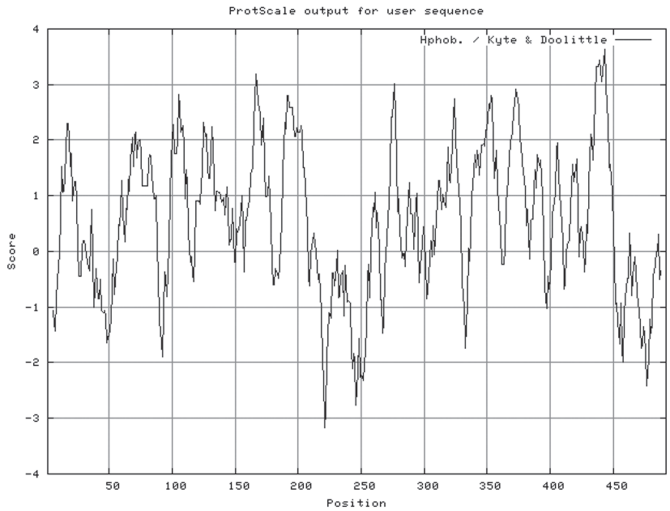

Fig. 2: Hydropathy plot from Protscale for GLUT1

programming based on the dynamic algorithm designed (Fig. 3) (10; 11; 12; 13). So the atomic composition of each and every protein sequence was extracted and were formulated into the excel sheet. After that the respective percentage of carbon was calculated on basis of number of carbon atoms and number of total atoms present in every protein sequences.

Proteins were also classified into broad categories on basis of their function like transport protein, catalytic protein, regulatory protein etc.

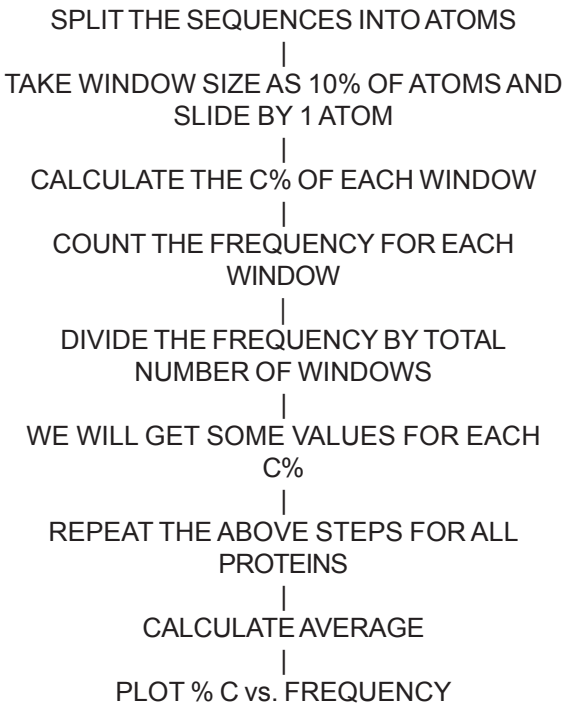

Fig. 3: Flow chart for the dynamic programming algorithm

The scrutiny of the atomic percentages calculated for the proteins revealed that there is a specific range of carbon percentage for all the *Escherichia coli* proteins that is 30%-33%. Broad classification of proteins also showed that all proteins strictly followed the range.

Results and Discussion:

We got amazing results from our research work. Carbon percentages in all the protein sequences lied between 30%-33% no matter which types of amino acids where present in protein sequences (Table 1). So we can conclude that on the basis of carbon atoms, demarcation can be done. And after analyzing the carbon content in every proteins, percentages of other components can be taken out and studied for further uses. The atomic level analysis of the protein sequence does lead to a new venture of scrutiny of many long stranded questions.

The arenas of molecular biology, pharmacy, drug designing, enzymology, proteomics and many other fields including genetics and phylogenetic are wedged on certain facets which can possibly be answered by the carbon content analysis of protein sequences. The carbon level analysis of protein sites for post translational modification would lead towards new and profound ways of understanding them (14).

Carbon percentage in protein sequence would be the next parameter for prediction of secondary protein structure. Developments in microarray technologies, which would be based on the carbon content of protein, are required. Chromatography techniques which imply carbon as a parameter may also evolve. Drug development and designing must be implied for detection of active site and potential drugs based on carbon content. The development of tool for prediction of ligand binding site in globular proteins, based on average carbon percentage and distribution, was developed for mouse mitochondrial aspartate aminotransferase. This technique has huge potential to further develop for a large spectrum of proteins (15).

Table 1: Carbon percentages in various types of proteins in *E. coli*

S.No	Types of Protein	Range of Carbon (%)
1	Regulatory proteins	29.95%-32.32%
2	Catalytic Proteins	30.82%-32.97%
3	Transport protein	30.37%-32.15%
4	Enzymatic proteins	29.91%-33.65%
5	Transfer proteins	31.13%-32.58%

A new and fascinating concept is of **'Carbon bar coding'.** The concept is to make carbon as the stricture for width of bars. The protein sequence may be converted into its carbon bar code which would be universal. This presentation would be path breaking and very convenient size wise.

Acknowledgement:

Authors are grateful to Dr. A. K. Chauhan, Founder President & Mr. Aseem Chauhan, Chancellor Amity University Haryana & Chairperson Amity Lucknow for providing necessary facilities and support. We also extend our gratitude to Maj. Gen. K.K Ohri, AVSM (Retd.), Pro Vice Chancellor, Amity University, Uttar Pradesh Lucknow Campus for constant support and encouragements.

References

1. Johri, P. and Gokhale, M. (2013). A New Perspective for Sequence Analysis – Carbon content. Research and Review: Journal of Computational Biology, 2:1-6.
2. Rajasekaran, E., Akila, K. and Vennila, J.J. (2011). Carbon Contents of H1N1 Proteins**.** International Conference on Biosciences, Biochemistry and Bioinformatics, 5:27-29.
3. Akila, K. and Rajasekaran, E. (2009). What Might be the Difference in Viral Proteins? International Journal of Bioinformatics Research,1:1-3.
4. Rajasekaran, E., Asha, J. and Klaus, H. (2012). Magnitude of Thymine In Different Frames of Messenger RNAs. International Journal of Bioinformatics Research, 4:273-275.
5. Senthil, R., Sathish, S., Vennila, J.J. and Rajasekaran, E. (2011). Prediction of Ligand Binding Site in Globular Proteins. Journal of Advance Bioinformatics Application and Research, 2:98-99.
6. Akila, K., Kaliaperumal, R. and Rajasekaran, E. (2012).Carbon Distribution to Toxic Effect in Toxin Proteins. Bioinformation Discussion at the Interface of Physical and Biological Science, 8:720-721.
7. Rajasekaran, E. and Vijayasarathy, M. (2011). CARBANA: Carbon Analysis Program for Protein Sequences. Bioinformtaion, 5:455-457.
8. Rajasekaran, E. (2012) CARd: Carbon Distribution Analysis Program for Protein Sequences. Bioinformation, 8:508-512.
9. Chase, M.W. and Fay, M.F. (2009). Barcoding of Plants and Fungi. Science, 325:682-683.
10. Nsimama, P.D., Mamboya, A.F., Amri, E. and Rajasekaran, E. (2012). Corelation Between The Mutated Colour Tunings and Carbon Distributions in Luciferase Bioluminescence. Journal of Computational Intelligence In Bioinformatics, 5:105-112.
11. Rajasekaran, E., Rajadurai, M., Vinobha, C.S. and Senthil, R. (2008). Are The Proteins Being Hydrated During Evolution ? Journal of Computational Intelligence In Bioinformatics,1:115-118.
12. Akila, K., Sneha, N. and Rajasekaran, E. (2012). Study of Carbon Distribution at Protein Regions of Disorder. Journal of Bioscience, Biochemistry and Bioinformatics, 2:58-60.
13. Johri, P., Trivedi, M. and Siddiqui, M.H, and Gokhale, M. (2016). A Study On The Presence and Distribution of Carbon Percentage in and Around the Sites of Glycosylation for Eukaryotic Proteins. Journal of Chemical and Pharmaceutical Research, 8:52-63.
14. Johri, P., Trivedi, M., Singh, A. and Siddiqui, M.H. (2016). Towards The Atomic Level Protein Sequence Analysis. Journal of Chemical and Pharmaceutical Research, 8:204-207.
15. Johri, P. (2013). Atomic Level Sequence Analysis- a Review. International Journal of Computational Bioinformatics and Insilco

Current Trends in Biotechnology and Pharmacy
Vol. 12 (4) 371-376, October 2018, ISSN 0973-8916 (Print), 2230-7303 (Online)

Molecular Phylogenetic Analysis of Indian Apple Snail

Silpi Sarkar and S. Krupanidhi
Department of Biotechnology, VFSTR
Vadlamudi, 522213 A P, India
Corresponding author : krupanidhi.srirama@gmail.com

Abstract

Apple snails (Ampullariidae) belong to a diversified freshwater family which occurs in pan-tropical habitats. The Indian apple snail, *Pila globosa* and other operculate snails are grouped in Architaenioglossa which also includes Viviparidae and Cyclophoridae. In our study, a concise relationship of Ampullariidae with Viviparidae and Cyclophoridae has been elucidated by using partial nucleotide sequence of cytochrome b gene. *Pila globosa* was collected from freshwater habitats of Berhampore (West Bengal) and its morphometric analysis is determined as an addendum to its phylogeny. The multiple sequence alignment is performed in MEGA v5.2 to reconstruct molecular affinities within the family, Ampullariidae. The phylogenetic tree is constructed with 1000 bootstrap replications in RAxML software. The outgroup species considered for the analysis in our study is chosen from Heterobranchia as it is a sister group to the clade Caenogastropoda. It is observed that family Ampullariidae formed a nested cluster and showed a polyphyletic affinity with Viviparidae and Cyclophoridae.

Keywords: - *Pila globosa*, Morphometry, Cytochrome b gene, RAxML , MEGA-v5.2

Introduction

The Phylum Mollusca is an extensive group of unsegmented and soft-bodied coelomates which have a prominent ventral foot and dorsal visceral mass (1). Phylum Mollusca consists of seven classes, among which class Gastropoda belongs to large assemblage of soft bodied invertebrates such as slugs and hard shelled snails which are adapted to varied habitats in comparison to rest of the representatives of molluscs (2). The genera of class Gastropoda, represented in all realms as their habitat varies namely benthic, epifaunal, burrowers, pelagic drifters, active swimmers, detritus, sedentary and suspension feeders (3). Gastropods are commercially exploited due to ornamental, edible and medicinal value and thus there is a risk for their sustainability (4). The clade Caenogastropoda as mentioned in taxonomic classification of Bouchet and Rocroi 2005 is the largest and most diverse among the living snails which consist of 136 extant, 65 extinct and 41 superfamilies. Caenogastropoda includes a) Architaenioglossa (Cyclophoridae - a major group of operculate land snails) and b) freshwater families – Ampullariidae and Viviparidae (5). The taxonomic history, affinities and systematic positions within the families namely Ampullariidae, Viviparidae and Cyclophoridae were studied to reconstruct the phylogenetic affinities (6). Thus, the morphology and phylogeny related study would give an insight into the deeper aspects of these families. The evolutionary hypothesis for major groups within the phylum is controversial due to varied habitats adaptability and extreme diversity of the phylum. A recent insight into the correlation and taxonomic identity of the studied genera with the existing findings on caenogastropods by Ponder and Linderberg (1997), Simone (2001, 2004, 2005) and Strong (2002) had been deduced

within this article (7). Ampullariids are freshwater amphibious snails of tropics and sub-tropics of Africa, America and Asian continents, where they are found as major native freshwater molluscan fauna. Our study is based on the characterisation of morphological features which includes morphometric analysis of *Pila globosa* (Ampullariidae) and construction of its phylogenetic affinities using partial nucleotide sequence of cytochrome b, which is a highly conserved representative of mitochondrial enzymes. The MT-Cyb gene provides the necessary instructions to make a protein called cytochrome b. There are 11 components forming group of proteins called complex III among which cytochrome b is one among the 11 components. Complex III performs a step of a process known as oxidative phosphorylation in mitochondria where oxygen and sugars are used in synthesis of adenosine triphosphate (ATP), cells main energy source. During oxidative phosphorylation, the protein complexes which include complex III, carries the production of ATP through a step-by-step transfer of negatively charged particles called electrons. Cytochrome b is mainly involved in the transfer of these negatively charged particles through complex III. In complex III cytochrome b is the only component which is produced from a gene found in the mitochondrial DNA (8).

Materials and methodology

A) Collection of Samples : *Pila globosa,* also known as apple snails, are freshwater dwelling animals habituated in ponds, streams, lakes, rice fields and in rivers. They are collected by skimming from the riverine areas of Berhampore, West Bengal. A total size of ten samples is procured in the months of the monsoon from June to August 2016 because of their abundance in freshwater habitats. The coordinates for the study area are Lat. 24.098 N and Long 88.267 E for specific taxonomical identifications.

B) Maintenance of the samples prior to study **:** The procured snails after collection from the river site are taken to the laboratory, washed properly to remove the dirt and greenish algae attached to its shell, kept in tubs with water and fed them with lettuce and green leaves available from the market (9).The snails are kept for observation for a week to check for their mortality rates. To maintain the health of snails it is appropriate to change the water in the tubs daily.

C) Morphometric Study : The cleaned snails are kept aside over a bed of filter papers separately for 24 hours to remove the excess water. The colouration of *P.globosa* shell is generally pale to dark brownish with a globose shape in appearance. The collected *Pila* specimens are medium, large adults in size, body whorls are 5-6 in number. Morphologically the specimens' shells are transverse with oblique suture, sculpture coarser and less regular. The size and weight of snails are recorded on the live samples and it varied externally (10). The height, width of the *P.globosa* is measured using Vernier callipers to 0.1 mm precision as shown in Fig.1. The shell height (H), shell breadth (B), length of the operculum (LO) and breadth of operculum (BO) of *Pila globosa* are measured. The measurement of length and breadth of operculum provided information on the shell shape and hence the calculated values are determined from the ratio given in Table 1 whether any variation in shape existed within the species of snails which is not possible to visualize by apparent vision. The operculum of *Pila* is hard, concentric and calcareous. Also, the morphometric analysis might give an insight to the characters to be explored for further studies with large sample size. These studies may give the possibility to identify the cryptic species, which are morphologically identical can be hidden in a same species without proper taxonomical classification but literally belonging to different species and cannot interbreed among themselves within a particular geographical region (11).

D) DNA extraction by phenol- chloroform : The snails before dissected are kept aside separately and the snails are narcotized to isolate 0.5 g foot muscle tissue for genomic DNA extraction. Genomic DNA of good quality is vital as it is significant in deciphering the information which can be required to study evolutionary

interrelationships among taxa. There has been a recent study that developed a new methodology to generate high quality genomic DNA from terrestrial gastropod *Achatina fulica* (12). In our study, we followed the total genomic DNA extraction by the well known phenol-chloroform method (13). The purity of the extracted genomic DNA is checked and it is found to be 1.68 ng/ml respectively. The samples are loaded to 0.8% agarose gel prepared in 0.5 X TBE (Tris-Borate-EDTA) buffer which contained 0.5 mg/ml ethidium bromide. The gels are visualized in a UV transilluminator (Genei) and the image is captured under UV light using Gel documentation system (Bio-Rad). For PCR amplification, the 100 ng template DNA is taken (14).

E) PCR amplification : PCR is performed in a 20 µl reaction volume which contained 100 ng template DNA, 5 pmol of each specific primers, 0.2 mM of each dNTPs, 1.0 U *Taq* DNA polymerase and 1X PCR buffer contained 1.5 mM of $MgCl_2$. The PCR is driven for 40 cycles in a Thermal Cycler (Effendorf, Germany). The partial cyt b gene is amplified using the template DNA with reported universal primers (15).The PCR products are run on 1.2% agarose gel prepared in 0.5X TBE buffer containing 0.5 mg /ml ethidium bromide against a DNA ladder. The gel is visualised in UV transilluminator (Genei) and the image is captured under UV light using the gel documentation system (Bio-Rad). The size of amplicon of cytochrome b is found to be 490 bp (Fig.2).

F) Phylogenetic Analysis : The PCR product of cytb (Fig.2) is eluted. The sequencing of the eluted gene is carried by Big Dye Terminator 3.1 v sequencing kit to acquire partial nucleotide sequences of cytb in *P.globosa.* The sequences obtained are annotated and submitted to NCBI. The sequence is given the accession number viz., KR297240. The BLAST analysis is performed to check the similarity and match identity of the species, after which the alignment is done with default parameters in Clustal W algorithm using MEGA v5.2 (16). Regions of excess gaps and lengthy inserts are exempted during the alignment analysis in MEGA. The FASTA format generated is uploaded in ALTER (Alignment Transformation Environment), to be used in RAxML software. The software package RAxML GUI V 1.3 is used in the construction of phylogenetic tree for maximum likelihood analysis. This method is based on a firm statistical principles and is most powerful in recovering correct tree topologies by computer simulation studies. The unpartitioned nucleotide sequences are subjected to ML phylogenetic analysis through RAxML GUI v1.3 software package supported with 1000 bootstrap replications (17). The bipartition file obtained from RAxML is opened in Fig Tree v4 software to obtain the final cladogram.

Results and Discussion

The morphological parameters of *P.globosa* such as weight, colour and shape of shell are

Fig.1 Measurement of height of shell of Pila globosa (H) using a Vernier Callipers.

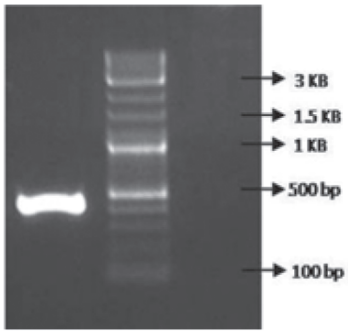

Fig.2. PCR amplification of partial Cyt b gene with an amplicon stretch of 490 bp in 1.2% agarose gel electrophoresis.

given in Table 1. The shell of the *P.globosa* is globose shaped like an apple and hence commonly known as 'Indian Apple snail'. Analyses using morphological and molecular approaches invariably highlight the phylogenetic affinities among the genera of Ampullariidae, Viviparidae and Cyclophoridae (18). The morphometric analysis of snails collected is studied to check whether any unusual variation exists among the population from the Berhampore region. In the present study, 11 species of Architaenioglossa are retrieved based on the available closest sequences of species obtained from GenBank. The representative species of families namely Ampullariidae, Cyclophoridae and Viviparidae are selected to derive phylogenetic affinities. Maximum likelihood (ML) phylogenetic analysis of 12 genera including *P.globosa* belonging to Architaenioglossa is shown in Fig.3 and the derived tree using RAxML tool is rooted on the outgroup taxon namely *Anguispira* (19).The tree does not show nodal support to the genera, *Pomacea* and *Pila* though both of them belong to Ampullariidae and the same might be in compliance with their divergent habitats due to their geographical location. This result also indicated that the ampullariids are polyphyletic within Architaenioglossa as they are clustered with the species of Cyclophoridae and Viviparidae. Our focal taxa, *P. globosa* formed a tertiary cluster with the genera of Viviparidae. Thus, the Maximum Likelihood tree reconstructed with the species of families, Ampullariidae, Viviparidae and Cyclophoridae within the Architaenioglossa is in synchronicity with Ponder and Lindberg's (1997) based topology which is also strongly supported by taxonomical classifications of Bouchet and Rocroi 2005. The bootstrap values of the cladogram supported the clustering of the chosen genera of families of Ampullariidae and Cyclophoridae despite their divergent habitats (20). It is further reported by Healy (1988) that Ampullariidae and Cyclophoridae shared a few specialized features namely eusperm and parasperm (21).

Conclusion

Understanding, the freshwater fauna of gastropods is essential as India has a peculiar diverse biota of invertebrate species which encompasses greater than 99 % animal biodiversity (22). The freshwater gastropods species are representative of Caenogastropoda

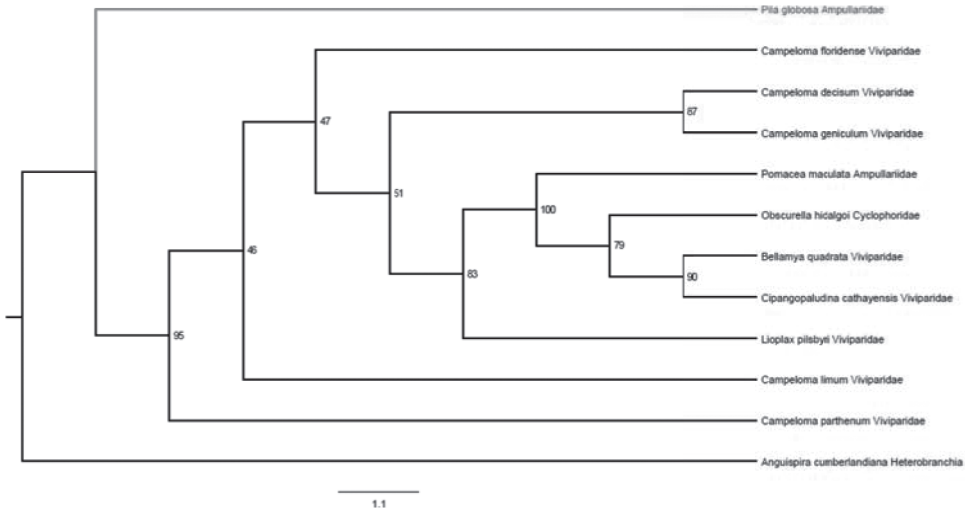

Fig.3. Maximum Likelihood cladogram based on RaXML analysis of the full concatenated dataset on the nucleotide sequence of partial gene, cytochrome b of the chosen gastropod taxa with 1000 bootstrap replications.

Table 1 The morphometric analysis of *Pila globosa* sampled from Berhampore (WB), India.

No. of samples	Snails weight g.	Vol. ml	Height of shell in mm (H)	Height up to 2nd whorl (H2)	Breadth of shell in mm (B)	Length of operculum in mm (LO)	Breadth of Operculumn in mm (BO)	Operculum shape LO/BO	Shell shape H2/B
5	28.82 ±12.56	42.4 ±7.83	46.24 ±4.08	45.60 ±0.38	40.04 ±6.18	35.53 ±2.70	24.44 ±1.40	1.453 ± 1.92	1.13 ±0.061

and pulmonate heterobranchs. In India, phylogeny studies of *Pila globosa* (Ampullariidae) along with other sister taxa families of Cyclophoridae and Viviparidae have not been done previously. In this study, it was found that Ampullariidae is found to be polyphyletic and showed a sister taxon relationship both with Cyclophoridae and Viviparidae although there is no apparent variation among the morphometric study done using the snails from Berhampore West Bengal. Nevertheless, an increase in number of *Pila globosa* from diverse areas is required which needs to be considered to deduce a definitive conclusion. To find out the diversity of Ampullariidae species, which can add to the evolutionary relationships in the reconstruction of phylogeny tree for Indian Apple snails, it is necessary to identify and locate these species through a scaling up process which explores the conservation stragies of freshwater gastropod species in a holistic way.

Acknowledgements:

Prof. S Krupanidhi thanks DST MRP (SB/SO/AS-138/2012), New Delhi India for providing financial support to carry out the work presented in this article. Authors acknowledge DST FIST (2015-20) support to the Department of Biotechnology, VFSTR during the time of which the present work was done.

References

1. Jena, C., Sarkar, S., Jalaja, N. and Krupanidhi, S. (2017).Molecular Phylogenetic relations of *Achatina fulica* based on partial sequence of COI gene. *National Academy of Science Letters.* 40(2):101-103.
2. Sarkar, S. and Sreerama, K. (2018). Phylogenetic Affinities Of Indian Apple Snails- An Insight into the Tibetan Tectonic Terranes. *Proceedings of Zoological Society* 71(2):194-201; https://doi.org/10.1007/s12595-017-0257-4.
3. Rao, S.N.V. (1989). Handbook Freshwater Molluscs of India. Zoological Survey of India, Kolkata, pp 411.
4. Baby, R.L., Hasan, I., Kabir, K.A. and Naser, M.N. (2010).Nutrient analysis of some commercially important molluscs of Bangladesh. *Journal of Scientific Research* 2(2): 390-396.
5. Bouchet, P. and Rocroi J.P. (2005). Classification and nomenclator of gastropod families. *Malacologia*., 47(1–2) :1– 397.
6. Colgan, D.J., Ponder,W.F., Beacham, E. and Macaranas, J. (2007). Molecular phylogenetics of Caenogastropoda (Gastropoda: Mollusca). *Molecular Phylogenetics and Evolution*. 42: 717–737.
7. Hayes, K.A., Burks, R.L., Vazquez, C.A., Darby, P.C., Heras H., Martin, R.P., Qui, W.J.,Thiengo, C.S., Vega,A.I., Wada,T., Yusa,Y., Burela,S., Cadierno, P.M., Cueto, A.J., Dellagnola, A.F., Dreon,S.M., Frassa, V.M., Billoud,G.M., Godoy, S.M., Ituarte, S., Koch, E., Matsukura, K., Pasquevich, Y.M., Rodriguez, C., Saveanu, L., Seuffert, E.M., Strong E.E., Sun, J., Tamburi, E.N., Tiecher,J.M., Turner,L.R., Darby- Valentine L.P. and Cowie, H.R.(2015). Insights from

an Integrated View of the Biology of Apple snails (Caenogastropoda: Ampullariidae). *Malacologia* .58(1-2): 245-302.

8. Esposti, D.M., Vries, De. S., Crimi, M., Ghelli, A., Patamello, T. and Meyer, A.(1993) Mitochondrial cytochrome b: evolution and structure of the protein. *Biochimica et Biophysica Acta.,*1143(3):243-271.

9. Ramakrishna and Dey,A. (2007). Handbook on Indian freshwater molluscs. Zoological Survey of India. Kolkata. pp1- 399.

10. Strong, E.E. (2003). Refining molluscan characters: morphology, character coding and a phylogeny of Caenogastropoda. *Zoological Journal of Linnean Society*.137(4): 447- 554.

11. Ponder, W.F. and Lindberg, D.R. (1997). Towards a phylogeny of gastropod molluscs: an analysis using morphological characters. *Zoological Journal of Linnean Society*. 119: 83–265.

12. Ayyagiri, V.S., Jalaja,N. and Krupanidhi,S.(2017).Optimization of the Isolation procedure of genomic DNA from a mucus laden pulmonate gastropod, *Achatina fulica.*40(2):109-112.

13. Sambrook, J., Fritsch, E.F. and Maniatis, T. (1989). Molecular cloning: a laboratory manual, 2nd edn. Cold Spring Harbor Laboratory Press, Cold Spring Harbor.

14. Brown, T.A. (1991). Essential molecular biology, A practical approach. (Volume 2) Oxford University Press, New York pp 296.

15. Meritt, T.J.S. and Shi, L.(1998). Universal cytochrome b primers facilitate intraspecific studies in molluscan taxa. *Molecular Marine Biology and Biotechnology.* 7(1):7–11.

16. Tamura, K., Peterson, D., Peterson, N., Stecher, G., Nei, M., and Kumar, S. (2011). MEGA5: Molecular Evolutionary Genetics Analysis Using Maximum Likelihood, Evolutionary distance, and Maximum Parsimony Methods. *Molecular Biology and Evolution*., 28: 2731- 2739.

17. Stamatakis, A., Hoover, P. and Rougemont, J. (2008). A rapid bootstrap algorithm for the RAxML web servers. *Systemic Biology*.57: 758–771.

18. Thompson, J.D., Plewniak, F. and Poch, O. (1999). A comprehensive comparison of multiple sequence alignment programs. *Nucleic Acids Research*. 27: 2682–2690.

19. Raven, J.G.M. (1990). A revision of Obscurella Clessin, 1889 (Gastropoda Prosobranchia: Cyclophoridae) *Basteria*. 54:17-62.

20. Harasewych,M.G.,Adamkewicz,S.L. and Gillevet, P.M. (1998). Phylogenetic relationships of the lower Caenogastropoda (Mollusca, Gastropoda, Architaenioglossa, Campaniloidea, Cerithioidea) as determined by partial 18s rDNA sequences. *Zoologica Scripta*. 27(4) : 361–372.

21. Healy, J.M. (1988). Sperm Morphology and its systematic importance in the Gastropoda *Malacological Review Supplement*. 4: 251-266.

22. Sarkar, S. and Krupanidhi, S. (2018) (in press). A review to necessitate conservation of Indian terrestrial and freshwater gastropods. *Journal of Threatened Taxa.*

Current Trends in Biotechnology and Pharmacy
Vol. 12 (4) 377-389, October 2018, ISSN 0973-8916 (Print), 2230-7303 (Online)

Evaluation of factors affecting L-asparaginase activity using experimental design

Rania A. Zaki, Mona S. Shafei, Heba A. El Refai *, Abeer A. El-Hadi and Hanan Mostafa
Chemistry of Natural and Microbial Products Department, National Research Center, (ID:60014618), Dokki, Giza, Egypt
*Corresponding author: E mail: dr.heba_ar@yahoo.com

Abstract

The present study aims for the purification and characterization of L-asparaginase produced by *Fusarium solani*. Microbial L-Asparaginase has attracted considerable attention, owing to the cost effective and eco-friendly nature. The most common use of asparaginases is as a processing aid in the manufacture of food. L-asparaginase used to reduce the formation of acrylamide, a suspected carcinogen, in starchy food products such as baked or fried snacks and biscuits. Extracellular L-asparaginase was produced by solid-state fermentation (SSF) using sequential statistical strategy as optimization for some vital factors; wheat bran concentration, fermentation time, moisture content, inoculum size, temperature, culture age and asparagine concentration which were adjusted by the sequential two design of response surface methodology. *Fusarium solani* produced the highest L-asparaginase level (254 I/U) using Placket-Burman design andimprovement up to 290 U/gds upon applying the Box–Behnken design. Partial purification of the enzyme using acetone was done, the specific activity increased to 709.24/mg in the fraction of 40-60 % acetoneThe optimum temperature and pH of the enzyme were 40ºC and 7, respectively. The K_m and V_{max} of the partially purified enzyme were 9.1×10^{-2} mμ and 20 U/mg proteins respectively. The impact of L-asparaginase on the acrylamide content reduction after high heat treatment in a model system as well as in potato based material was investigated.

Keywords : *Fusarium solani* -L-Asparaginase - Solid State Fermentation- partially purified enzyme- sequential statistical strategy.

Introduction

Therapeutic enzymes have a wide variety of applications as replacement for metabolic deficiencies and as anticoagulants and anti-tumor. In the field of medicine, L-asparaginase is considered as an effective antitumor agent (Baskar and Renganathan, 2009). It is used in the treatment of lymphoblastic leukemia. An enzyme called asparagine synthetase in human is responsible for the synthesis of L-asparaginase from central metabolic pathway intermediates inside the cells. L-asparaginase helps in the hydrolysis of L-asparagine into L-aspartic acid and ammonia (Jha *et al*., 2012). The normal cells are able to synthesize their own asparagine while the leukemic cells need a great amount of it to keep up with their rapid malignant growth, L-asparaginase (ASNase) triggers metabolic reprogramming of leukemic cells which is part of the adaptation process to stress caused by amino acid depletion (Hermanova *et al.*, 2016). Also, L-asparaginase is known for its importance in food application, this enzyme is used in food industry to prevent the acrylamide formation when foods are processed in high temperatures. This use is important because acrylamide is a neurotoxin classified as potentially carcinogenic to humans (Cachumba *et al*., 2016). Previously, bacteria are considered as a great source for producing L-asparaginase and a series of preclinical and

clinical tests. Nowadays, fungi, actinomycetes, plants and animals are different sources for the enzyme. L-asparaginasefrom fungal sources is preferred to that of bacterial sources as they don't cause allergic reactions and anaphylaxis (Kumar *et al*., 2012).

The submerged fermentation technique (SF) is the most adopted method used throughout the world for L- asparaginase production. This method has some limitations which can be overcome by solid state fermentation technique (SSF). The latter method has many advantages such as low energy used, high product, low cost and water use in addition to simple fermentation media used (Chavez-Gonzalez *et al*., 2011).

Agricultural wastes can be used as a source of nutrients; e.g. agro-wastes from leguminous crops (Mishra, 2006), rice bran (Venil *et al*., 2009), soybean meal (Hosamani and Kaliwal, 2011).These wastes are cost effective and environment friendly (Couto and Sanroman, 2005).

The objectives of this work were to study the various effects that influence the production of L-asparaginase using *F. solani* from different agro-wastes using solid state fermentation and analyze the mutual interactions among the variables in a statistically valid manner using Placket-Burman design. Partial purification of the enzyme and its kinetic properties also application of the partially purified in food industry were also examined.

MATERIALS AND METHODS

Chemicals : All chemicals used in this study were of analytical grade.

Microorganism and inoculum preparation : The fungus used through this study was *Fusarium solani* provided by culture collection Centre of the National Research Center, Cairo, Egypt. The culture was maintained on the modified Czapek-dox agar medium supplemented with L-asparagine 1.5 % (w /v), incubated at 30ºC for 3 days, the stock culture was preserved at –80°C in 50% (v/v) glycerol with regular monthly transfer. Fungal suspension was prepared from freshly raised seven days old culture of *Fusarium solani* on Czapek-dox agar slants by suspending in 10 ml of o.85% sterile saline.

Fermentation medium : Wheat bran obtained from local market was used as the substrate for the production of L-asparaginase by *F. solani*. One gram of the substrate was taken in 250 ml Erlenmeyer flasks and moistened by modified Czapek medium under solid state fermentation (SSF). The flasks were autoclaved at 121ºC for 20 min, then cooled and followed by inoculation with 2 ml of spore suspension. The flasks were mixed thoroughly and incubated at room temperature for different incubation periods. Afterwards, the moldy substrate was analyzed for L-asparaginase production.

Extraction of L-asparaginase in SSF : Samples were withdrawn after different time intervals of fermentation and L-asparaginase activity was tested. A solution of NaCl (1 %), Trition X-100 (1 %) was used to transfer the solid media to liquid one so that the enzyme could be extracted by incubating the solution in a shaker at 180 rpm for 2 h at 30ºC (Vaseghi *et al*., 2013).

Qualitative estimation of L-asparaginase : L-asparaginase was assayed calorimetrically according to (Usha *et al.*, 2011). A standard curve was prepared with ammonium sulphate. One L-asparaginase (1U) is defined as the amount of enzyme that librates 1µmol of ammonia per minute under optimal assay conditions.

Partial purification of L-asparaginase : The purification was carried out using crude enzyme extract according to the following steps at 40ºC (Shafei *et al*., 2015).

Acetone precipitation : The enzyme was precipitated in a sequential manner using different acetone concentrations (v/v %). The mixture was centrifuged at 6000 rpm at 4ºC for 30 min and the precipitate was collected and stored at 4ºC.

Characterization of the partially purified L-asparaginase : Determination of optimum pH and temperature : Optimum pH and temperature

were determined by changing individually the condition of the reaction mixture assay: pH from 5.0 to 7.0 using citrate-phosphate buffer and 8.0 to 9.0 using tris buffer while temperature varied from 30º to 50º C.

Thermal stability of the partially purified enzyme : The thermal stability of the enzyme was evaluated by measuring the residual activity. Samples were incubated at different temperatures from 40º-60ºC in tris buffer (1M, pH 8.0) for different time intervals.

Substrate specificity and determination of V_{max}&K_m : Identical reaction mixtures containing the same amount of enzyme preparation were made each received different concentration of L-asparagine (0.02M-0.12M).The maximum reaction velocity (Vmax), Michaelis–Menten constant (Km) - defined as the substrate concentration at half the maximum velocity- of the partially purified enzyme were measured according to Lineweaver-Burk plots relating 1/v to 1/s**.**

Statistical optimization

Placket-Burman design : Seven different fermentation variables were prepared in two levels (-1) for the low level and (+1) for the high level according to Placket-Burman design (1969). The design is practical especially when there are large numbers of factors and implemented in the setting that produce optimal or near optimum responses (Strobel and Sullivan, 1999).Table ² showed the factors under investigations as well as the levels of each factor used in the experimental design; the Placket-Burman experimental design is based on the first order model:

$$Y=â_0+ © â_1xi$$

Where Y is the responses, $â_0$ is the model intercept and $â_1$ is the variables estimates. This model evaluates the important factors that affect the production of L-asparaginase using SSF. The effect of each variable was determined by the following equation:

$$E(x) =© M^+ - M^- /N$$

where E(x) is the effect of the tested variable, M^+ and M^- represent L-asparaginase activity from the trials where (x) measured was at the high and low concentration respectively and N is the number of trials.

Box-Behnken design for modified Czapekdox media under SSF: Table IIpresents the design matrix of 13 trials using this design (Box and Behnken, 1960), factors of the highest main effect were prescribed into three coded levels (-1, 0, +1) for low, middle and high concentrations respectively). For predicting the optimal point, a second-order polynomial function was fitted to correlate the relationship between variables and responses (L-asparaginase activity). For the three factors, the equation is as follows:

$$Y=â_0+ â_1x_1+â_2x_2+â_3X_3+â_{12}x_1x_2+â_{13}x_1x_3+â_{23}x_2x_3+â_{11}x_1^2+â_{22}x_2^2+â_{33}xâ_3^2.$$

Where Y is the predicted response; $â_0$ in the model constant; X_1, X_2 and X_3 are the independent variables; $â_1$, $â_2$ and$â_3$ are the linear coefficients, $â_{12}$, $â_{13}$ and$â_{23}$ are the cross product coefficients and $â_{11}$, $â_{22}$and$â_{33}$are the quadratic coefficients. The values of the coefficients were calculated and the optimum concentrations were predicted using JMP software. The quality of the fit of the polynomial model equation was expressed by R^2 (regression coefficient). The quality of fit of the polynomial model equation was expressed by the coefficient of determination R^2. All experimental designs were randomized to exclude any bias. Experiments were carried out in duplicates and mean values were given. The SE of the concentration effect was the square root of the variance of an effect, and the significant level (P-value) of each concentration effect was determined using student's t-test.

$$T(x) = E(x)/SE$$

Where E(x) is the effect of the variable x

Validation model : The statistical model was validated with respect to L-asparaginase production under the conditions predicted by the model. Samples were withdrawn at the desired

intervals and L-asparaginase assay was carried out.

Effect of moisture level in SSF : The solid substrate i.e. wheat bran was moistened using modified Czapek medium the composition of which was reported previously. Different levels of moisture were tested 3%, 4% and 5% ml to determine the optimum moisture level for enzyme production. The enzyme was the extracted and assayed.

Application of L-asparaginase in food : Potato chips were washed, peeled and cut into 2mm thick chips using a slicer. The chips were soaked for 10 min with 5 ml of 0.5 % (w/v) glucose solution. Five ml of partially purified enzyme solution and 15% (w/v) of tri-chloroacetic acid were incubated in Tris-buffer (1M, pH 8 at 37°C. The chips were then fried in oil for 8min at 190°C. The quantification of acrylamide was performed by an Agilent 1100 model HPLC system (Waldbrann, Germany). The chromatographic separations were performed in Zorbax ODS column using the mobile phase (7% v/v) methanol in 0.025 mol/L sodium dihydrogen phosphate) at a flow rate of 1ml/ min. The acrylamide was detected at 215nm with continuous monitoring the peak spectra within the range of 190-350nm. Control samples were also prepared, using untreated potato chips (Ahn *et al*., 2002).

RESULTS AND DISCUSSION

Evaluation of medium composition and operating condition affecting L-asparaginase production by Placket-Burman design: In solid state fermentation, seven factors namely; wheat bran concentration, fermentation time, moisture content, inoculum size, temperature, culture age and asparagine concentration were tested using Placket- Burman design (1946) for the enzyme production. Variations of enzyme activity ranging from 65 to 254 U/ml in the nine trials were observed (Table I). This variation shows that both medium composition and the operating conditions have great influence on the enzyme activity. The main effects of the tested variables on L-asparaginase production were calculated and represented in Figure 1. The enzyme activity was positively affected by wheat bran concentration, temperature, culture age and inoculum size while the other three factors time, moisture level and asparagine concentration showed negative effect on L-asparaginase activity. In order to approach the optimum response of L-asparaginase activity, the effective independent variables, including the temperature (X_1), wheat bran concentration (X_2) and moisture level (X_3), were further investigated each at three levels according to the Box and Behnken design (Table II). These results obtained were used for ANOVA analysis (Table III). Mathematical model equation 3 represents relationship between L-asparaginase activity (Y) and temperature (X_1), wheat bran (X_2) and moisture level (X_3) in coded levels was as follows:

$$\mathbf{Y = 250-0.5X_1+11.875X_2+ 25.375X_3+ 2.75X_1X_2-1.75X_1X_3-5X_2X_3-12.25X_1^2+X_2^2+11.5X_3^3}$$

The variables X_1X_2, X_1X_3 and X_2X_3 are interaction effects of temperature-wheat bran concentration, temperature-moisture level and wheat bran concentration-moisture level respectively. The significance of each coefficient was determined by the F and P-values.

Low P-values of the linear terms for wheat concentration and moisture level and low P-values for quadratic terms for temperature and moisture showed high linear and quadratic effects of this parameter on enzyme production. Temperature showed high P-value (0.7584) for linear term and high quadratic term for wheat bran concentration which indicated insignificant linear and quadratic effect of these variables. It should be noted that the interaction effect of these variables were significant. From the ANOVA, the high F-value (44.3095) and low P-values ($P<0.0001$) indicate that the regression model were valid.

Lack of fitness more than 0.05 indicate that the model is significant for enzyme production. Also (R^2) which is multiple correlation coefficients indicate the correctness of the model also the predicted value is very close to the actual value.

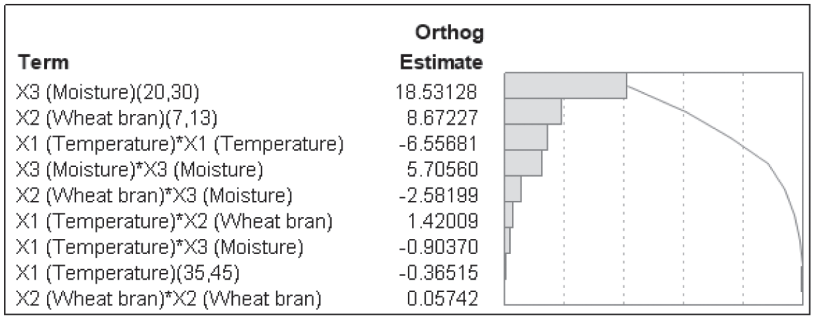

Term	Orthog Estimate
X3 (Moisture)(20,30)	18.53128
X2 (Wheat bran)(7,13)	8.67227
X1 (Temperature)*X1 (Temperature)	-6.55681
X3 (Moisture)*X3 (Moisture)	5.70560
X2 (Wheat bran)*X3 (Moisture)	-2.58199
X1 (Temperature)*X2 (Wheat bran)	1.42009
X1 (Temperature)*X3 (Moisture)	-0.90370
X1 (Temperature)(35,45)	-0.36515
X2 (Wheat bran)*X2 (Wheat bran)	0.05742

Fig 1Pareto chart for Box behnken design under SSF

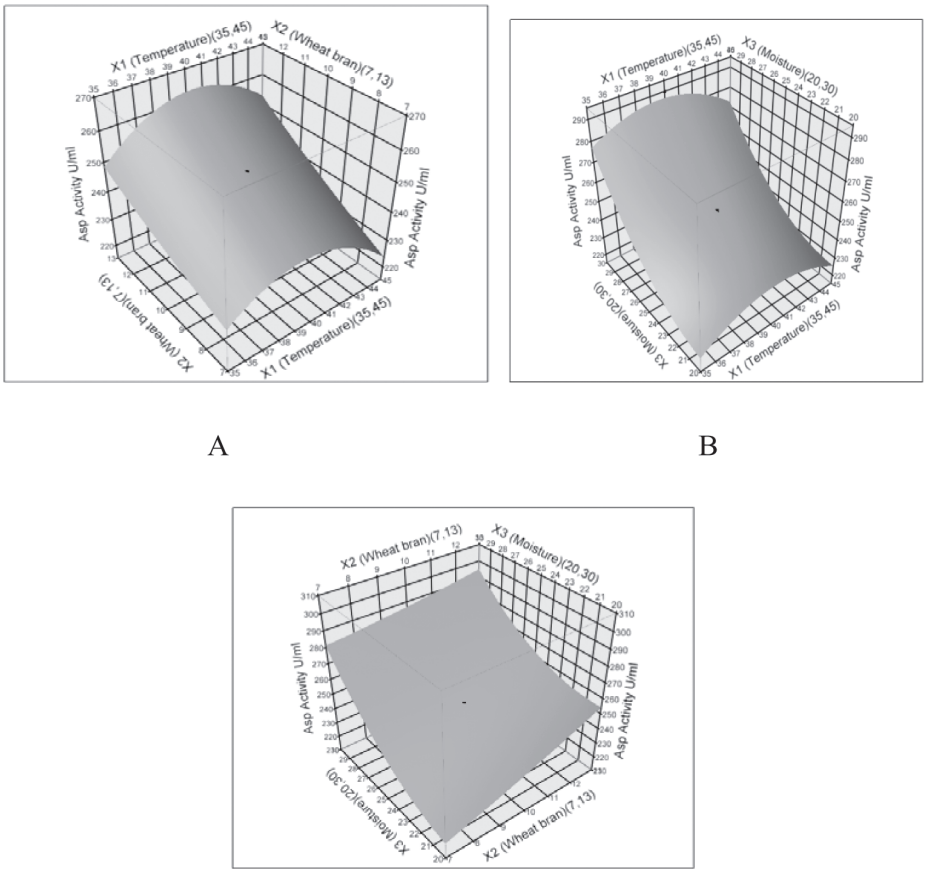

A B C

Fig. 2: Response surface plots showing the effects of the most significant independent variables on L-asparaginase production. (A) Wheat bran and temperature (B) Temperature and moisture content (C) Wheat bran and moisture content

R^2 value is 0.987617 which shows that the predicted value is very close to 1.0 and also very close to the actual one.The surface plot and the pareto chart (Figure 2) showed that near to moderate levels of wheat bran concentration, temperature and moisture level supported high L-asparaginase activity.

In each 3D curve (Figure 3 a, b, c), the effect of two factors on enzyme activity are shown, keeping other variables constant at zero level. From the statistical analysis, the moisture content had the most significant effect on the enzyme activity. Results obtained are in accordance with other findings where it was reported that high initial moisture content is accompanied by a decrease in enzyme production due to decrease in substrate porosity, gas volume and fungal growth in addition to change in structure of substrate particles. On the contrary, low moisture content decrease the nutrients solubility, substrate swelling and water retention by the substrate. All these factors influence the fungal growth and consequently the enzyme production (Baysal *et al*., 2003; Hosamani and Kaliwal, (2011); Beniwal *et al*., (2013).

Validation of the model: The maximum experimental response for L-asparaginase activity was in strong agreement with the predicted values.

Partial purification of L-asparaginase : The partial purification of the enzyme crude extract was carried out using acetone precipitation where the most active fraction was (40-60 %).The enzyme activity increased with every step of purification (Table IV). The partial purification steps were rapid and cost-effective; the fractions were collected and examined for enzyme activity and protein content. The total protein decreased from 62, 8 to 21.9 mg for the crude extract and the final preparation, respectively. The specific activity increased to709.24/mg in the fraction of 40-60 % acetone. The purification fold increase to 3.64.Similar results were obtained by (Thakur *et al*., 2014) on the purification of extracellular L-asparaginase from *Mucor hiemalis* by acetone, also (Bora and Bora, 2012)who reported that fewer steps of purification are more preferred as a loss of about 10% enzyme yield is recorded at each step of purification.

Kinetic properties of the purified L-asparaginase : Some properties of L-asparaginase from *F.solani* were investigated as

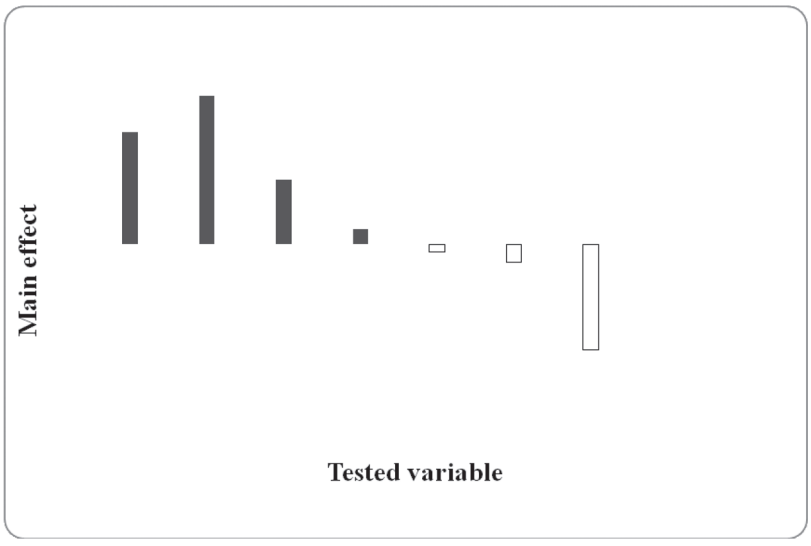

Fig (3): Main effect of variables affecting L-asparaginase activity under solid state

shown in Table V . The enzyme was active between pH values 5.0-9.0 with an optimum activity at pH 7.0, at higher pH values, L-asparaginase activity decreased. Nearly similar results were obtained by using *Penicillium sp* where the enzyme showed maximum activity at pH 7.0. (Patro and Goupta, 2012).(Amruthae*t al*., 2014) recorded the pH profile of L-asparaginase from *Fusarium sp* not only showed optima at pH 9.0 but also was active in the acidic pH that was in accordance with the studies of Sahue*t al*., 2007 who indicated that L-asparaginase is pH-dependent.

A temperature profile showed that the enzyme was measured at various ranges from 25-50°C. Maximum activity was obtained at 40°C. At higher temperatures, the reaction rate declined gradually until it lost nearly 57.3 %. Nearly similar results were shown by the purified L-asparaginase from *Penicillium brevicompactum* NRC 829 which was active at a wide range of temperature from 30-75°C with maximum activity at 37°C (El shafei *et al*., 2012).

The temperature tolerance of the enzyme showed it was stable at 40°C for 15 min, 30 min and 1 h and may be quite stable at 45°C (FIGURE IV). There was a progressive loss in enzyme activity at higher temperatures. L-asparaginase lost about 23.4 % of its activity after incubation at 50°C for 15 min while a rapid decrease (65 %) was observed after incubation at 55°C for 15 min. Kirshna and Gupta (2012) reported near results for the temperature stability of L-asparaginase at 37°C from *Penicillium sp.* On the contrary, enzyme activity from *Aspergillus terreus* KLS_2 showed stability at temperature 70°C for 30 and 60 min (Shafei *et al*., 2015).

L-asparaginase of different microorganisms expresses a great variety of substrate affinities and consequently plays ecophysiological roles in the enzyme activities. The effect of L-asparagine substrate concentrations (0.02-0.12 mμ/mol) on the partially purified enzyme was studied. The K_m and V_{max} of the partially purified enzyme were 9.1×10^{-2} mμ and 20 U/mg proteins respectively. The affinity of the enzyme to its substrate shows the degree of

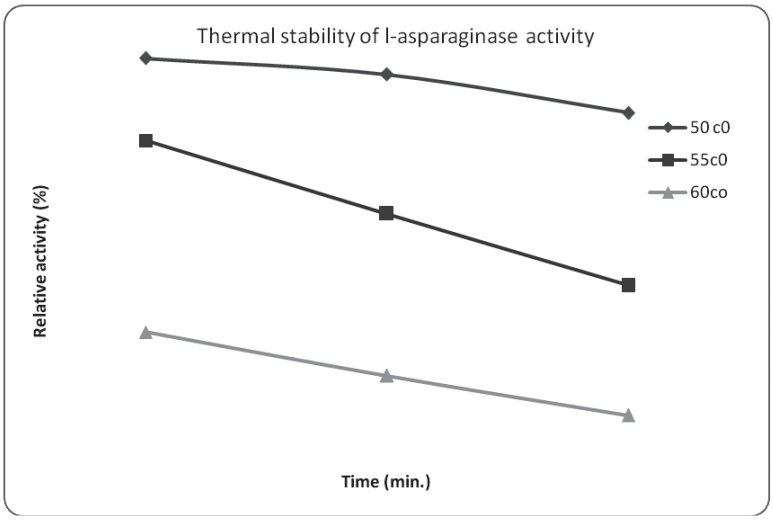

Fig. 4 : Thermal stability L-asparaginase produced by *F. solani*

Evaluation of factors affecting L-asparaginase activity

its effectiveness towards tumors. L-asparaginase of different microorganisms has different substrate affinities and probably plays different physiological roles in the enzyme activity. The linearity of the Linweaver-burk double reciprocal plot also indicates that our enzyme followed Michaelis-Menten kinetics (Gaffes, 1975). Also Km and Vmax values of L-asparaginase from Pseudomonas aeruginosa 50071 were 0.147 mM and 35.7 IU, respectively (El-Bessoumy *et al.*, 2004).Lower K_m values were reported for other microorganisms like *Vibrio succinogens* (Prabhu and Chandrasekaran, 2000).

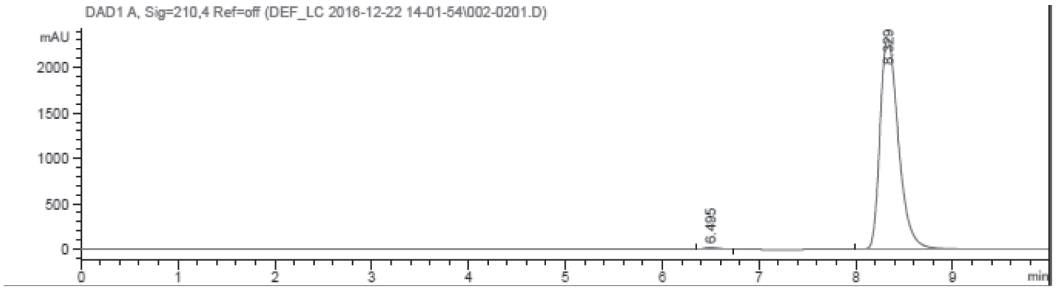

A

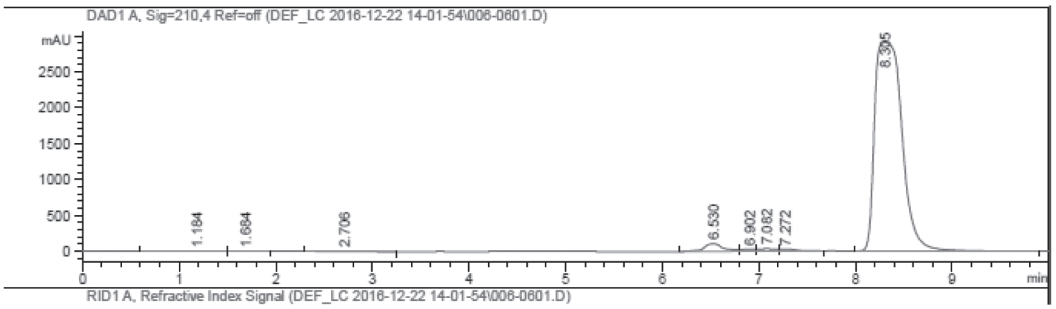

B

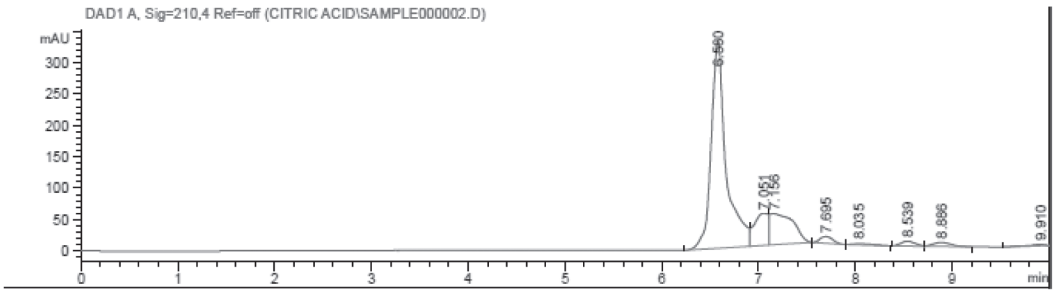

Fig (5): HPLC chart of (A) Standard acrylamide (B) the untreated fried potato chips (C) the enzyme (partial purified) treated fried potato chips

Table (1): Plackett-Burman experimental design for evaluation of factors (Coded levels and real values) affecting L-asparaginase activity under SSF

Trial	Wheat bran (g) x_1	Time (h)x_2	Moisture (%)x_3	Inoculum size (ml) x_4	Temp°Cx_5	Age of culture (day) x_6	Asparagine conc (g) x_7	Asp. Activity U/ml
1	-(3)	-(8)	-(30)	+(6)	+(35)	+(10)	-(0.3)	254
2	+(7)	-(8)	-(30)	-(4)	-(25)	+(10)	-(0.3)	222
3	-(3)	+(12)	-(30)	-(4)	-(25)	-(4)	+(0.5)	208
4	+(7)	+(12)	-(30)	+(6)	+(35)	-(4)	-(0.3)	205
5	-(3)	-(8)	+(50)	+(6)	-(25)	-(4)	+(0.5)	105
6	+(7)	-(8)	+(50)	-(4)	+(35)	-(4)	+(0.5)	222
7	-(3)	+(12)	+(50)	-(4)	-(25)	+(10)	-(0.3)	131
8	+(7)	+(12)	+(50)	+(6)	+(35)	+(10)	+(0.5)	245
9	0(5)	0(10)	0(40)	0(5)	0(30)	0(7)	0(0.4)	65

Table (2): Box-Behnken factorial design for optimization for L-asparaginase production using SSF

Trial	Independent Variables			Asp. ActivityU/ml
	Temperature°CX_1	Wheat bran(g)X_2	Moisture level%X_3	
1	- (35)	-(7)	0(25)	228
2	+(45)	-(7)	0(25)	222
3	-(35)	+(13)	0(25)	250
4	+(45)	+(13)	0(25)	255
5	-(35)	0(10)	-(20)	220
6	+(45)	0(10)	-(20)	222
7	-(35)	0(10)	+(30)	280
8	+(45)	0(10)	+(30)	275
9	0(40)	-(7)	-(20)	225
10	0(40)	+(13)	-(20)	255
11	0(40)	-(7)	+(30)	280
12	0(40)	+(13)	+(30)	290
13	0(40)	0(10)	0(25)	250

Table (3): Analysis of variance for L-asparaginase production by *F. solani* under SSF

Term	Coefficient estimate	DF	SE	SS	t-value	F-ratio	P-value
Corrected Model	-	9	-	7556.9833	-	44.3095	0.0003*
Intercept	250	1	2.513298	-	99.47	-	<.0001*
X1(Temperature)	-0.5	1	1.539074	2.0000	-0.32	0.1055	0.7584
X2 (Wheat bran)	11.875	1	1.539074	1128.1250	7.72	59.5317	0.0006*
X3 (Moisture)	25.375	1	1.539074	5151.1250	16.49	271.8272	<.0001*
X_1X_2	2.75	1	2.17658	30.2500	1.26	1.5963	0.2621
X_1X_3	-1.75	1	2.17658	12.2500	-0.80	0.6464	0.4579
X_2X_3	-5	1	2.17658	100.0000	-2.30	5.2770	0.0700
X_1^2	-12.25	1	2.265456	554.0769	-5.41	29.2389	0.0029*
X_2^2	1	1	2.265456	3.6923	0.44	0.1948	0.6773
X_3^2	11.5	1	2.265456	488.3077	5.08	25.7682	0.0038*

SS: Sum of squares.DF: Degrees of freedomSE: Standard error
R^2 =R Squared = 0.987617 (Adjusted R Squared = 0.965328)*Significant at 5% level.

Table (4): Summary of steps employed in partial purification of L-asparaginase produced by*F. solani*

Acetone Concentration	Total activity (u/F)	Recovered activity%	Total protein of fraction (mg/F)	Recovered Protein(%)	S.E.A (U/mg)	Purification fold
Crude enzyme	9825	100	62.8	100	156.45	0.80
0-20	1313	13.36	8.45	13.45	155.40	0.79
20-40	655	6.66	3.625	5.77	180.68	0.93
40-60	4213.3	42.88	5.941	9.46	709.20	3.64
60-80	615	6.26	3.885	6.18	158.30	0.51
Total	6796.3	69.17	21.90	25.6	194.90	1

Specific activity= total activity of fraction /protein of fraction
Culture filtrate means before precipitation
mg/f= milligram / fraction
U/f= unit/ fraction
U/mg protein= unit/ milligram protein

Table (5) Some properties of partially pure L-asparaginase produced by *F. solani*

Properties	Relative activity (%)
pH	
5.0	90.9
6.0	100.6
7.0	143.1
8.0	100
8.5	75.9
9.0	50.5
Temperature °C	
25	55.6
30	64.7
35	79.5
40	100
45	70.6
50	42.7
Substrate concentration mM/ml	
0.02 M	54.1
0.04 M	100
0.06 M	46.2
0.08 M	31.2
0.1 M	11.6
0.12 M	5.6

Application of L-asparaginase from *F. solani* in potatoes : The partially purified enzyme was tested for its impact in potato chips. The released ammonia confirmed the conversion L-asparaginase present in potato to L-aspartic acid. Upon frying the potato chips treated with L-asparaginase from *F. solani*, the acrylamide formed was approximately 99.3405 % lower than that with the untreated potatoes (FIGURE V). This is due to reduction of L-asparaginase in the external layer of the potato chips that could be reached by the enzyme. Thus, indicating the formation of L-aspartic acid and ammonia and accordingly preventing the formation of Millare reaction product and reduction in the high L-asparagine content in potato (Shafei*et al*., 2015).

CONCLUSION

Extracellular*Fusariumsolani* L-asparaginase was produced by solid-state fermentation (SSF)using sequential statistical strategy as optimization for some vital factors; wheat bran concentration, fermentation time, moisture content, inoculum size, temperature, culture age and asparagine concentration. Partial purification of the enzyme using acetone was done, the specific activity increased to709.24/mg in the fraction of 40-60 % acetone The optimum temperature and pH of the enzyme were 40ºC and 7, respectively. The Km and Vmax of the partially purified enzyme were 9.1×10-2 mμ and 20 U/mg proteins respectively. The impact of L-asparaginase on the acrylamide content reduction after high heat treatment in a model system as well as in potato based material was investigated.

ACKNOWLEDGEMENT

The authors would like to thank the National Research Centre,Egypt for financial support in the frame ofNRC/VPRA/GDRPADU/FSEIRPC/F 28)P100222).

REFERENCES

1. Ahn,JS, Castle, L, Clark, DB, Lioyd, AS, Philo, MR and Speck DR.(2002).Verification of the findings of acrylamide in heated food. Food Addit.Contam.19:1116-1124.
2. Amrutha, Vg, Audipudi, Ng,,Supriya, R, Pallavi,Mp, Ganga. (2014)Characterization of L-asparaginase producing endophytic fungi isolated from ripened fruit of capsicum frutescence.Int*J* Pharm. Dev. Tech. 4: 52–57.
3. Baskar G, RenganathanindianS. (2009). Application of latin square design for the evaluation and screening of supplementary nitrogen source for L-asparaginase production by *Aspergillus terreus* MTCC 1782. J. Sci.Technol.2: 50-54.
4. Baysal E, Peker H, Kemal M,Temiz A. (2003). Cultivation of oyster mushroom on waster paper with some added

supplementary materials. Bioresour. Technol.89: 95-97.

5. Beniwal, V, Goel, G, Kumar, A, Chhokar, V. (2013). Production of tannase through solid state fermentation using Indian Rosewood (Dalbergia Sissoo) sawdust a timber industry was te. Ann.Microbiol.63: 583-590.

6. Bora, L, Bora, M. (2012).Optimization of extracellular thermophilic highly alkaline lipase from thermophilic *bacillus sp* isolated from hotspring of Arunachal Pradesh, India. Braz. J. Microbiol.43: 30-42.

7. Boxgep, Behnken, DW. (1960).Some new three level designs for the study of quantitative variables. Technometrics. 2:455–475.

8. Cachumbajm, Felipe, AFA, Guilherme, FDP, Larissa, PB, Júlio C. DS, Silvio, SDS.(2016).Current applications and different approaches for microbial l-asparaginase production *Braz. J. Microbiol*.47: 77–85.

9. Chavez-Gonzalez M, Rodrigues-DuránLv, Balagurusamy N, Prado-Barragán A, Rodrigues R, ConherasJc, Aguilar Gn. (2011).Biotechnological advances and challenges of tannase: an overview. Food Bioprocess Technolinpres.Doi 10.1007/s11947-011-0608-5.

10. Couto, R,Sanroman, MA.(2005).Review Application of solid-state fermentation to ligninolytic enzyme production S. *Biochemical Engineering Journal*,22: 211–219.

11. El-Shafei,AM, Mohamed, H M, Abd-Elmontasr,AM, Mahmoud, DA, Elghonemyd H. (2015).Purification, characterization and antitumor activity of L-asparaginase from *Penicillium brevicom pactum* NRC 829.Br Microb Res J.2:158–174.

12. El-Shafeiam, Hassan, MM, Abd-Elmontasr, M, Mahmoudda,Elghonemy, DH.(2012).L-asparaginase from *Penicillium brevicom pactum* NRC 829.Brit. Microbial.Rese.J.2: 158-174.

13. Gaffar, SA,and Shethna, YI. (1977). Purification and some biological properties of Asparaginase from *Azoto bactervinel andii*.Appl. Environ.Microbiol.33:508-514.

14. Hermanovaa, Arruabarrena-Aristorena, KV, Nuskovahalberich-Jorda, M, Fiser K, Fernandez-Ruiz, S, Kavan, D, Pecinova, A, Niso-Santanom, Zaliova M, Novak P, Houstek J, Mracek T, Kroemer G, Carracedo A, Trka J, Starkova J. (2016).Pharmacological inhibition of fatty-acid oxidation synergistically enhances effect of l-asparaginase in childhood ALL cells. Leukemia.30: 209–218.

15. Hosamani, Kaliwal, Bb. (2011).L-asparaginase- an antitumor agent production by *Fusarium equiseti*using solid state fermentation. International Journal of Drug Discovery. 3(2):88-99.

16. Jha,Sk, Pasrija, D, Sinha,Rk, Singh,Hr, Nigam,Vk, Vidyarthi, As. (2012). Microbial L-Asparaginase: A Review On Current Scenario And Future Prospects. International Journal of Pharmaceutical Sciences and Research.3 (9): 3076-3090.

17. Krishna, RP, Gupta, N. (2012). Extraction, purification and characterization of L-asparaginase from *Penicillium sp*. by submerged fermentation.International Journal for Biotechnology and Molecular Biology Research.3(3):30-34.

18. Kumar D, Sobha K. (2012). L-Asparaginase from microbes: a comprehensive review. AdvBiores.3:137–157.

19. Lineweaver,H, Burk D. (1934). The determination of enzyme dissociation constants. J. Am. Chem. Soc.1: 658-666.

20. Mishra, A. (2006).Production of L-Asparaginase, an anticancer agent, from

Aspergillusniger using agricultural waste in solid state fermentation. Appl. Biochem. Biotechnol.135:33-42.

21. Thakur, M,Lincoln, L, Francois, NN, Sunill, SM. (2014).Isolation, Purification and Characterization of Fungal extracellular L-AsparaginasefromMucorhiemalis., Journal of Biocatalysis and Biotransformation. 2(2).

22. Patro, KR, Gupta,N. (2012). Extraction, purification and characterization of L-asparaginase from *Penicillium sp*.by submerged fermentation. International Journal for Biotechnology and Molecular Biology Research.3(3): 30-34.

23. Plackett,Rl,Bunnan, JP. (1946). The design of multifactorial experiments.*Biometrika*.33: 305-325.24.

24. Prabhu, GN, Chandrasekaran, M. (2000).Purification and Characterization of an Anti-cancer Enzyme Produced by Marine Vibrio Costicola Under A Novel Solid State Fermentation Process. Nature.227: 1136-1137.

25. Shafei, MS, Heba, AE, Hanan, M, Abdel-Monem,HE, Fawkia,ME, Saadia, ME, Sanaa, KG. (2015). Purification, Characteriza-tion and Kinetic Properties of *Penicillium cyclopium* L-Asparaginase: Impact of l-asparaginase on a crylamide content in potato products and its cytotoxic activity. 9(2): 130-138.

26. Sahu, MK, Sivakumar, k, Poorani, E,Thangaradjou,T,Kannan, L. (2007).Studies on L-asparaginase of actinomycetes isolated from estuarine fishes. J. Environ. Biol.28 (2): 465-474.

27. Strobel, RJ, Sullivan, GR. (1999). Experimental design for improvement of fermentation.In Manual of Industrial Microbiology and Biotechnology.

28. Usha, R, Mala, KK, Venil, CK, Palaniswamy, M.(2011).Screening of actinomycetes from mangrove ecosystem for L-asparaginase activity and optimization by response surface methodology. PolishJ. Microbial. 60:213-221.

29. Vaseghi, G, Andalib,S, Rabani, M, Sajjadi, S, Jafarian, A. (2013).Hypnotic Effect of Salvia ReuteranaBoiss for Treatment of Insomnia.J Med Plants.12(45):7–13.

30. Venil, CK, Nanthakumar, KK,arthikeyan, K, Lakshmanaperumalsamy, p. (2009). Production of L-asparaginase by serratiamarcescens SB08: Optimization by response surface methodology. Iranian J. Biotech.7: 10-18.

Current Trends in Biotechnology and Pharmacy
Vol. 12 (4) 390-405, October 2018, ISSN 0973-8916 (Print), 2230-7303 (Online)

Modelling and optimization of L-Asparaginase production from *Bacillus stratosphericus.*

Madhuri Pola[1], Chandrasai Potla Durthi[1], Satish Babu Rajulapati[1*], Rajeswara Reddy Erva[2]
[1]National Institute of Technology, Warangal
[2]National Institute of Technology, Andhra Pradesh
*Corresponding author : satishbabu@nitw.ac.in, rsatishbabur@gmail.com

Abstract:

L-Asparaginase has gained importance as one of the most important medications used to treat Acute Lymphocytic Leukemia (ALL). The goal of the current study is to maximize the L-Asparaginase activity besides minimizing the L-Glutaminase activity. Shorter half-life and side effects remain the drawbacks of the commercially available L-Asparaginase drugs. To overcome the drawbacks, L-Asparaginase has been isolated from endophytes of *Ocimum tenuiflorum*. The novel endophyte shown highest L-Asparaginase activity and it was identified as *Bacillus stratosphericus* using 16S rRNA sequencing analysis. With unoptimized medium, the maximum activity for L-Asparaginase was 7.81 IU/ml and for L-Glutaminase 6.51 IU/ml at 48h, pH-7.0 and temperature 25˚C. It was observed that the L-Asparaginase activity was increased to 18 IU/ml by (One-Factor-at-a-Time) OFAT method. Further medium was optimized by Plackett-Burman method. It was observed that Time, Temperature, pH and L-Asparagine were identified as significant variables, which were further optimized by Response Surface Methodology (RSM). After RSM, the L-Asparaginase activity increased to 25.28 IU/ml whereas the L-Glutaminase activity diminished to 3.09 IU/ml.

Keywords: L-Asparaginase, ALL, endophytes, OFAT, Plackett-Burman method, RSM

Introduction

Acute Lymphocytic Leukemia (ALL) (1-5) was the foremost observed disease in children (6, 7). Currently, many therapies are in use to diagnose ALL (8). However, in recent days treating ALL by L-Asparaginase has gained attention. In addition, it has been employed in industries for acrylamide degradation of fried foods (9-13). L-Asparaginase primarily breaks L-Asparagine into aspartate and ammonia (14,15). L-Asparagine is the nonessential amino acid (16), which cannot be synthesized by the cancerous cells. Hence, they will move in search of L-Asparagine within the blood plasma making the cancer cell malignant (17). External supply of L-Asparaginase can break down the free L-Asparagine within the plasma making cancer cell deficit of L-Asparagine (18), and hence they will die. L-Asparaginase from *E.coli* and *Erwinia cartovora* has both medicinal (to treat ALL) (16,19,20) as well as industrial importance (acrylamide degradation) (10,21-23). The L-Asparaginase produced from *E.coli* has high specificity, but the half-life was very less (1,16,24), vice versa with the L-Asparaginase isolated from *Erwinia cartovora* (25-26). The L-Glutaminase activity of L-Asparaginase leads to side effects (27) like allergies etc. due to prolonged treatment. To overcome the side effects of the commercially available L-Asparaginase research is going on to produce L-Asparaginase having same therapeutic effects but serologically different (28-30).

In this study, L-Asparaginase has been isolated from endophytes (31,32) of *Ocimum tenuiflorum*. Endophytes lives in plants (33, 34), animals, fungi (35), and others. Endophytes are rich sources of bioactive compounds having

therapeutic properties (36,37). However, the isolated endophytes produced extra-cellular enzyme making the downstream process simple (38, 39). Culture media composition and the physical parameters play a significant role on the enzyme activity(40). The optimum concentrations of media and physical parameters can be identified by various optimization studies. Statistical optimization studies were conducted to explore the interactions between parameters (28, 41-43) and to reduce the time required for the production of enzyme. Enzyme activity was estimated by Nesslerization method.

Screening and analysis of nutritional factors play a crucial role in bioprocess development. Hence, One-Factor-at-a-Time (OFAT) studies were conducted for both the media components (Carbon, Nitrogen and L-Asparagine) and physical factors (Time, Temperature, RPM and pH). As OFAT studies are tedious to examine the interactions between the components, statistical optimisation techniques were employed to minimise the L-Glutaminase activity economically. Plackett-Burman experimental studies were conducted to identify the factors influencing on enzyme activity. The significant variables obtained from the Plackett-Burman studies were further optimized by using Response Surface Methodology (RSM) studies.

Materials and methods

Isolation and screening and identification of endophytes : Endophytes were isolated from *Ocimum tenuiflorum* (44) on M-9 agar medium and screened by rapid plate assay. The endophyte that produced maximum pink zone formation has been identified by 16s rRNA sequencing studies.

Analytical methods : Enzyme activity was estimated by Nesslerization. Ammonium sulphate was used to develop the standard graph. The equation obtained from the standard graph was implied to calculate the enzyme activity in terms of IU/ml. All the experiments were performed in triplicates.

Production and optimization studies of L-Asparaginase

Primary inoculum and production studies : The pre-culture was made by the addition of one loop of pure culture into the nutrient broth (pH-7.0) which incubated at 25°C, for 24h. 1ml from the pre culture was taken and added to the production medium, incubated at 25°C, 120 RPM and for 72h.

One factor at a time optimisation (OFAT) studies: The impact of physical variables incubation time (0-72h), Temperature (25°C-40°C), pH (6.0-9.0) and RPM (100-150) were studied. By substituting the glucose (3 g/L) with Fructose/ Maltose/Starch/Cellulose/Trisodium citrate the catalytic activity was calculated. The best carbon substitute concentration was varied from 2-6 g/L. Similarly, Yeast extract was substituted by Beef extract/Ammonium sulphate/Potassium nitrate/ Soybean peptone. The best nitrogen source concentrations was varied and evaluated for highest activity. The effect of different concentrations of L-Asparagine on L-Asparaginase and L-Glutaminase was also evaluated.

Plackett-Burman design : Optimization process involving OFAT studies takes long time and therefore the analysis of interactions among the factors becomes difficult. The primary goal of bioprocess development is to maximize the product in an economical manner. Hence, statistical methods are economically designed to minimize the error for predicting the optimum values of individual factors. The factors that affect the productivity were identified and further optimized using RSM.

A two level factorial Plackett-Burman design was developed to study 11 different variables. Eleven variables namely Maltose, Yeast extract, L-Asparagine, Na_2HPO_4, KH_2PO_4, NaCl, Time, Temperature, pH, RPM and Dissolved oxygen (v/v) were considered. A total of 13 experiments were generated, both L-Asparaginase and L-Glutaminase activities were estimated by Nesslerization method. Central Composite Design studies were employed on significant variables whose probability <0.05.

Optimization of L-Asparaginase by Response Surface Methodology (RSM) : Design-Expert offers several designs depending on the number of design factors to find desirable location (maximum or minimum). In this study, Central Composite Design was chosen for optimization studies. Quadratic model coefficients with face-centered design (alpha=1.00) were analyzed at two different levels.

A second order experimental design was developed by sequential experimentation and predicting the level of factors to get an optimal response through regression analysis. The effect of four independent variables Time, Temperature, pH, and L-Asparagine on maximization of L-Asparaginase and minimization of L-Glutaminase production has been studied at five different levels. A full factorial central composite design was designed to build a total of 30 experiments, having 2^4= 16 cube points plus 6 centre points (4 in cube and 2 in axial positions) and (4× 2 = 8) star points. The experimental design and statistical analysis of results were done by using Design Expert 6.0v. The 3D surface plots were used to analyze the optimum levels of variables to obtain low L-Glutaminase and high L-Asparaginase activity.

Results

Isolation, screening, and identification of endophyte : The endophyte that produced maximum pink zone (Fig 1) was chosen for further identification. Microscopic observation revealed that the endophyte was a rod-shaped and gram-positive *Bacillus* bacterium. Based on data of 16S rRNA sequencing, the organism B16 has been identified as *Bacillus stratosphericus*.

L-Asparaginase primary production studies : The production medium was incubated at 25˚C, 120 RPM for 72h. For every regular interval of 8 h, samples were taken, centrifuged and filtered. The supernatant acts as the crude enzyme. The enzyme activities obtained for L-Asparaginase and L-Glutaminase at 48 h were estimated as 7.88 IU/ml and 6.51 IU/ml respectively.

One-variable-at-a-time (OFAT) studies: Effect of incubation time

The enzyme activities shown in Fig 2, for L-Asparaginase and L-Glutaminase at 48h were estimated as 7.88 IU/ml and 6.51 IU/ml respectively. With gradual increase in incubation time L-Glutaminase activity was increased.

Effect of Temperature : Enzyme activity initiated at 8h of incubation, the maximum activity attained was 6.88 IU/ml for L-Asparaginase at 48h of incubation. From Fig 3 it was analyzed that the activity for L-Asparaginase declined after 48h.The enzyme activity obtained at 40˚C for L-Asparaginase was 27.92 IU/ml, and for L-Glutaminase the activity was 24 IU/ml. The enzyme activities obtained at 25˚C was 15.4 IU/ml (L-Asparaginase) and 4.7 IU/ml (L-Glutaminase). There was no much difference observed between L-Asparaginase and L-

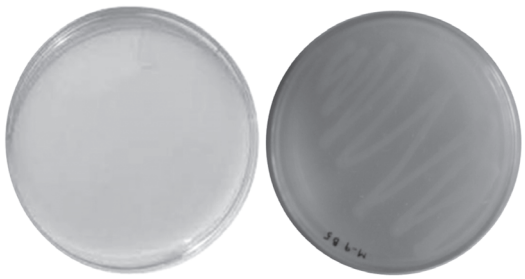

Fig 1.Qualitative assay for Identifying L-Asparaginase producing endophyte

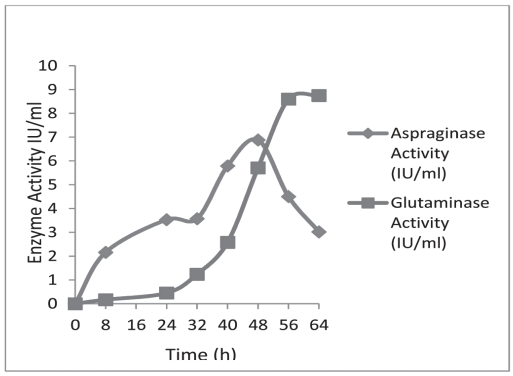

Fig 2.Effect of enzyme activities w.r.t Time (h)

Glutaminase activity with the increase in temperature. Hence the optimum temperature chosen was 25˚C because of low L-Glutaminase activity.

Effect of pH : From Fig 4, pH-6.0 was found to be as optimum pH. Low pH favoured high L-Asparaginase activity. The enzyme activities obtained at pH-6.0 was 15.8 IU/ml (L-Asparaginase) and 5.7 IU/ml (L-Glutaminase).

Effect of RPM : With increase in RPM L-Glutaminase activity was increased. The optimum RPM found was found to be 120.

Effect of carbon sources : The effect of carbon source on activity was checked with different carbon sources were shown in Fig 5. It was observed that Maltose showed low L-Glutaminase and high L-Asparaginase activity. The L-Asparaginase activity obtained with Maltose at 48h pH-6.0, temperature 25˚C, and 120 RPM was found to be 8.25 IU/ml besides there was a decrease in L-Glutaminase activity to 3.27 IU/ml. Increased concentration of the Maltose favoured high L-Glutaminase activity was shown in Fig 6. No enzyme was produced with Fructose as a carbon source.

Effect of nitrogen source : From Fig 7 it was observed that Yeast extract gave the best results among all other nitrogen sources. The concentration of Yeast extract was varied from 5 g/L to 20 g/L was shown in Fig 8 Yeast extract optimum concentration was found to be 15 g/L. At optimum concentration, the enzyme activities were observed as 17.1 IU/ml and 9.43 IU/ml for L-Asparaginase and L-Glutaminase respectively.

Effect of L-Asparagine concentration : L-Asparagine was the inducer which triggers the production of L-Asparaginase. The concentration of L-Asparagine was varied from 3 g/L to 15 g/L shown in Fig 9. The optimum concentration was found to be 15 g/L. The enzyme activities were observed as 18.1 IU/ml and 5.7 IU/ml for L-Asparaginase and L-Glutaminase respectively at 48h, pH-6.0, Temperature 25˚C and RPM-120.

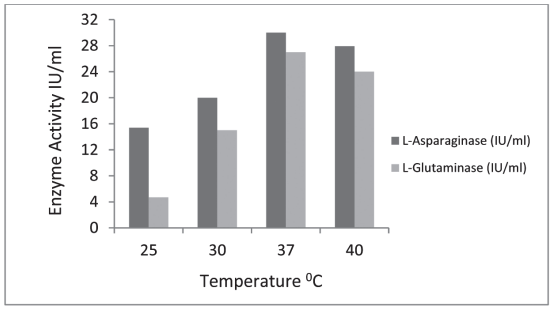

Fig 3.Effect of Temperature (^{O}C) at 48h of incubation

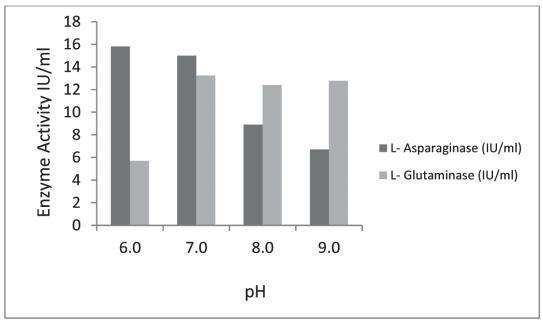

Fig 4.Effect of pH at 48h of incubation

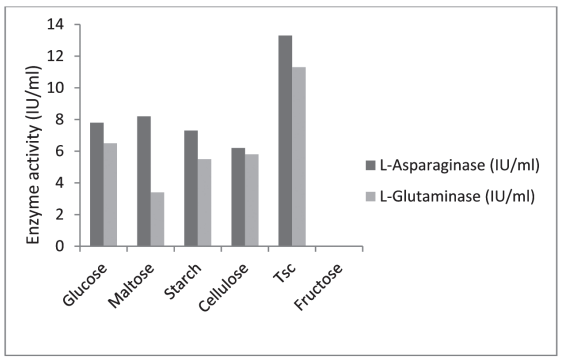

Fig 5.Effect of Different Carbon sources (2g/L) at 48h

From process of optimization by OFAT studies, there was approximately 2.6 fold increase in the L-Asparaginase activity from 7.8 IU/ml to 18.4 IU/ml, and decrease in L-Glutaminase activity from 6.51 to 5.7 IU/ml was observed.

Plackett –Burman design studies : Plackett-Burman design experiments listed Table 1 were conducted to identify the factors influencing on the production. The square root transformation is

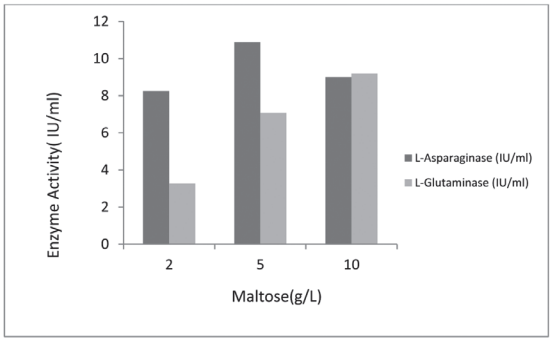

Fig 6.Effect of different concentrations of Maltose

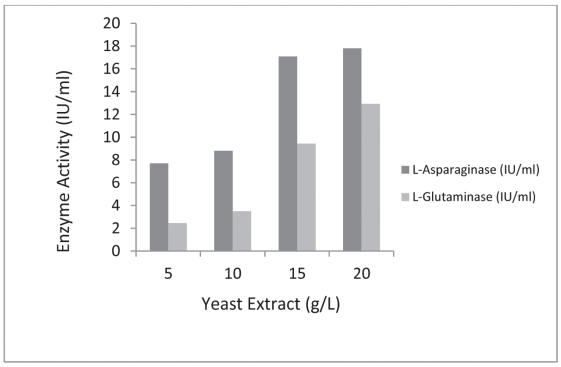

Fig 8.Effect of different concentrations of Yeast Extract

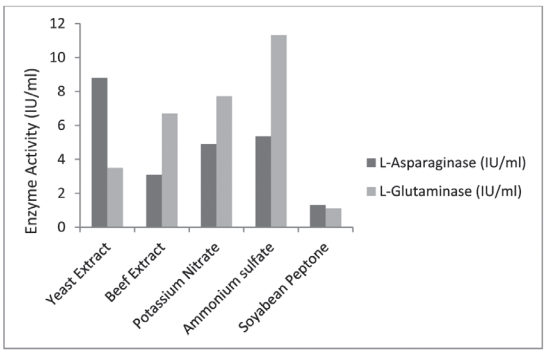

Fig 7.Effect of Different Nitrogen sources (15g/L) at 48h

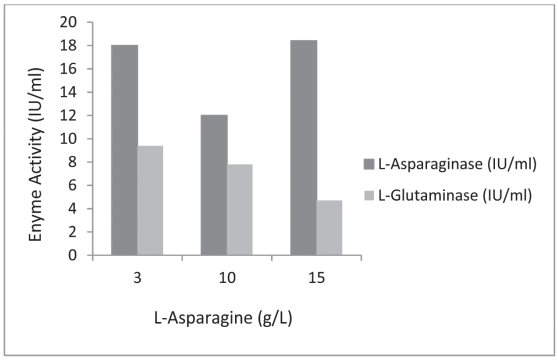

Fig 9.Effect of different concentrations of L-Asparagine

used as the ratio of maximum to minimum activity is >10. From Table 2 ANOVA based regression investigation was employed. It was affirmed that L-Asparagine, Time, Temperature, pH were identified as significant variables. The R^2 value, mean and standard deviation of the obtained model were reported as 97.12, 2.31 and 0.51 respectively.

The model F-value of 282.95 implies that the model was significant. There was only a 4.62% chance that a "Model F-Value" this large could occur due to noise. In the Pareto chart of L-Asparaginase, all the factors have shown positive effect.

The final equation obtained in terms of coded factors for L- Asparaginase was shown below:

sqrt(L-Asparaginase)=-1.98+0.37* Maltose+0.34* Yeast Extract +0.35* L-Asparagine + 0.042 *Temperature+0.17* pH+0.019* Time+7.39 E-003*RPM+0.048* D.O2+1.51* KH_2PO_4+5.61* NaCl

For L-Glutaminase the responses ranged from 2.04 to 16.14.The proportion of maximum to minimum was observed as 7.86. Hence, transformation is not required. From Table 3 the model F-value of 24.59 implies that the model is significant with the regression coefficient of 99.83%. Maltose showed a negative impact on L-Glutaminase activity.

The final equation obtained from ANOVA in terms of coded factors is shown below:

L-Glutaminase=-13.58+1.16* Yeast Extract +0.49* L-Asparagine + 0.23* Temperature + 0.47 * pH +0.052* Time+0.060* RPM+0.83* DO_2+1.25* Na_2HPO_4-9.3*NaCl

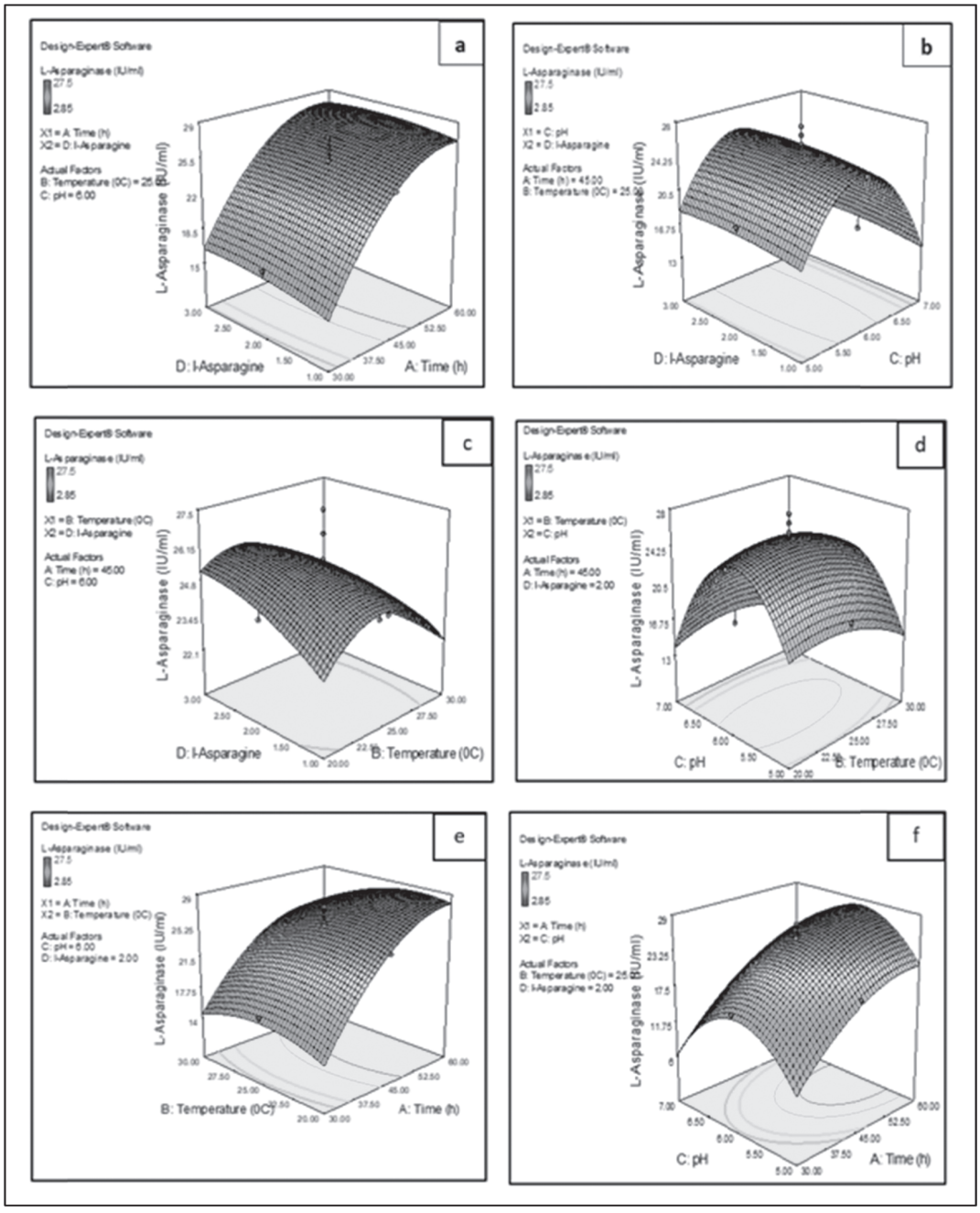

Fig 10.3D response surface plots showing the interactive effects of significant variables on L-Asparaginase production:**a:**Concentration of L-Asparagine and Time**b**: Concentration of L-Asparagine and pH **c**: Concentration of L-Asparagine and Temperature d: pH andTemperature**e**: Temperature and Time**f**: pH and Time

Vol. 12 (4) 390-405, October 2018, ISSN 0973-8916 (Print), 2230-7303 (Online)

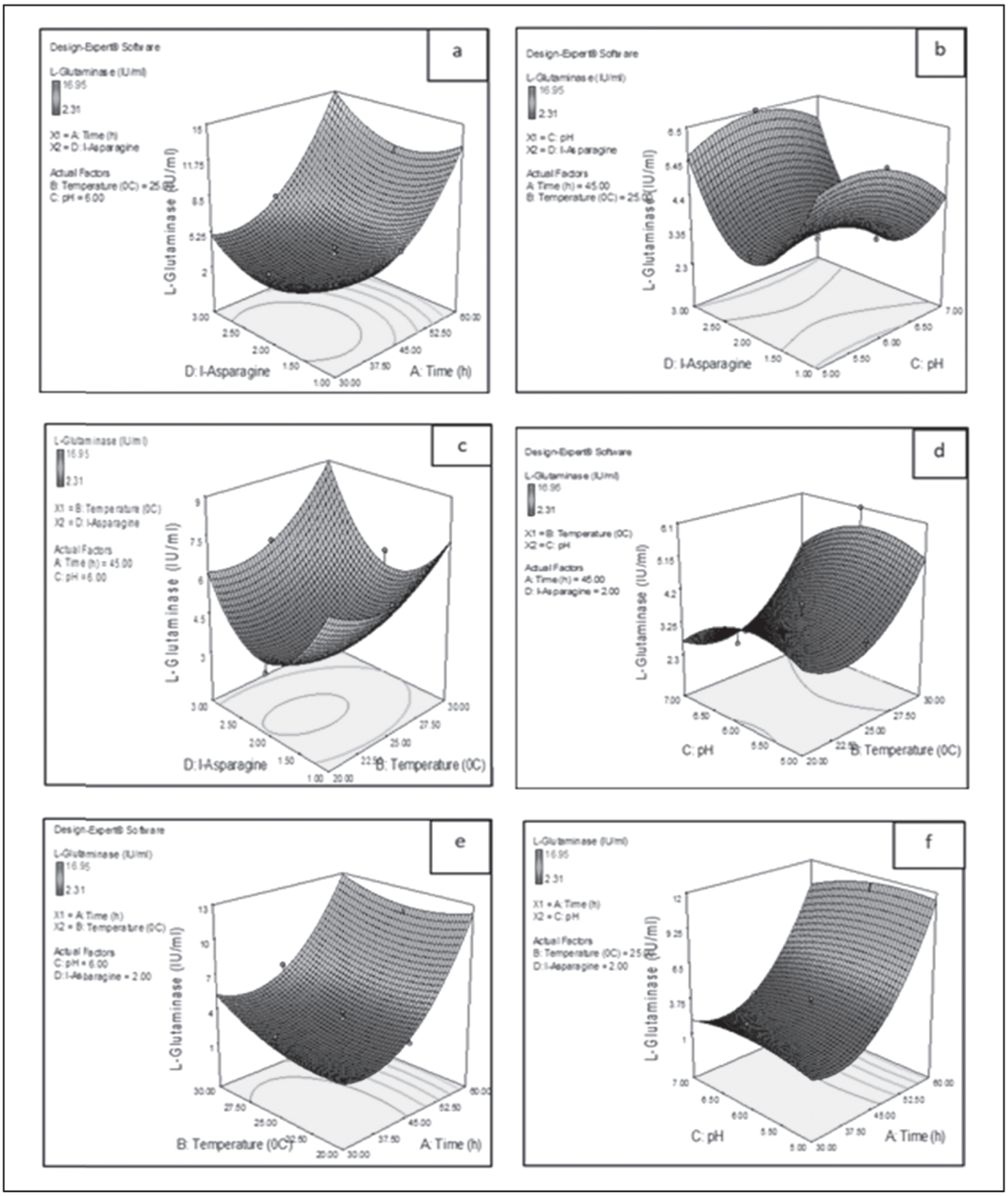

Fig 11.3D response surface plots showing the interactive effects of significant variables on L-Glutaminase production:**a:** Concentration of L-Asparagine andTime b: Concentration of L-Asparagine and pH **c**: Concentration of L-Asparagine and Temperature **d**: pH and Temperature**e**: Temperature and Time**f**: pH and Time

Table 1.Plackett-Burman Design

Std	Run	Maltose (g/L)	Yeast Extract (g/L)	L-Asparagine (g/L)	Temperature (^{0}C)	pH	Time (h)	RPM	DO2	Na_2HPO_4 (g/L)	KH_2PO_4 (g/L)	NaCl (g/L)	L-Asparaginase (IU/ml)	L-Glutaminase (IU/ml)
6	1	0.1	0.1	0.3	40	5	72	150	1	1	0.5	0.1	22.01	12.08
2	2	0.1	1.5	2	20	8	72	150	1	0.3	0.1	0.1	23.96	10.63
8	3	0.4	1.5	0.3	20	5	72	100	4	1	0.1	0.1	13.02	9.00
4	4	0.1	1.5	0.3	40	8	24	150	4	1	0.1	0.01	14.40	16.14
7	5	0.4	0.1	0.3	20	8	24	150	4	0.3	0.5	0.1	13.74	8.20
1	6	0.4	1.5	0.3	40	8	72	100	1	0.3	0.5	0.01	24.88	12.31
10	7	0.1	1.5	2	40	5	24	100	4	0.3	0.5	0.1	21.56	10.66
12	8	0.1	0.1	0.3	20	5	24	100	1	0.3	0.1	0.01	2.051	2.05
13	9	0.25	0.8	1.15	30	6.5	48	125	2.5	0.65	0.3	0.05	22.9	9.87
11	10	0.4	0.1	2	40	8	24	100	1	1	0.1	0.1	16.11	9.22
5	11	0.1	0.1	2	20	8	72	100	4	1	0.5	0.01	18.05	10.04
3	12	0.4	0.1	2	40	5	72	150	4	0.3	0.1	0.01	20.09	15.82
9	13	0.4	1.5	2	20	5	24	150	1	1	0.5	0.01	12.83	8.45

Finally, in numerical optimization, the goal for L-Asparaginase is set to maximum and vice versa for L-Glutaminase. The optimum concentration of factors was shown in Table 4. Time, Temperature, pH and L-Asparagine were chosen as significant variables which were further studied by RSM method.

Optimization by Response Surface methodology (RSM) : Based on the Table 5 generated from Central Composite Design (CCD), experiments have been performed in triplicates, and the responses were noted.

L-Asparaginase ANOVA analysis : The ratio of maximum to minimum response is <10. The quadratic model was chosen based on the lack of fit test. The lack of fit F-Value 2.53 from Table 6 indicates that the model is significant. The standard deviation, mean and regression coefficient (R^2) obtained were 1.36, 16.93 and 98.60% respectively.

From the above data it was observed that A,B,C,AB,A^2,C^2 were significant model terms. The interactions between the factors were in significant if P>0.5.

The second order polynomial equation related to L-Asparaginase activity is shown below:

L-Asparaginase (IU/ml) =-374.98+2.15* Time (h)+3.51*Temperature (˚C)+99.95* pH + 5.99*L-Asparagine(g/L)-0.012*Time (h)*Temperature (˚C)-0.013*Time (h)*pH-0.013*Time (h)*L-Asparagine(g/L)+0.11*Temperature (˚C)*pH-0.124*Temperature (˚C)*L-Asparagine (g/L)+0.013* pH *L-Asparagine (g/L)-0.015* Time $(h)^2$ -0.07*Temperature $(˚C)^2$-8.64* pH^2-0.479* L-Asparagine $(g/L)^2$

The 3D surface model graphs will be useful when the response is transformed. It can be viewed in both in transformed and original scale. These graphs were plotted to study the interactions between two factors while keeping the other factors constant. The 3D surface plots obtained for L-Asparaginase were shown in Fig 10.

L-Glutaminase ANOVA analysis : The significant terms obtained from regression analysis were A,

Table 2. Plackett-Burman ANOVA analysis for L-Asparaginase

Response-L-Asparaginase						
Transform:	Square root	Constant:	0			
ANOVA for selected factorial model						
Analysis of variance table [Partial sum of squares - Type III]						
				F	p-value	
Source	Sum of Squares	df	Mean Square	Value	Prob > F	
Model	10.01	10	1.00	282.95	0.0462	significant
A-carbon	0.038	1	0.038	10.77	0.1883	
B-nitrogen	0.71	1	0.71	202.87	0.0446	
C-L-ASPARAGINE	1.10	1	1.10	312.67	0.0360	
D-TEMPERATURE	2.20	1	2.20	622.9	0.0255	
E-pH	0.85	1	0.85	242.28	0.0408	
F-TIME	2.74	1	2.74	776.19	0.0228	
G-RPM	0.41	1	0.41	115.99	0.0589	
H-D.O2	0.06	1	0.064	18.283	0.1463	
K-kh2po4	1.10	1	1.10	311.10	0.0361	
L-Nacl	0.76	1	0.76	216.44	0.0432	
Curvature	0.55	1	0.55	157.87	0.0506	not significant
Residual	0.003	1	0.003			
Cor Total	10.57	12				

Table 3. Plackett-Burman ANOVA analysis for L-Glutaminase

Response-L-Glutaminase						
ANOVA for selected factorial model						
Analysis of variance table [Partial sum of squares - Type III]						
	Sum of		Mean	F	p-value	
Source	Squares	df	Square	Value	Prob > F	
Model	150.50	9	16.72	127.10	0.0078	significant
B-Yeast Extract	7.988	1	7.988	60.722	0.0161	
C-L-Asparagine	2.126	1	2.126	16.160	0.0567	
D-Temperature	64.68	1	64.68	491.68	0.0020	
E-pH	5.988	1	5.988	45.517	0.0213	
F-Time	19.17	1	19.17	145.78	0.0068	
G-RPM	27.06	1	27.06	205.75	0.0048	
H-DO2	19.04	1	19.04	144.79	0.0068	
J-Na2HPO4	2.308	1	2.308	17.545	0.0525	
L-NaCl	2.105	1	2.105	16.007	0.0572	
Curvature	0.242	1	0.242	1.8422	0.3076	not significant
Residual	0.2631	2	0.131			
Cor Total	151.0	12				

Table 4. Final Concentrations of individual factors obtained from Plackett-Burman design

Maltose (g/L)	Yeast Extract (g/L)	L-Asparagine (g/L)	Temperature (^{0}C)	pH	Time (h)	RPM	DO2	Na_2HPO_4	KH_2PO_4	NaCl	L-Asparaginase (IU/ml)	L-Glutaminase (IU/ml)
0.4	0.96	1.99	22.92	7	50	132.1	1.2	0.37	0.5	0.1	22.59	8.130

Table 5. RSM CCD design for four independent variables

Std	run	Time (h)	Temperature (^{O}C)	pH	L-Asparagine (g/L)	L-Asparaginase (IU/ml)	L-Glutaminase (IU/ml)
9	1	30	20	5	3	6.98	3.01
29	2	45	25	6	2	25.65	3.81
2	3	60	20	5	1	19.12	15.43
5	4	30	20	7	1	2.89	4.45
24	5	45	25	6	3	24.78	6.5
11	6	30	30	5	3	6.34	6.76
19	7	45	20	6	2	24.267	3.345
20	8	45	30	6	2	22.34	6.09
3	9	30	30	5	1	6.45	6.98
28	10	45	25	6	2	27.5	3.21
4	11	60	30	5	1	17	13.98
15	12	30	30	7	3	5.65	7.32
23	13	45	25	6	1	24.45	5.89
7	14	30	30	7	1	2.85	7.07
17	15	30	25	6	2	16.88	3.86
16	16	60	30	7	3	13.65	15.82
6	17	60	20	7	1	15.88	12.65
1	18	30	20	5	1	6.42	5.34
26	19	45	25	6	2	24.9	3.09
27	20	45	25	6	2	26.6	3.74
21	21	45	25	5	2	19.12	3.421
18	22	60	25	6	2	26.53	10.48
25	23	45	25	6	2	25.6	3.8
14	24	60	20	7	3	16.89	14.65
10	25	60	20	5	3	24.087	14.45
12	26	60	30	5	3	15.14	16.95
13	27	30	20	7	3	4.98	4.06
22	28	45	25	7	2	13.78	2.31
8	29	60	30	7	1	15.78	12.31
30	30	45	25	6	2	25.3	3.21

Table 6. RSM ANOVA analysis for L-Asparaginase

ANOVA for Response Surface Quadratic Model –L-Asparaginase IU/ml						
Analysis of variance table [Partial sum of squares - Type III]						
	Sum of		**Mean**	**F**	**p-value**	
Source	Squares	df	Square	Value	Prob > F	
Model	1939.832	14	138.55	75.29	< 0.0001	significant
A-Time (h)	608.272	1	608.27	330.55	< 0.0001	
B-Temperature (^{0}C)	14.785	1	14.78	8.035	0.0126	
C-pH	44.515	1	44.51	24.191	0.0002	
D-l-Asparagine	3.257	1	3.25	1.77	0.2032	
AB	13.008	1	13.008	7.069	0.0179	
AC	0.691	1	0.691	0.375	0.5490	
AD	0.702	1	0.702	0.38	0.5459	
BC	5.0254	1	5.02	2.73	0.1192	
BD	6.159	1	6.15	3.34	0.0873	
CD	0.002	1	0.0028	0.0015	0.9692	
A^2	29.768	1	29.76	16.17	0.0011	
B^2	8.312	1	8.31	4.51	0.0506	
C^2	193.617	1	193.61	105.21	< 0.0001	
D^2	0.596	1	0.59	0.323	0.5777	
Residual	27.602	15	1.84			
Lack of Fit	23.043	10	2.30	2.527434	0.1589	not significant
Pure Error	4.558	5	0.911			
Cor Total	1967.435	29				

B, C, AC, BC, A^2, B^2 and C^2 was shown in Table 7.The "Pred R-Squared" of 0.8958 is in reasonable agreement with the "Adj R-Squared" of 0.9518.The value of Adeq Precision 18.615 indicates an adequate signal. Hence this model can be used to navigate the design space.

L-Glutaminase (IU/ml) =29.54-0.87 *Time (h)-1.93*Temperature(˚C)+8.83*pH-16.77*L-Asparagine(g/L)-7.82E-003*Time (h)*Temperature (˚C)-0.025*Time (h)*pH+0.042*Time (h)*L-Asparagine(g/L)+3.37E-003* Temperature (˚C)*pH+0.102*Temperature (˚C) * L-Asparagine (g/L)+0.37* pH* L-Asparagine (g/L)+0.015*Time $(h)^2$+0.044*Temperature (˚C)^2-0.73* pH^2 + 2.59* L-$Asparagine^2$

The 3D surface plots obtained for L-Glutamine are shown in Fig 11.

The final optimal concentrations obtained from RSM analysis were shown in Table 8.

Conclusion:

To minimize the side effects of the commercially available forms of L-Asparaginase an alternative source has been identified in this study. Out of 30 endophytes which were isolated from *Ocimum tenuiflorum*, the one that gave the maximum activity was screened and identified as *Bacillus stratosphericus* by 16 S rRNA sequencing studies. The enzyme activities obtained with M-9 media for L-Asparaginase and L-Glutaminase were 7.8 IU/ml and 6.51 IU/ml respectively. By traditional

Table 7.RSM ANOVA analysis for L-Glutaminase

ANOVA for Response Surface Quadratic Model - L-Glutaminase IU/ml						
Analysis of variance table [Partial sum of squares - Type III]						
	Sum of		**Mean**	**F**	**p-value**	
Source	Squares	df	Square	Value	Prob > F	
Source	Squares	df	Square	Value	Prob > F	
Model	640.490	14	45.749	131.848	< 0.0001	significant
A-Time (h)	336.874	1	336.874	970.859	< 0.0001	
B-Temperature (0C)	14.036	1	14.036	40.452	< 0.0001	
C-pH	1.793	1	1.793	5.167	0.0381	
D-L-Asparagine	1.632	1	1.632	4.703	0.0466	
AB	5.511	1	5.511	15.882	0.0012	
AC	2.395	1	2.395	6.902	0.0190	
AD	6.490	1	6.490	18.703	0.0006	
BC	0.005	1	0.005	0.013	0.9103	
BD	4.213	1	4.213	12.141	0.0033	
CD	2.198	1	2.198	6.334	0.0237	
A^2	33.012	1	33.012	95.139	< 0.0001	
B^2	3.233	1	3.233	9.317	0.0081	
C^2	1.400	1	1.400	4.034	0.0630	
D^2	17.441	1	17.441	50.263	< 0.0001	
Residual	5.205	15	0.347			
Lack of Fit	4.628	10	0.463	4.012	0.0692	not significant
Pure Error	0.577	5	0.115			
Cor Total	645.695	29				

Table 8. Final composition of individual factors obtained from RSM CCD analysis

Time (h)	Temperature (°C)	pH	L-Asparagine (g/L)	L-Asparaginase (IU/ml)	L-Glutaminase (IU/ml)
43.93	23.27	5.91	2.06	25.28	3.09

optimization, L-Asparaginase activity increased to 18.4 IU/ml whereas L-Glutaminase activity decreased to 5.7 IU/ml. L-Asparagine, Time, Temperature, and pH was identified as significant variables from Plackett-Burman experimental design. Central Composite Design was employed for the four significant variables. There was a 3.24 fold increase in L-Asparaginase activity, i.e., 25.28 IU/ml besides minimizing the L-Glutaminase activity to 3.09 IU/ml. Hence, this work will provide a future direction for the enhancement of L-Asparaginase production from new source with minimal side effects.

Acknowledgments

Authors would like to thank Director, National Institute of Technology Warangal, Warangal, India, for the kind support in bringing out the above literature and providing lab facilities.

Conflict of interest: Authors have no conflict of interest regarding the publication of paper.

References

1. Avramis, V.I., Sencer, S., Periclou, A.P., Sather, H., Bostrom, B.C., Cohen, L.J., Ettinger, A.G., Ettinger, L.J., Franklin, J., Gaynon, P.S. and Hilden, J.M., (2002). A randomized comparison of native Escherichia coli asparaginase and polyethylene glycol conjugated asparaginase for treatment of children with newly diagnosed standard-risk acute lymphoblastic leukemia: a Children's Cancer Group study. Blood, 99(6), pp.1986-1994.
2. Clavell, L.A., Gelber, R.D., Cohen, H.J., Hitchcock-Bryan, S., Cassady, J.R., Tarbell, N.J., Blattner, S.R., Tantravahi, R., Leavitt, P. and Sallan, S.E., (1986). Four-agent induction and intensive asparaginase therapy for treatment of childhood acute lymphoblastic leukemia. New England journal of medicine, 315(11), pp.657-663.
3. Pieters, R., Hunger, S.P., Boos, J., Rizzari, C., Silverman, L., Baruchel, A., Goekbuget, N., Schrappe, M. and Pui, C.H., (2011). L-asparaginase treatment in acute lymphoblastic leukemia. Cancer, 117(2), pp.238-249.
4. Sassen, S.D., Mathôt, R.A., Pieters, R., Kloos, R.Q., de Haas, V., Kaspers, G.J., van den Bos, C., Tissing, W.J., te Loo, M., Bierings, M.B. and Kollen, W.J., (2017). Population pharmacokinetics of intravenous Erwinia asparaginase in pediatric acute lymphoblastic leukemia patients. haematologica, 102(3), pp.552-561.
5. Schrappe, M., Reiter, A., Ludwig, W.D., Harbott, J., Zimmermann, M., Hiddemann, W., Niemeyer, C., Henze, G., Feldges, A., Zintl, F. and Kornhuber, B., (2000). Improved outcome in childhood acute lymphoblastic leukemia despite reduced use of anthracyclines and cranial radiotherapy: results of trial ALL-BFM 90. Blood, 95(11), pp.3310-3322.
6. Ogawa, C., Taguchi, F., Goto, H., Koh, K., Tomizawa, D., Ohara, A. and Manabe, A., (2017). Plasma asparaginase activity, asparagine concentration, and toxicity after administration of Erwinia asparaginase in children and young adults with acute lymphoblastic leukemia: Phase I/II clinical trial in Japan. Pediatric blood & cancer, 64(9).
7. Pui, C.H., Pei, D., Raimondi, S.C., Coustan-Smith, E., Jeha, S., Cheng, C., Bowman, W.P., Sandlund, J.T., Ribeiro, R.C., Rubnitz, J.E. and Inaba, H., (2017). Clinical impact of minimal residual disease in children with different subtypes of acute lymphoblastic leukemia treated with response-adapted therapy. Leukemia, 31(2), p.333.
8. Hunger, S.P. and Mullighan, C.G., (2015). Acute lymphoblastic leukemia in children. New England Journal of Medicine, 373(16), pp.1541-1552.
9. Dias, F.F.G., Junior, S.B., Hantao, L.W., Augusto, F. and Sato, H.H., (2017). Acrylamide mitigation in French fries using native l-asparaginase from Aspergillus oryzae CCT 3940. LWT-food Science and Technology, 76, pp.222-229.
10. Mahajan, R.V., Saran, S., Kameswaran, K., Kumar, V. and Saxena, R.K., (2012). Efficient production of L-asparaginase from Bacillus licheniformis with low-glutaminase activity: optimization, scale up and acrylamide degradation studies. Bioresource technology, 125, pp.11-16.
11. Pedreschi, F., Kaack, K. and Granby, K., (2008). The effect of asparaginase on

acrylamide formation in French fries. Food chemistry, 109(2), pp.386-392.

12. Xu, F., Oruna-Concha, M.J. and Elmore, J.S., (2016). The use of asparaginase to reduce acrylamide levels in cooked food. Food chemistry, 210, pp.163-171.

13. Zyzak, D.V., Sanders, R.A., Stojanovic, M., Tallmadge, D.H., Eberhart, B.L., Ewald, D.K., Gruber, D.C., Morsch, T.R., Strothers, M.A., Rizzi, G.P. and Villagran, M.D., (2003). Acrylamide formation mechanism in heated foods. Journal of agricultural and food chemistry, 51(16), pp.4782-4787.

14. Kumar SS, Abdulhameed S. Therapeutic Enzymes. Bioresour. Bioprocess Biotechnol., (2017), p. 45–73.

15. Polgár, L., (2005). The catalytic triad of serine peptidases. Cellular and Molecular Life Sciences CMLS, 62(19-20), pp.2161-2172.

16. Keating, M.J., Holmes, R., Lerner, S. and Ho, D.H., 1993. L-asparaginase and PEG asparaginase - past, present, and future. Leukemia & lymphoma, 10(sup1), pp.153-157.

17. Kwong, Y.L., 2005. Natural killer-cell malignancies: diagnosis and treatment. Leukemia, 19(12), p.2186.

18. Sabu, A., (2003). Sources, properties and applications of microbial therapeutic enzymes.

19. Asselin, B.L., Whitin, J.C., Coppola, D.J., Rupp, I.P., Sallan, S.E. and Cohen, H.J., (1993). Comparative pharmacokinetic studies of three asparaginase preparations. Journal of Clinical Oncology, 11(9), pp.1780-1786.

20. Castaman, G. and Rodeghiero, F., (1993). Erwinia-and E. coli-derived L-asparaginase have similar effects on hemostasis. Pilot study in 10 patients with acute lymphoblastic leukemia. Haematologica, 78 (6 Suppl 2), pp.57-60.

21. Batool, T., Makky, E.A., Jalal, M. and Yusoff, M.M., (2016). A comprehensive review on L-asparaginase and its applications. Applied biochemistry and biotechnology,178(5), pp.900-923.

22. Huang, L., Liu, Y., Sun, Y., Yan, Q. and Jiang, Z., (2014). Biochemical characterization of a novel L-Asparaginase with low glutaminase activity from Rhizomucor miehei and its application in food safety and leukemia treatment. Applied and environmental microbiology, 80(5), pp.1561-1569.

23. Kornbrust, B.A., Stringer, M.A., Lange, N.E.K. and Hendriksen, H.V., (2009). Asparaginase–an enzyme for acrylamide reduction in food products. Enzymes in Food Technology, Second edition, pp.59-87.

24. Capizzi, R.L., Bertino, J.R., Skeel, R.T., Creasey, W.A., Zanes, R., Olayon, C., Peterson, R.G. and Handschumacher, R.E., (1971). L-asparaginase: clinical, biochemical, pharmacological, and immunological studies. Annals of internal medicine, 74(6), pp.893-901.

25. Asthana, N. and Azmi, W.,(2003). Microbial l-asparaginase: a potent antitumour enzyme.

26. Lopes, A.M., Oliveira-Nascimento, L.D., Ribeiro, A., Tairum Jr, C.A., Breyer, C.A., Oliveira, M.A.D., Monteiro, G., Souza-Motta, C.M.D., Magalhães, P.D.O., Avendaño, J.G.F. and Cavaco-Paulo, A.M., (2017). Therapeutic l-asparaginase: upstream, downstream and beyond. Critical reviews in biotechnology, 37(1), pp.82-99.

27. Kumar, S., Dasu, V.V. and Pakshirajan, K., (2011). Purification and characterization of glutaminase-free L-asparaginase from Pectobacterium carotovorum MTCC 1428. Bioresource technology, 102(2), pp.2077-2082.

28. El-Naggar, N.E.A., El-Ewasy, S.M. and El-Shweihy, N.M., (2014). of Acute Lymphoblastic Leukemia: The Pros and Cons. International Journal of pharmacology, 10(4), pp.182-199.

29. Erva, R.R., Goswami, A.N., Suman, P., Vedanabhatla, R. and Rajulapati, S.B., (2017). Optimization of L-asparaginase production from novel Enterobacter sp., by submerged fermentation using response surface methodology. Preparative Biochemistry and Biotechnology, 47(3), pp.219-228.

30. Shinnick, S.E., Browning, M.L. and Koontz, S.E., (2013). Managing hypersensitivity to asparaginase in pediatrics, adolescents, and young adults. Journal of pediatric oncology nursing, 30(2), pp.63-77.

31. Martinez-Klimova, E., Rodríguez-Peña, K. and Sánchez, S., (2017). Endophytes as sources of antibiotics. Biochemical pharmacology, 134, pp.1-17.

32. Rajamanikyam, M., Vadlapudi, V. and Upadhyayula, S.M., (2017). Endophytic Fungi as Novel Resources of natural Therapeutics. Brazilian Archives of Biology and Technology, 60.

33. Krishnapura, P.R., Belur, P.D. and Subramanya, S., (2016). A critical review on properties and applications of microbial l-asparaginases. Critical reviews in microbiology, 42(5), pp.720-737.

34. Tanvir, R., Javeed, A. and Bajwa, A.G., (2017). Endophyte bioprospecting in South Asian medicinal plants: an attractive resource for biopharmaceuticals. Applied microbiology and biotechnology, 101(5), pp.1831-1844.

35. Jalgaonwala, R.E., Mohite, B.V. and Mahajan, R.T., (2017). A review: natural products from plant associated endophytic fungi. Journal of microbiology and biotechnology research, 1(2), pp.21-32.

36. Golinska, P., Wypij, M., Agarkar, G., Rathod, D., Dahm, H. and Rai, M., (2015). Endophytic actinobacteria of medicinal plants: diversity and bioactivity. Antonie Van Leeuwenhoek, 108(2), pp.267-289.

37. Ludwig-Müller, J., (2015). Plants and endophytes: equal partners in secondary metabolite production?. Biotechnology letters, 37(7), pp.1325-1334.

38. Kusari, S., Singh, S. and Jayabaskaran, C., (2014). Biotechnological potential of plant-associated endophytic fungi: hope versus hype. Trends in biotechnology, 32(6), pp.297-303.

39. Venugopalan, A. and Srivastava, S., (2015). Endophytes as in vitro production platforms of high value plant secondary metabolites. Biotechnology advances, 33 (6), pp.873-887.

40. Nannipieri, P., Kandeler, E. and Ruggiero, P., (2002). Enzyme activities and micro-biological and biochemical processes in soil. Enzymes in the environment. Marcel Dekker, New York, pp.1-33

41. El-Naggar, N.E.A., Moawad, H. and Abdelwahed, N.A., (2017). Optimization of fermentation conditions for enhancing extracellular production of L-asparaginase, an anti-leukemic agent, by newly isolated Streptomyces brollosae NEAE-115 using solid state fermentation. Annals of microbiology, 67(1), pp.1-15.

42. Kenari, S.L.D., Alemzadeh, I. and Maghsodi, V., (2011). Production of l-asparaginase from Escherichia coli ATCC 11303: Optimization by response surface methodology. Food and Bioproducts Processing, 89(4), pp.315-321.

43. Muralidhar, R.V., Chirumamila, R.R., Marchant, R. and Nigam, P., (2001). A response surface approach for the comparison of lipase production by Candida cylindracea using two different carbon

sources. Biochemical Engineering Journal, 9(1), pp.17-23.

44. Larran, S., Perello, A., Simon, M.R. and Moreno, V., (2002). Isolation and analysis of endophytic microorganisms in wheat (Triticum aestivum L.) leaves. World Journal of Microbiology and Biotechnology, 18(7), pp.683-686.

45. Janssen, P.H., (2006). Identifying the dominant soil bacterial taxa in libraries of 16S rRNA and 16S rRNA genes. Applied and environmental microbiology, 72(3), pp.1719-1728.

46. Liu, W.T., Marsh, T.L., Cheng, H. and Forney, L.J., (1997). Characterization of microbial diversity by determining terminal restriction fragment length polymorphisms of genes encoding 16S rRNA. Applied and environmental microbiology, 63(11), pp.4516-4522.

47. Marchesi, J.R., Sato, T., Weightman, A.J., Martin, T.A., Fry, J.C., Hiom, S.J. and Wade, W.G., (1998). Design and evaluation of useful bacterium-specific PCR primers that amplify genes coding for bacterial 16S rRNA. Applied and environmental microbiology, 64(2), pp.795-799.

48. Frank, J.A., Reich, C.I., Sharma, S., Weisbaum, J.S., Wilson, B.A. and Olsen, G.J., (2008). Critical evaluation of two primers commonly used for amplification of bacterial 16S rRNA genes. Applied and environmental microbiology, 74(8), pp.2461-2470.

49. Kim, O.S., Cho, Y.J., Lee, K., Yoon, S.H., Kim, M., Na, H., Park, S.C., Jeon, Y.S., Lee, J.H., Yi, H. and Won, S., (2012). Introducing EzTaxon-e: a prokaryotic 16S rRNA gene sequence database with phylotypes that represent uncultured species. International journal of systematic and evolutionary microbiology, 62(3), pp.716-721.

50. Altschul, S.F., Gish, W., Miller, W., Myers, E.W. and Lipman, D.J., (1990). Basic local alignment search tool. Journal of molecular biology, 215(3), pp.403-410.

51. Edgar, R.C., (2004). MUSCLE: multiple sequence alignment with high accuracy and high throughput. Nucleic acids research, 32 (5), pp.1792-1797.

52. Guindon, S. and Gascuel, O., (2003). A simple, fast, and accurate algorithm to estimate large phylogenies by maximum likelihood. Systematic biology, 52(5), pp.696-704.

53. Chevenet, F., Brun, C., Bañuls, A.L., Jacq, B. and Christen, R., (2006). TreeDyn: towards dynamic graphics and annotations for analyses of trees. BMC bioinformatics, 7(1), p.439.

Vol. 12 (4) i - v October 2018, ISSN 0973-8916 (Print), 2230-7303 (Online)

NEWS ITEM

Researchers from IIT (BHU) found a breakthrough in detoxifying toluene

Using bacteria isolated from soil and effluents near an oil refinery, researchers from the University of Delhi and Indian Institute of Technology (BHU), Varanasi, have successfully degraded toluene into less-toxic by products. Toluene is one of the petrochemical wastes that get released without treatment from industries such as refineries, paint, textile, paper and rubber. Toluene has been reported to cause serious health problems to aquatic life, and studies point that it has genotoxic and carcinogenic effects on human beings.To the soil and effluent samples containing some bacteria 100 mg/L of toluene was added and incubated for four weeks. The bacteria were isolated from the samples, identified and studied for their toluene-degrading abilities. They isolated eight to 10 strains of bacteria and found that a particular bacteria Acinetobacter junii showed good degrading potential - about 80% of toluene (50 ppm) in a liquid medium was degraded within 72 hours. A consortium of A. junii bacteria was found to be more effective than using a single strain. Different bacterial strains have different characteristic potential to degrade intermediate by-products formed during the degradation process and, hence, increase the efficiency, says Pardeep Singh. Another interesting find was that when exposed to toluene, these bacteria changed their morphology to escape toxicity. Electron microscopy studies revealed that the cylindrical cells transformed into an ovoid or spherical structure. The researchers also examined the pathway by which the bacteria were doing the degradation and found it to be general aerobic biodegradation pathway. The researchers also tested the bacterial strain for the degradation of benzene, phenol, and xylene and they showed effective results towards degradation of these compounds - both individual compounds and their mixtures.

Researchers from JNCASR reports restoration of memory in Alzheimer's mice

Using a small molecule that activates two enzymes (CBP/p300 histone acetyltransferases), researchers from India and France have been able to completely recover long-term memory in mice with Alzheimer's disease. Neuron-to-neuron connections that form the network were re-established leading to memory recovery in the diseased mice. The therapeutic molecule used in the study was synthesised by a team led by Tapas Kundu from the Molecular Biology and Genetics Unit at Jawaharlal Nehru Centre for Advanced Scientific Research (JNCASR), Bengaluru. The small molecule was found to activate the two enzymes, and the two enzymes by virtue of being the master regulators activate several genes that are important for memory. In a June 2013 paper in the Journal of Neuroscience, Prof. Kundu's team had demonstrated the small molecule's ability to generate new neurons and induce long-term memory in normal mice.If it is able to induce memory in normal mice, we wondered if it can induce and recover lost memory in mice with Alzheimer's,recalls Prof. Kundu. We found the molecule activating the two enzymes in the diseased mice and producing new neurons. Also, 81 genes whose expression was repressed in mice with Alzheimer's were activated to normal levels. Besides completely recovering lost memory, other symptoms of Alzheimer's such as balance problem was also addressed. The amyloid plaques and neurofibrillary tangles contribute to the degradation of the neurons leading to memory loss in Alzheimer's. The plaques and tangles absorb these two enzymes. So once the enzymes are activated by the small molecule, the whole process of neurodegeneration gets reversed, he says.

Shells of Sea Snails are dissolving due to Climate change

Researchers from the University of Plymouth in the UK and the University of Tsukuba, Japan assessed the impact of rising carbon dioxide levels on the large predatory "triton shell" gastropod. They found those living in regions with predicted future levels of CO2 were on average around a third smaller than counterparts living in conditions seen throughout the world's oceans today. However there was also a noticeable negative impact on the thickness, density, and structure of their shells, causing visible deterioration to the shell surface, researchers said. The study, published in the journal Frontiers in Marine Science, found that the effects are down to the increased stresses placed on the species in waters where the pH is lower, which

reduce their ability to control the calcification process. The researchers have warned other shellfish are likely to be impacted in the same way, threatening their survival and that of other species that rely on them for food. Using computed tomography (CT) scanning, the scientists measured the thickness, density and structure of the shells, with shell thickness halved in areas with raised CO2 while average shell length was reduced from 178mm in sites with present day levels to 112mm.In some cases, these negative effects left body tissue exposed and the shell casing dissolved, with the corrosive effects of acidification far more pronounced around the oldest parts of the shell.

Researchers from IIT Guwahati invents superior scaffold which aids in cartilage repair

Implanting cartilage alone or injecting cells found in healthy cartilage (chondrocytes) at the site of injury to heal the damaged cartilage in patients with osteoarthritis does not produce favourable results. Similarly, implanting two different scaffolds joined together to simultaneously regenerate the cartilage and reconstruct the bone too has many limitations.The problem arises because the interface between the cartilage and bone scaffolds, which are made of different materials, is not connected but has a distinct boundary. As a result, the interface tends to delaminate and degrade. Now, researchers from Indian Institute of Technology (IIT) Guwahati have addressed this shortcoming by fabricating a silk scaffold where the junction between the cartilage and bone scaffold is continuous and seamless and hence less prone to damage under load-bearing environment of the joint.A team led by Biman B. Mandal from the Department of Biosciences and Bioengineering has fabricated the biphasic scaffold where the top portion is highly porous and spongy thus mimicking the cartilage, while the bottom portion is reinforced with silk fibre thus imparting more stiffness and less porous to mimic the bone. Since the entire scaffold is made of silk, the interface merges with one another and is seamless despite having different porosities and stiffness. The results of the study were published in the Journal of Materials Chemistry B.The researchers made scaffolds using both wild silkworm (Antheraea assamensis) and mulberry silk (Bombyx mori) and found scaffolds made of non-mulberry silk were superior to the one made of mulberry silk in all respects. To make the biphasic scaffold we prepared silk solution by completely dissolving the silk. We then added chopped silk fibres to the solution so the bottom half portion of the scaffold becomes fibre-reinforced silk composite while the rest of the top portion had only the silk solution, says Prof. Mandal.

Scientists from IISc finds novel ways to dismantle Tuberculosis bacteria

Oxidative stress can directly damage the DNA, proteins and lipids of most of the bacteria and eventually kill them. However, disease-causing bacteria have evolved mechanisms to survive such stressful conditions. One of the ways bacteria overcome oxidative stress is by condensing or compacting the DNA (nucleoid). Compacted DNA has reduced surface area and hence lower vulnerability to oxidative stress.The role of several nucleoid-associated proteins produced by bacteria in condensing the DNA is also well known. But for the first time a protein (WhiB4) that condenses the DNA of TB-causing bacteria in response to oxidative stress has been found by a multi-institutional team led by Prof. Amit Singh from Indian Institute of Science (IISc), Bengaluru.Though the role of proteins in condensing DNA and the connection between DNA compaction and bacteria's ability to survive oxidative stress are already known, this is the first time the role of a protein to condense DNA upon directly sensing oxidative stress in any bacteria has been reported,says Prof. Singh. The results were published in the journal Redox Biology.While DNA compaction helps the bacteria survive stressful conditions, the compaction has to be only for a brief period and should be reversible. Prolonged compaction could adversely impact bacterial multiplication, conversion of DNA into RNA, and formation of protein molecules.The active form of WhiB4 protein is produced in the presence of oxidative stress leading to compaction of TB bacterial DNA. The protein level reduces after a while and thus preventing long-lasting condensation, and also allows the compacted DNA to revert to its original state.

Researchers reports micro spheres which traps water pollutants

Scientists have created tiny spheres that can catch and destroy bisphenol A (BPA), a synthetic chemical used to make plastics that often contaminates water.BPA is commonly used to coat the insides of food cans, bottle tops and water supply lines, and was once a component of baby bottles.

While BPA that seeps into food and drink is considered safe in low doses, prolonged exposure is suspected of affecting the health of children and contributing to high blood pressure.Scientists at Rice University in the U.S. have developed something akin to the Venus' flytrap of particles for water remediation.The supple petals provide plenty of surface area for researchers to anchor cyclodextrin — a benign sugar-based molecule often used in food and drugs. It has a two-faced structure, with a hydrophobic (water-avoiding) cavity and a hydrophilic (water-attracting) outer surface.BPA is hydrophobic and naturally attracted to the cavity. Once trapped, reactive oxygen species (ROS) produced by the spheres degrades BPA into harmless chemicals.The size of the particles is less than 100 nanometers. Because of their very small size, they're very difficult to recover from suspension in water,said Mr. Zhang, lead author of the study published in the journal Environmental Science & Technology.

Study reported that human eyes have innate mode for night vision

Our eyes have in-built night vision mode, say scientists who found that to see under starlight and moonlight, the retina changes both the software and hardware of its light-sensing cells.Retinal circuits that were thought to be unchanging and programmed for specific tasks are adaptable to different light conditions. However, scientists have now identified how the retina reprograms itself for low light.To see under starlight, biology has had to reach the limit of seeing an elementary particle from the universe, a single photon, said Greg Field, an assistant professor at Duke University in the US.The findings, published in the journal Neuron, show that the reprogramming happens in retinal cells that are sensitive to motion. Even in the best lighting, identifying the presence and direction of a moving object is key to survival for most animals.In humans, these directional neurons account for about 4% of the cells that send signals from the retina to the brain. In a study with mouse retinas conducted under a microscope equipped with night vision eye pieces in a very dark room, researchers found that the retinal cells sensitive to upward movement change their behaviour in low light.The 'up' neurons will fire upon detecting any kind of movement, not just upward. When there is much less light available, a weak signal of motion from the 'up' neurons, coupled with a weak signal from any of the other directional cells can help the brain sense movement.The loss of motion perception is a common complaint in human patients with severe vision loss. Field said this finding about the adaptability of retinal neurons may help the design of implantable retinal prosthetics in the future.

Pathway for Klebsiella's colistin resistance unearthed

A study carried out in Chennai has found bacteria resistant to colistin drug, a last-line antibiotic, in 51 of the 110 (46%) fresh food samples (poultry, mutton, fish, and vegetables) tested. Though colistin-resistant bacteria have been found in food samples in more than 30 countries, this is the first time researchers in India have looked for and found them in fresh food.More importantly, the researchers, led by Dr. Abdul Ghafur of Apollo Cancer Institute, Chennai, have for the first time uncovered the mechanism by which Klebsiella pneumoniae bacteria in food samples develop resistance to colistin.While mcr-1 gene in E. coli confers resistance to colistin drug, mutations and insertional inactivation in mgrB gene are responsible for colistin resistance in Klebsiella. In the case of insertional inactivation, an external genetic element (called insertion sequence) gets inserted into a normal mgrB gene leading to its inactivation. Once the mgrB gene gets inactivated, the Klebsiella bacteria become resistant to colistin antibiotic.In clinical settings, the mcr-1 gene is less significant than the mgrB gene mutations for colistin resistance. This is because most of colistin resistance seen in clinical settings comes from Klebsiellabacteria and not E. coli,says Dr. Ghafur. The results of the study were published in the Journal of Global Antimicrobial Resistance.The researchers first identified colistin-resistant Klebsiella in the food samples. Then they looked and found mgrB gene mutation in Klebsiella. We identified 30 samples with colistin-resistant Klebsiella. Of the 30 samples, six had insertion sequences. This is the first time that mgrB gene mutation and the presence of insertion sequence have been identified in food Klebsiella, he says. This finding has remarkable public health significance as colistin resistance in Klebsiella can spread to humans.

Researchers reports DNA aptamer prohibiting Tuberculosis bacteria' entry into cells

By using a small single-stranded DNA molecule (DNA aptamer) that specifically binds to a single protein (HupB) present in TB bacteria, researchers have been able to achieve 40-55% reduction in the bacteria's ability to enter into human

cells and infect them. Besides facilitating entry into host cells, HupB also helps the TB bacteria survive various stresses encountered inside host cells.The HupB protein was discovered in late 1990s by Prof. H. Krishna Prasad, formerly with AIIMS, while looking at specific TB bacterial antigens that induced immune response in humans. He found the protein was associated with the DNA of the bacteria (Tubercle and Lung Disease journal).Since it is associated with the DNA, we didn't expect it to be found on the surface of the bacteria. But to our surprise, it was seen on the surface of the TB bacteria too," recalls Prof. Prasad. Further studies showed that the HupB protein was able to interact and bind to proteins found on the surface of host cells, which will facilitate the entry into host cells. HupB is an essential protein of TB bacteria and so an attractive drug target, says Prof. Jaya Sivaswami Tyagi from the Department of Biotechnology at AIIMS and one of the corresponding authors of a paper published a few days ago in the journal Molecular Therapy - Nucleic Acid.From a collection of two types of DNA libraries, the researchers selected 23 aptamers. Of the 23, only two aptamers (4T and 13T) were chosen based on high binding affinity and specificity to the HupB protein. Both the aptamers remained stable when exposed to serum, an essential requirement for an inhibitor. The aptamers were found to bind at different positions of the protein.

Researchers from IIT – B worked out Biomarkers for lung cancer detection, air pollutants and explosives

Researchers at the Indian Institute of Technology (IIT) Bombay have set the stage to possibly sniff out in about a minute early-stage lung cancer from exhaled breath. A two-member team led by Chandramouli Subramaniam from the institute's Department of Chemistry has developed a platform that detects volatile organic compounds such as benzene, acetone, benzaldehyde and ethanol in a gas phase at single molecular levels. These organic compounds in exhaled breath are clinically established biomarkers for early stage lung cancer. The same platform can also be used to monitor air-pollution levels or detect explosives like TNT (trinitrotoluene).The volatile compounds have been detected using lab samples and clinical applications for detecting early-stage lung cancer will become possible once validated on human subjects. The results were published in the journal ACS Sustainable Chemistry and Engineering. Since Raman scattering is an inherently weak phenomenon, the researchers turned to surface-enhanced Raman scattering to dramatically increase the sensitivity of the platform such that it detects molecules at extremely low concentrations using a small amount of sample. We put the molecule of interest on a gold or silver nanoparticle and then record the Raman spectrum. When we shine light [laser] on the sample [molecule plus the nanoparticle], the Raman spectrum of the molecule gets enhanced,says Prof. Subramaniam. The intensity enhancement of Raman spectrum happens predominantly through the interaction of localised electromagnetic field on the nanoparticles surface with the vibrational modes of the molecule.

Can the human's retina be regenerated just like the zebra fish does, IISER Mohali researchers founds new pathway?

In stark contrast to mammals, the zebrafish has the ability to completely regenerate its retina and restore vision after an injury. Researchers from Indian Institute of Science Education and Research (IISER) Mohali, have decoded the signals and genes behind this tremendous feat and hope to uncover valuable clues as to why we humans fail at such regeneration.A particular signalling system — sonic hedgehog (Shh) — in zebrafish has been previously reported to aid in developmental and tissue regeneration activities. To decipher the influence of Shh signalling on retina regeneration, the researchers first inhibited its function. They found that impairing this signal made 90% of the zebrafish embryo exhibit a birth defect called cyclopia. Cyclopia is also seen in humans, where there is a single median eye or a partially divided eye. Detailed understanding of this signalling may provide insights into the rare defect. Since this signalling is also responsible for retina regeneration in zebrafish, the researchers are trying to understand why the signalling does not bring about retina regeneration in humans.They performed whole retina RNA sequencing at various time points post-retinal injury to the zebrafish eye. Several genes (zic2b, foxn4, mmp9) were found to be upregulated through Shh signalling. Zic2b and foxn4 are essential components for development and tissue regeneration, whereas mmp9 is an enzyme which makes the environment congenial for freshly formed cells. Individual knockdowns of these genes also revealed that these are indeed essential for normal retina regeneration.They further carried out studies on mice models by injecting the protein.

Vol. 12 (4) i - v October 2018, ISSN 0973-8916 (Print), 2230-7303 (Online)

SCIENTIFIC NEWS

Mission embarked to sequence Indian genomes announced : A group of Indian scientists and companies are involved with a 100k GenomeAsia project, led out of the Nanyang Technological University (NTU), Singapore, to sequence the whole genomes of 100k Asians, including 50,000 Indians. India is planning a major mission to sequence the genes of a "large" group of Indians — akin to projects in the United Kingdom, China, Japan and Australia — and use this to improve health as well as buck a global trend of designing 'personalised medicine.'This was among the key decisions taken at the 1st Prime Minister's Science, Technology and Innovation Advisory Council (STIAC) in its first meeting on Tuesday.The Ministry of Health and Family Welfare and the Department of Biotechnology would be closely associated with the project.Ever since the Council of Scientific and Industrial Research in 2009 announced that it had sequenced the genome of an Indian, then making India one of six countries to achieve such a feat.

Study suggests declining rate of wetlands exceeds thrice that of forests : Wetlands, among the world's most valuable and biodiverse ecosystems, are disappearing at an alarming speed amid urbanisation and agriculture shifts.We are in a crisis, Martha Rojas Urrego, head of the Ramsar Convention on Wetlands, told reporters in Geneva, warning of the potential devastating impact of wetland loss, including on climate change.The convention, adopted in the Iranian city of Ramsar nearly a half-century ago, on Thursday issued its first-ever global report on the state of the world's wetlands.The 88-page report found that around 35% of wetlands — which include lakes, rivers, marshes and peatlands, as well as coastal and marine areas like lagoons, mangroves and coral reefs — were lost between 1970 and 2015.Today, wetlands cover more than 12 million square km , the report said, warning that the annual rates of loss had accelerated since 2000.We are losing wetlands three times faster than forests, Mr. Rojas Urrego said, describing the Global Wetland Outlook report as a red flag. While the world has been increasingly focused on global warming and its impact on oceans and forests, the Ramsar Convention said wetlands remain dangerously undervalued.The Ramsar Convention has been ratified by most of the world's nations, including the U.S., China and India, & has designated more than 2,300 sites of international importance.

Japanese and European Spacecraft embarked on Mercury journey : European and Japanese space agencies said an Ariane 5 rocket successfully lifted a spacecraft carrying two probes into orbit on Saturday for a joint mission to Mercury, the closest planet to the sun.The European Space Agency and the Japan Aerospace Exploration Agency said the unmanned BepiColombo spacecraft successfully separated and was sent into orbit from French Guiana as planned to begin a seven-year journey to Mercury. They said the spacecraft, named after Italian scientist Giuseppe "Bepi" Colombo, was in the right orbit and has sent the first signal after the liftoff.ESA says the 1.3 billion-euro (USD 1.5 billion) mission is one of the most challenging in its history. Mercury's extreme temperatures, the intense gravity pull of the sun and blistering solar radiation make for hellish conditions.

Post-Doctoral Research Fellows

1.Indian Govt. Fellowships - Fellowship of Ministry of Science & Technology (DST/ DBT / CSIR(DSIR)/ SERB): Different Indian Govt. Fellowships are available for different streams of science and engineering like life sciences, chemical sciences, physical sciences and others, please refer http://dst.gov.in/fellowship-opportunities-researchers

2. ***Institute of Nano Science and Technology, Mohali:*** The applicants should Either hold a Ph.D. degree in Science/ Engineering or should have submitted the PhD thesis in Science/ Engineering. Proven research competence in any of the above related areas. Please refer **http:// www.inst.ac.in/careers.php**

3. Indian Institute of Technology (IIT Delhi) PDF : IIT Delhi invites applications from qualified Indian Nationals, Persons of Indian Origin (PIOs) and Overseas Citizens of India (OCIs) for the Post Doctoral Fellows (PDF) in the various Departments/Centres/Schools (in the fields mentioned alongwith them). Please refer **https:// recruit.iitd.ac.in**

4. IISER Pune Postdoctoral Research Associate : Applications are invited for Postdoctoral Research Associate (PRAs) positions at the Indian Institute of Science Education and Research (IISER) Pune, India. These positions are open for candidates with 0-5 years of experience after the submission of their PhD thesis. Candidates should provide evidence of having carried out high quality research. Appointments will be made for two years at a time with a maximum tenure of three years. Please refer **http://www.iiserpune.ac.in/opportunities / postdoctoral-research**

☆ ☆ ☆ ☆

The 12th Annual Convention of ABAP &
International Conference on
BIODIVERSITY, ENVIRONMENT AND HUMAN HEALTH : INNOVATIONS AND EMERGING TRENDS
(BEHIET - 2018)
12 - 14 November, 2018
Auditorium, Mizoram University
Aizawl, Mizoram, India

THEMES

* Biodiversity and Environmental Protection
* Pharmacology and Drug Development
* Omics of Food, Water, Health and Environment
* Environmental Pollution

IMPORTANT DATES

Abstract (Oral and Poster) Submission	31st July, 2018
Notification of Acceptance/Rejection	3 August, 2018
Full paper submission	15 August, 2018
Registration deadline	31 Aust, 2018
Nomination for Awards	15 September, 2018

Contact

The Organizing Secretary

The School of Life Science, Mizoram University

Aizawl - 796004;

Email : abapmzu@gmail.com

Registered with Registrar of News Papers for India
Regn. No. APENG/2008/28877

Association of Biotechnology and Pharmacy

(Regn. No. 28OF 2007)

Executive Council

Advisory Board

Executive Members

Printed, Published and owned by Association of Bio-Technology and Pharmacy # 6-69-64 : 6/19, Brodipet, Guntur - 522 002, Andhra pradesh, India. **Printed at :** Don Bosco Tech. School Press, Ring Road, Guntur - 522 007. A.P., India **Published at :** Association of Bio-Technology and Pharmacy # 6-69-64 : 6/19, Brodipet, Guntur - 522 002, Andhra pradesh, India.
Editors : Prof. K.R.S. Sambasiva Rao, Prof. Karnam S. Murthy